Surface and Topography Metrology in Firearm Evidence Identification and Engineering Surface Quality Control

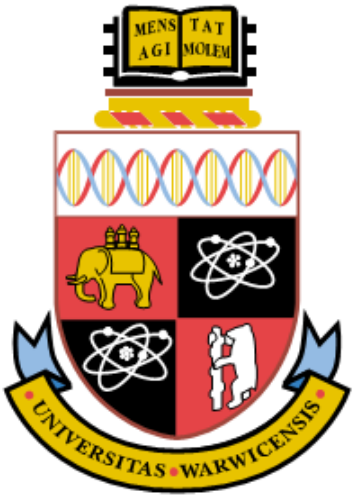

By

Junfeng J. Song

A thesis submitted in partial fulfillment of the requirements for the degree of Doctor of Philosophy in Engineering

School of Engineering, University of Warwick
April, 2017

ABSTRACT

This thesis is a topical review on the application of Surface and Topography Metrology in Firearm Evidence Identification and Engineering Surface Quality Control. It summarizes my research work at the National Institute of Standards and Technology (NIST) from 1987 to present, where I'm a Project Lead for the Forensic Topography and Surface Metrology since 1997.

I started my research in surface metrology since 1982 -- after my MS study at the Harbin Institute of Technology (HIT, Harbin, China) from 1978 to 1981. In 1985, I designed, manufactured and patented the Precision Random Profile Roughness Specimens in Beijing aimed to provide a reference standard for quality control of smooth engineering surfaces [1]. These specimens were manufactured with *R*a values ranging from 0.015 μm to 0.1 μm -- less than 1/10 of the similar specimens developed by PTB (Physikalisch-Technische Bundesanstalt) in Germany. These specimens were successfully used by U.S. manufacturers for measurement unification and quality control of smooth engineering surfaces, and were included in ASME B46 surface standard in 1995.

Microform metrology is a subfield of surface metrology that involves surface measurements of complex geometry features on the micrometer scale. In 1995, I led a team at NIST which established a Microform Calibration System with the lowest calibration uncertainty in the world for calibration of Rockwell hardness (HR) diamond indenters. Based on the precision calibration of HR indenters and the control of other influencing quantities, I proposed a "Metrological Approach" to unifying international HRC scales with metrological traceability. I led an international HRC comparison among five National Metrological Institutes (NMIs). The comparison results strongly supported the proposed Metrological Approach. I drafted a joint paper for five NMIs entitled "Establishing a worldwide unified Rockwell hardness scale with metrological traceability" which was published at the *Metrologia* **34,** 1997 in Paris [4].

Surface and topography metrology provides strong support to firearm evidence identifications. Based on my experience in developing surface standards, measurement systems, uncertainty and traceability procedures, I led a research team which developed the NIST Standard

Reference Material (SRM) Bullets and Cartridge Cases, and the NIST 2D/3D Topography Measurement System [5]. We formulated a National Traceability and Quality System using the SRM Bullets and Cartridge Cases to support ballistics identifications within the National Integrated Ballistics Information Network (NIBIN) in the United States [6]. I have recently invented a Congruent Match Cells (CMC) method for accurate ballistics identification and error rate estimation [7], which can serve as a statistical foundation for estimating error rates in firearm evidence identifications, thus emulating methods used for forensic identification of DNA evidences [8].

Keywords: Surface metrology, microform, topography, roughness, Rockwell hardness, forensics, ballistics identification, congruent match cells, CMC.

ACKNOWLEDGEMENTS

The author would like to express his thanks to his supervisor Dr. Xianping Liu, for her encouragement and supportive suggestions during the research, and for her help in reviewing and correcting the thesis. The author is grateful to Prof. Kai Cheng of the Brunel University London, and to Prof. Nigel Jennett of the University of Coventry for their review, comments and suggestions on my Ph.D. Thesis.

Many thanks go to my colleagues and team members in the Engineering Physics Division (EPD) of the Physical Measurement Laboratory (PML) at NIST, especially, Dr. T V Vorburger, Dr. R M Silver, Dr. J A Soons, Ms. S M Ballou, Mr. R M Thompson, Mr. S Low, Dr. J Yen, Mr. T B Renegar, Mr. A Zheng, Mr. R Clary and Mr. E Whitenton; to NIST guest researchers Prof. X Zhao, Prof. Y Yuan, Dr. L Ma, Dr. W Chu, and Dr. H Zhang; as well as to NIST Post-Doc. Associate Dr. D B Ott, Dr. A Hilton and to Ph.D. students Mr. M Tong and Mr. Z Chen.

The indispensable part of the Ph.D. project is the financial support, coming from the Physical Measurement Laboratory (PML) and Special Program Office (SPO) of NIST, which is greatly appreciated by the author.

Finally, the author would like to express his deepest gratitude to his wife, Fan (Helen) Hou, for her general support, patient and understanding during my research work for Ph.D. degree.

TABLE OF CONTENTS

1. Song J, "Random profile precision roughness calibration specimens," *Surface Topography*, 1988, **1**: p29-40.
2. Song J, Vorburger T V, "Verifying measurement uncertainty using a control chart with dynamic control limits," *MEASURE* (Journal of NCSL-International), NCSL-International, 2007, **2**(3): p76-80.
3. Song J, Rudder F Jr, Vorburger T V, Smith J, "Microform calibration uncertainties of Rockwell diamond indenters," *Journal of Research of NIST*, 1995, **100**(5): p543-561.
4. Song J, Low S, Pitchure D, Germak A, DeSogus S, Polzin T, Yang H, Ishida H, Barbato G, "Establishing a worldwide unified Rockwell hardness scale with metrological traceability," *Metrologia*, BIPM, Paris, 1997, **349**(4): p331-342.
5. Song J, Whitenton E, Kelley D, Clary R, Ma L, Ballou S, "SRM 2460/2461 standard bullets and casings project," *Journal of Research of NIST*, 2004, **109**(6): p533-542.
6. Song J, Vorburger T V, Ballou S, Thompson R, Yen J, Renegar T B, Zheng A, Silver R, Ols M, "The national ballistics imaging comparison (NBIC) project," *Forensic Science International*, 2012, **216**: p168-182. http://dx.doi.org/10.1016/j.forsciint.2011.09.016.
7. Song, J., "Proposed Congruent Matching Cells (CMC) method for ballistics identification and error rate estimation," *AFTE Journal*, 2015, **47**(3): p177-185.
8. Song J, Vorburger T V, Chu W, Yen J, Soons J A, Ott D B, Zhang N-F, "Estimating error rates for firearm evidence identifications in forensic science," passed NIST review, to be submitted to *Forensic Science International* for publication.

LIST OF FIGURES

LIST OF TABLES

Chapter 1. Introduction

This thesis summarizes my research work at NIST's projects in surface metrology, microform metrology and forensic topography metrology since 1987 to present. My major contributions in these filelds are shown in below, which are summarized in my eight key publications [1-8] and are submitted with my PhD thesis for review.

Surface metrology for engineering surface quality control:

- Designed and manufactured the Precision Random Profile Roughness Specimens for quality control of smooth engineering surfaces [1] with roughness *R*a values ranging from 0.015 μm to 0.1 μm -- less than 1/10 of the similar specimens developed by PTB (Physikalisch-Technische Bundesanstalt) in Germany. These specimens were included in ASME B46 surface standards in 1995.
- Proposed a Dynamic Control Chart for measurement quality control of engineering surfaces [2].

Microform metrology for Rockwell hardness standardization:

- Established a Microform Calibration System at NIST with the lowest calibration uncertainty in the world for calibration of Standard Rockwell Diamond Indenters' microform geometry [3], developed uncertainty assessment procedures [3] and conducted initial calibrations of National Rockewll Indenters for five National Metrological Institutes (NMIs) [4].
- Proposed a "Metrological Approach" to unifying international Rockwell C hardness (HRC) scales based on precision calibration of microform geometry of HRC indenters and other influence quantities with traceability to base unites of length, mass and time [4], instead of the "Performance Approach" used at that time based on performance comparisons and corrections on different national HRC scales [4].
- Conducted international comparisons among five National Metrology Institutes (NMIs), drafted a joint paper entitled "Establishing a worldwide unified Rockwell hardness scale with metrological traceability" which was published at the *Metrologia* **34,** 1997 in Paris [4].

Topography metrology for firearm evidence identification and standardization:

- Designed NIST SRM (Standard Reference Material) 2460/2461Standard Bullets and Cartridge Cases, and NIST 2D/3D Topography Measurement System [5]; designed and led the manufacturing, inspection and certification process for the SRM Bulllets and Cartridge Cases [5].
- Proposed and led the National Ballistics Imaging Comparisons (NBIC) project for establlishing a Ttracceability and Quality System for ballistics measurement in the United States [6].
- Invented a Congruent Match Cells (CMC) method for accurate ballistics identfications and error rate estimation [7]; led the team and copmpleted the initial tests and error rate estimation; drafted a research paper which has passed NIST review for publication [8].

The objectives of this chapter are four fold. First, it starts with an introduction on surface, microform and topography metrology, and reviews my major publications in these fields. Second, it discusses background and identifies the major challenges in these fields. Third, it suggests some practical solutions for these challenges and explains the aims of the thesis. At last, it presents the layout of the thesis structure and a brief discreption of each chapter.

1.1. Foreword

1.1.1. Surface metrology

Metrology is the "*science of measurement*" [9]. Similarly, surface metrology is the science of surface measurement that involves a wide range of surface characterization represented by 2D and 3D surface parameters [10-12], measurement methods including the profile and areal method and instrumentation using contact and non-contact instruments based on different physical principles and engineering designs [10,11]. It also involves measurement traceability, quality control and uncertainty assessment procedures which may include the usage of different surface calibration and check standards, e.g. step height and surface roughness calibration and comparison specimens [1,13,14], using control charts with uncertainty and quality procedures [2,15].

1.1.2. Microform metrology

Microform metrology and topography metrology are subfields of surface metrology. Microform metrology involves surface measurements of complex geometry forms on the scale of micrometers, which may include a set of measurements on length, radius, angles, form and

alignment, as well as profile deviation and surface finish roughness [16]. A typical usage of microform metrology is the microform calibration of Standard Rockwell Hardness Diamond Indenters using the Microform Calibration System [3,17], which led to establishing a worldwide unified Rockwell C hardness scale with metrological traceability [4].

1.1.3. Topography metrology

Most metrics for describing surfaces are used to quantify the characteristics of a surface in vertical, horizontal or some combination of both dimensions [10-12]. However, topography metrology aims to compare the overall features of 2D profiles or 3D topographies and quantify the similarity of the compared profiles or topographies relative to each other [18,19]. The NIST 2D/3D Topography Measurement System was developed from NIST's Standard Reference Material (SRM) Bullet and Cartridge Case project [5,20,21]. The 2D profile comparison was also used for instrument characterization [22]; the 3D topography comparison was used for production quality control of the SRM cartridge cases [23]. Both the 2D and 3D topography measurements were used for firearm evidence identifications [24] and for establishment of measurement traceability and quality control for nationwide ballistics identifications [6,25,26].

1.2. Background and Challenges

1.2.1. Challenges to firearm evidence identifications in the United States

Side-by-side image comparisons for firearm identification have a history of more than a hundred year [27]. However, the scientific foundation of firearm and toolmark identification has been challenged by recent court decisions. As stated in the 2008 and 2009 National Academies Report [28,29]: "*The validity of the fundamental assumptions of uniqueness and reproducibility of firearms-related toolmarks has not yet been fully demonstrated…*" and "*Since the basis of all forensic identification is probability theory, examiners can never really assert a conclusion of an 'identification to exclusion of all others in the world,' but at best can only assert a very small (objective or subjective) probability of a coincidental match…*"

In order to response these fundamental challenges, a research plan with major research projects was developed by the Forensic Topography and Surface Metrology Project which was established at NIST in 1997. The major technical approaches are shown below (detailed information, significant accomplishments and impact will be described in Chapter 2):

- **Developing reference standards -- NIST SRM (Standard Reference Material) 2460 Bullets and SRM 2461 Cartridge Cases** for instrument calibration, measurement traceability and quality control to support nationwide ballistics identifications [5].
- **Developing a 2D/3D Ballistics Topography Measurement System.** Most of the existing ballistics identification systems are primarily based on comparisons of optical images acquired by microscopes under different lighting conditions. The correlation accuracy depends on image quality, which is largely affected by lighting conditions such as the type of light source, lighting direction, intensity, material color and reflectivity, and image contrast [24]. Since ballistics signatures are surface topographies by nature [30], it is necessary to develop a 2D/3D Ballistics Topography Measurement System, which is independent of optical lighting conditions, for quantitative and objective ballistics topography measurements [24].
- **Developing a Traceability and Quality System** to establish measurement traceability and quality control for nationwide firearm image measurements and identifications [6,25,26].
- **Developing a novel method for accurate ballistics identification and error rate report.** Accurate ballistics identification depends not only on image quality, but also on the capability of correlation software to identify the "valid correlation areas" and to eliminate the "invalid correlation areas" [7,8,31] from calculations. Currently, the final determination of a match (identification) or non-match (exclusion) in ballistics correlation is based on visual comparisons by an examiner having the experience required to exclude invalid correlation areas. It is necessary to develop a quantitative and objective method, called the "Congruent Match Cells (CMC)" method, for accurate ballistics identifications and error rate reporting [7,8,31-33].

1.2.2. Surface metrology for engineering surface quality control

- **Design, manufacturing and test of the Precision Random Profile Roughness Specimens**

  Many engineering surfaces, especially those of smooth engineering surfaces manufactured by grinding, lapping, polishing and honing etc., are random surfaces or with random components on their surfaces. In 1965, Häsing at PTB (Physikalisch-Technische Bundesanstalt, Germany) developed a random profile roughness specimen

to represent these types of random surfaces for quality control of medium machined engineering surfaces (Ra = 0.15 μm to 1.5 μm) [14]. With the development of modern science and technology, quality control for smooth engineering surfaces ($Ra \leq 0.1$ μm) becomes increasingly important, not only because of their important engineering functions, but also their high production costs [13]. NIST frequently receives requests to provide Standard Reference Material (SRM) Precision Random Profile Roughness Specimens for smooth surface measurements and quality control in U.S. industry.

- **Development of a dynamic control chart for engineering surface quality control**

  Reporting uncertainty is an important issue in surface metrology. A dynamic control chart is developed [2] using fixed and dynamic control limits for promoting the process of development and revising of uncertainty budgets and for verifying the developed measurement uncertainty. It can also be used for monitoring long term variation for measurement quality control [2]. These dynamic control charts have been used for quality control of national ballistics identifications and for establishing a Traceability and Quality System for the National Integrated Ballistics Information Network (NIBIN) in the United States [6].

1.2.3. Microform metrology for Rockwell hardness standardization

Rockwell Hardness C (HRC) is the most widely used mechanical testing method for metal products. However, international HRC scales are not unified. In the 1990's, I proposed a "Metrological Approach" to unifying international HRC scales [4], the key challenge being to establish a Microform Calibration System for precise calibration of the microform geometry of Standard Rockwell Diamond Indenters [3]; and to conduct international comparisons among National Metrological Institutes (NMIs) to verify the proposed Metrological Approach for establishing a worldwide unified Rockwell hardness scale with metrological traceability [4].

1.3. The Aim of the Thesis

In this Ph.D. thesis, I will present a Topical Review of my key publications to identify clearly the impact and key outcomes of my research works on:

- Surface metrology for quality control of engineering surfaces;

- Microform metrology for establishing a worldwide unified a Rockwell hardness C (HRC) scale;
- Topography metrology for firearm evidence identification and error rate estimation.

This thesis covers my research work at NIST from 1987 to present. I'm currently a Senior Research Engineer, a Post-Doc. Research Adviser and Project Lead at the Engineering Physics Division (EPD) of Physical Measurement Laboratory (PML) at NIST. I received a M.S. degree in Mechanical Engineering from the Harbin Institute of Technology (HIT), Harbin, China, in 1981. I came to NIST in 1987. From 1987 to 1997, my research was focused on surface and microform metrology, which were fundamental in precision engineering and advanced manufacturing. Since 1997, I have been working as the Project Lead and Post-Doc. Research Advisor for the Forensic Topography and Surface Metrology Project at NIST. I have published more than 150 papers, many are published in leading journals of U.S. and internationally, and celebrated in three NIST awards.

My thesis discusses how to use the general knowledge and fundamental principles in surface metrology to support engineering surface quality control and firearm evidence identifications. This includes how to define a measurable quantity and develop a reference standard; how to establish a measurement system; how to construct a traceability and quality system; and how to evaluate measurement uncertainty for engineering surface control and firearm evidence identification. The thesis also presents a review on some of the state-of-the-art technologies used in National Metrology Institutes (NMI) and measurement institutions in surface and topography metrology. It compares the advantages and limitations of some techniques and provides case studies and applications in R&D related industries that will be beneficial to different fields in precision engineering and metrology, advanced manufacturing, and firearm evidence identification.

The thesis is to be presented in accordance with the regulations for the Degree of Doctor of Philosophy by the High Degree Committee at the University of Warwick through the Ph.D. by Published Work Program of the Engineering School.

1.4. Outline of the Thesis

This thesis is outlined with a discussion on my recent research projects first, which is the topography measurements for firearm evidence identifications (from 1997 to present, see Chapter 2 and 3), then introduce my early research projects in surface metrology (from 1987 to 1992, see Chapter 4) and microform metrology (from 1993 to 1997, see Chapter 5), followed by a summary in Chapter 6:

- Chapter 1 starts with the background and challenges in surface, microform and topography metrology, and introduces my major published works in these fields.
- Chapter 2 discusses topography metrology for firearm evidence identification and error rate estimation. This includes developments of the NIST Standard Reference Material (SRM) Bullets and Cartridge Cases, the NIST 2D/3D Ballistics Topography Measurement System, the National Traceability and Quality System for U.S. firearm evidence identifications, and the proposed error rate assessment procedure for firearm evidence identifications based on the Congruent Match Cells (CMC) method.
- Chapter 3 describes the usage of 2D/3D topography measurements for instrument characterization and production quality control.
- Chapter 4 describes the Precision Random Profile Roughness Specimens, which were designed and manufactured before I came to NIST, aimed at quality control of smooth engineering surfaces. The development and application of a Dynamic Control Chart for engineering surface quality control are also described.
- Chapter 5 describes how to use Microform Metrology to establish worldwide unified Rockwell hardness scales with metrological traceability. This includes the proposed "Metrological Approach" and the NIST Microform Calibration System for microform calibration of Rockwell hardness diamond indenters, and the international comparison between five National Metrological Institutes (NMIs).
- Finally, Chapter 6 summarizes my major contributions, impacts and proposed future works in the fields of Surface and Topography Metrology in Firearm Evidence Identification and Engineering Surface Quality Control.

Chapter 2. Topography Metrology for Firearm Evidence Identification and Error Rate Estimation in Forensic Science

Accurate firearm evidence identifications depend on both the image quality and the capability of the correlation software to identify the "valid correlation areas" on the image of the firearm evidence for accurate firearm identification and error rate estimation [7,8]. This involves a ballistics calibration standard, a measurement and traceability system and correlation methods. My major contributions in this field are presented in the attached four key publications [5-8]:

- Designed the Virtual/Physical Ballistics Signature Standard -- NIST SRM 2460 Standard Bullets, designed and led the manufacturing process using numerically controlled (NC) diamond turning for manufacturing of the SRM bulllet [5].
- Proposed Cross Correlation Functions (CCF) for 2D/3D ballistics signature measurements, led the development and testing of the NIST 2D/3D Topography Measurement System, completed the measurement and certification of SRM bullets [5].
- Proposed electro-forming technique for SRM cartridge cases, proposed test of "decay factors" for optimization of the manufacture process [23].
- Proposed and led the National Ballistics Imaging Comparisons (NBIC) project to establlish a Traceability and Quality System for ballistics measurement in the United States [6].
- Invented a Congruent Match Cells (CMC) method for accurate ballistcs identfications and error rate estimation [7]; led the programing, testing and error rate estimation; drafted a research paper which has passed NIST review for publication [8].

2.1. Response to the Fundamental Challenge in Firearm Evidence Identifications in the United States

When bullets are fired and cartridge cases are ejected from a firearm, the parts of the firearm that make forcible contact with them create unique, characteristic tool marks on their surfaces called "ballistic signatures" [30]. Striation signatures (2D profile tool marks) on a bullet are caused by its passage through the gun barrel (see Fig.2-1 left [34]). Impression signatures (3D topography tool marks) on a cartridge case are caused by impact with the gun parts: firing pin,

breech face and ejector during firing (see Fig.2-1 right [34]). Both the 2D striation and 3D impression signatures are unique to the firearm [30]. By microscopically comparing these ballistic signatures, firearm examiners can determine whether a pair of bullets or cartridge cases were fired or ejected from the same firearm. Ballistics examiners can then connect a recovered firearm or other firearm evidence to criminal acts [30].

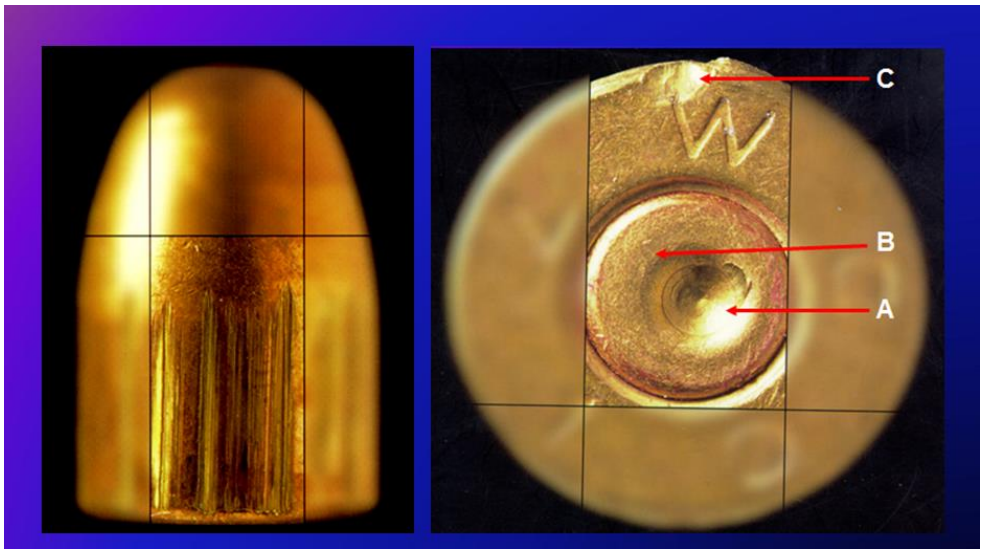

Fig.2-1. Bullet signature is a 2D profile signature (left), cartridge case signatures include those from firing pin A, breech face B and ejector mark C, all are 3D topography signatures (right) [34].

Side-by-side image comparisons using optical microscopes for ballistic identifications have more than a hundred years' history [27]. Since the late 1980s, different automated ballistics identification systems have been developed. These systems typically include a digitized optical microscope, a signature analysis station and correlation software [34]. In 1998, the National Integrated Ballistics Information System (NIBIN) [35] was established in the United States which currently included more than 150 local stations using the Integrated Ballistics Identification System (IBIS) [34] for ballistics identification and information sharing.

As a national metrology institute in the United States, NIST was requested to provide technical support on measurements and standards to NIBIN's nationwide ballistics identifications and measurement quality control. That includes developing reference standards and 2D/3D ballistics topography measurement system, formulating a traceability and quality system, and developing a novel method for accurate ballistics identification and error rate report.

2.2. NIST SRM 2460/2461 Standard Bullets and Cartridge Cases Project

2.2.1. Basic technical requirements

As a reference standard for ballistics signature measurements and firearm evidence identifications, basic technical requirements for NIST SRM 2460/2461 Standard Bullets and Cartridge Cases are specified as [5]:

- **Real firearm surface characteristics:** The bullet and cartridge case signatures must be obtained from real bullets and cartridge cases, which are duplicated on the surface of the physical standards -- the SRM Bullets and Cartridge Cases, with high fidelity. The shape, size, material and color of the physical Standard Bullets and Cartridge Cases should be as close as possible to those of the real bullets and cartridges.
- **Repeatability and reproducibility:** As a measurement standard, the profile signatures on the SRM Bullets and Cartridge Cases must show such a high degree of repeatability and reproducibility that when these SRM Bullets and Cartridges are distributed nationwide for checking instrument calibrations, they actually play the same function as a single SRM Bullet or SRM Cartridge does. Repeatability here means that the profile signatures are essentially identical over different SRMs produced at the same time. Reproducibility means that the profile signatures are highly uniform among different SRMs produced over time.
- **Measurement traceability:** The profile and topography measurements for SRM Bullets and Cartridges performed at the NIST Surface Calibration Laboratory must be traceable to the SI unit of length. By using these SRM Bullets and Cartridges, ballistics signature measurements using optical techniques, performed at local forensic laboratories, can be traced to the Bureau of Alcohol Tobacco and Firearms' (ATF) image standard established at ATF's National Laboratory Center using the SRM Bullets and Cartridge Cases.
- **Information technology:** It is advantageous to base the SRM Bullets on information technology. Thus, the digitized profile signatures may be stored in a computer and used to produce and re-produce the identical SRM Bullets at any time.

Considering the above technical requirements, the SRM 2460 Standard Bullets are designed as both a virtual and a physical bullet signature standard.

2.2.2. Establishment of a virtual bullet signature standard

The SRM Bullets are designed with six land engraved areas (LEA) which are the most popular used by handguns. The virtual standard of the bullet profile signatures is a set of six digitized profile signatures stored in a computer. The ATF's National Laboratory Center and the Federal Bureau of Investigation's (FBI) Central Laboratory provided NIST with a total of six master bullets -- three from each agency (Fig.2-2) [5], all were fired from different guns under

Fig.2-2. Six master bullets from ATF (top row) and FBI (bottom row), each of which was traced on a selected land engraved area. The six digitized bullet signatures were stored in a computer as the virtual bullet signature standard.

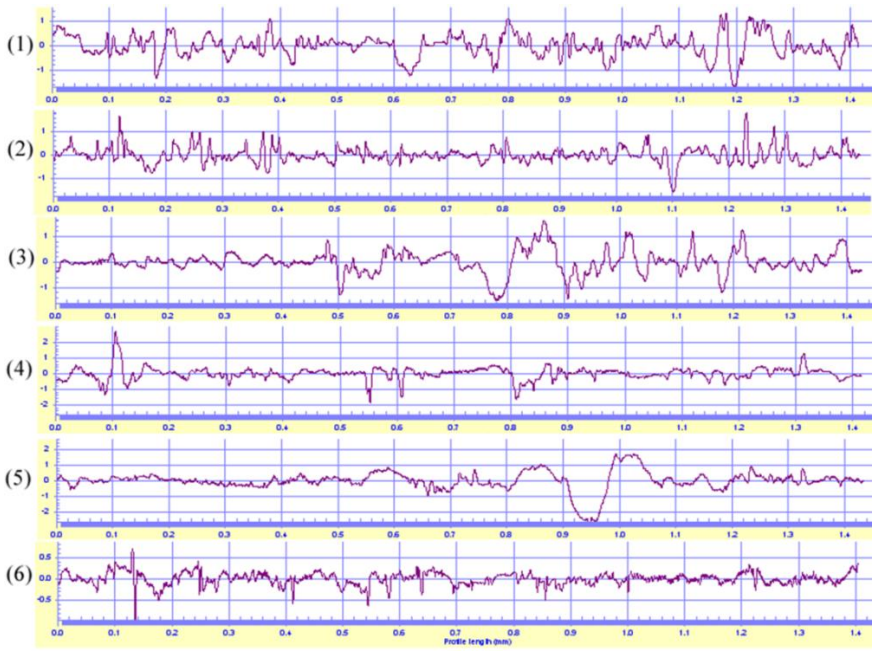

Fig.2-3. The virtual bullet signature standard consists of six digitized bullet profile signatures measured by a stylus instrument on six master bullets fired at the ATF and FBI. The virtual standard profiles shown above are modified profiles after curvature removal and Gaussian filtering with a short-wavelength cutoff of λs = 0.0025 mm and a long wavelength cutoff of λc = 0.25 mm [5]. The vertical scale is in µm; the horizontal scale is in mm.

standardized firing conditions. These master bullets underwent profile measurements at the NIST Surface Calibration Laboratory using a commercial stylus instrument. Each bullet was traced on one selected land engraved area (LEA). The resulting set of six digitized bullet profile signatures was used as the virtual standard for fabrication, and as a reference standard for measurement, of the SRM bullets [5]. The virtual standard profiles shown in Fig.2-3 are modified profiles after curvature removal and Gaussian filtering with a short-wavelength cutoff of $\lambda s = 0.0025$ mm and a long wavelength cutoff of $\lambda c = 0.25$ mm.

2.2.3. Manufacturing of the physical standard -- SRM 2460 Standard Bullets

The Engineering Physics Division at NIST has a long history of developing surface roughness specimens [36-38]. In 1998, a virtual/physical random profile surface roughness specimen was developed at NIST using a numerically controlled (NC) diamond turning process at the NIST's instrument shop [39]. Based on the same NC diamond turning technique for manufacturing random profile roughness specimens, the SRM standard bullets were developed [5].

The SRM Standard Bullets were manufactured by Mr. R. Clary of NIST using a Numerically Controlled (NC) diamond turning machine at the NIST Instrument Shop (Fig.2-4) [5]. The

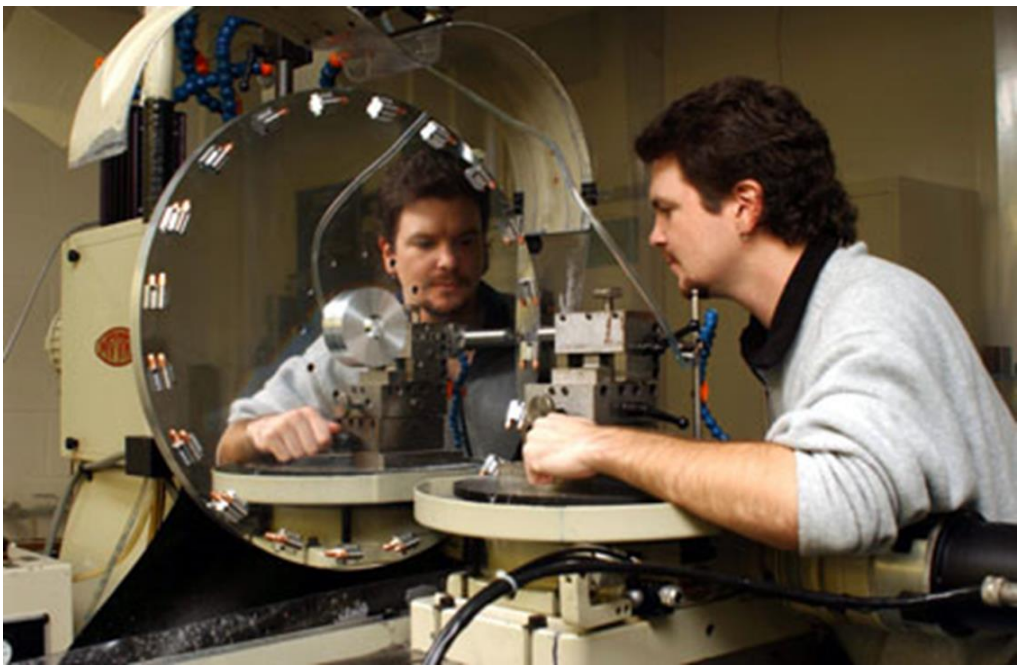

Fig.2-4. The SRM Standard Bullets were manufactured by Mr. R. Clary of NIST using a Numerically Controlled (NC) diamond turning machine at NIST's Instrument Shop. 20 bullets were cut at the same manufacturing set up.

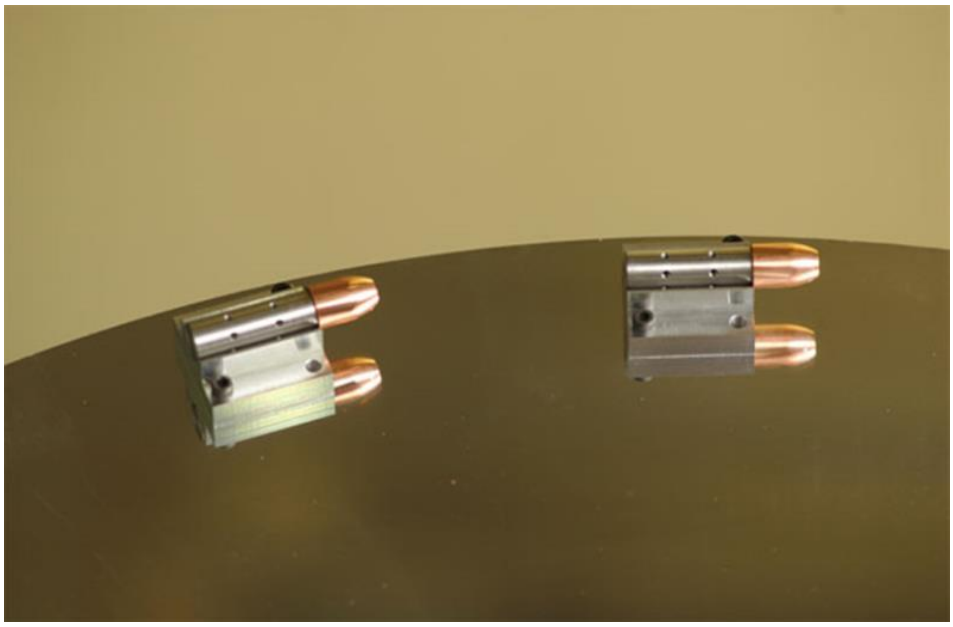

Fig.2-5. Manufacturing setup for SRM 2460 Standard Bullets: each bullet was fastened to a cylinder, which was mounted on a "V" block set on an aluminum wheel. 20 SRM bullets were manufactured at the same time. The cutting diameter was 22.5″ (572 mm).

SRM bullets are made of oxygen-free, high conductivity (OFHC) copper rod with about a 1 mm thick pure-copper coating to avoid the crystal boundary effect on the micro surface topography during diamond cutting [5]. Fig.2-5 shows the manufacturing setup on a NC diamond turning machine. The bullets were fastened to cylinders, which were mounted on V-blocks set on an aluminum wheel (Fig.2-5). Twenty SRM bullets were manufactured at the same setup (Fig.2-4). After cutting one signature, the cylinders were rotated 60° to cut the next signature until all six signatures were completed. There was a 5° tilt for the "V" block's alignment with the rotation direction of the aluminum wheel, so that a 5° twist in the bullet signature land could be made on the SRM bullets. That gave the SRM bullet a shape close to that of the master (see Fig.2-2) [5].

The manufacturing setup and cutting conditions are: the cutting diameter is 22.5" (572mm); the rotation speed is 300 rpm, or about 540 m-min^{-1}; the cutting depth is 10 μm; the cutting feed rate is 120 μm per minute or 0.4 μm per rotation. There are about 20 cuts to finish each signature, or about a total of 0.2 mm cutting depth for each signature. The diamond cutting tool is a natural diamond with a 2 μm nominal tip radius, which doesn't show significant change after the cutting of all signatures [5].

A SRM Bullet is shown in Fig.2-6. Six land engraved areas (LEA) are machined on the bullet surface by a NC diamond turning machine. Each LEA has a unique bullet signature in accordance with the virtual bullet signature standard (see Fig.2-3), but the SRM bullets are intended to be essentially identical to one another. The bullet's LEAs are produced with a 5° right hand twist, which makes the SRM 2460 resemble a real 9 mm Luger type bullet. The SRM 2460 Standard Bullet is mounted on a blue stub for initial setup on a microscope (Fig.2-6).

Fig.2-6. A NIST SRM 2460 Standard Bullet mounted on a blue stub for initial setup on a microscope.

2.2.4. SRM 2461 standard cartridge cases

The electro-forming technique has a long history for replication of surface specimens: a master specimen is put into a tank with electrolytes to produce a negative replica on the surface of the master. By repeating the same process on the negative replica, a positive replica is replicated with same surface topography as the master specimen [38]. The electro-forming technique was used for production of SRM 2461 Standard Cartridge Cases. In order to ensure that the SRM Cartridges are produced with virtually the same surface topography with the master, it is necessary to test the decay factors of the replication process, and design an optimum plan for the production of a large amount of SRM Cartridges with maximum uniformity of surface topography. Detailed information about the decay factor test can be found in Chapter 3.2 and Ref. 23.

For the NIST SRM 2461 Standard Cartridge Cases project, it was planned to produce 256 SRM Cartridges from the same ATF master with the similarity factor $CCF_{\max}$ [18, to be discussed in

Section 2.3.1] higher than 95 %. Based on the decay factors, we calculated the topography decays for two production plans. The first one, called "16 × 16", uses the ATF master to make 16 negative replicas, and then, uses each negative replica to make 16 SRM Cartridges. The CCF_{max} for the last SRM Cartridges is calculated as (97.37 ± 0.20) % [23]. The uncertainty (k = 1) is a Type A standard uncertainty derived from the parameter fitting. The second plan, called "4 × 4 × 4 × 4", uses the ATF master to make 4 negative replicas; and then, uses each negative replica to make 4 positive replicas; again, uses each positive replica to make 4 negative replicas; and finally, uses each negative replica to make 4 SRM Cartridges. The CCF_{max} for the last SRM Cartridge is calculated as CCF_{max} = (96.01 ± 0.25) % (also k = 1) [23]. Both plans can produce 256 SRM Cartridges with CCF_{max} values higher than 95 %.

Based on the production plan, 137 SRM 2461 Cartridge Cases were produced and certified for forensics / crime scene investigations [40]. Fig.2-7 (left) shows a SRM 2461 Standard Cartridge Case which is mounted on a brass cylinder holder. Fig.2-7 (right) shows the three certified areas of the SRM Cartridge Case: breech face impression (BF), firing pin impression (FP), and ejector mark (EM).

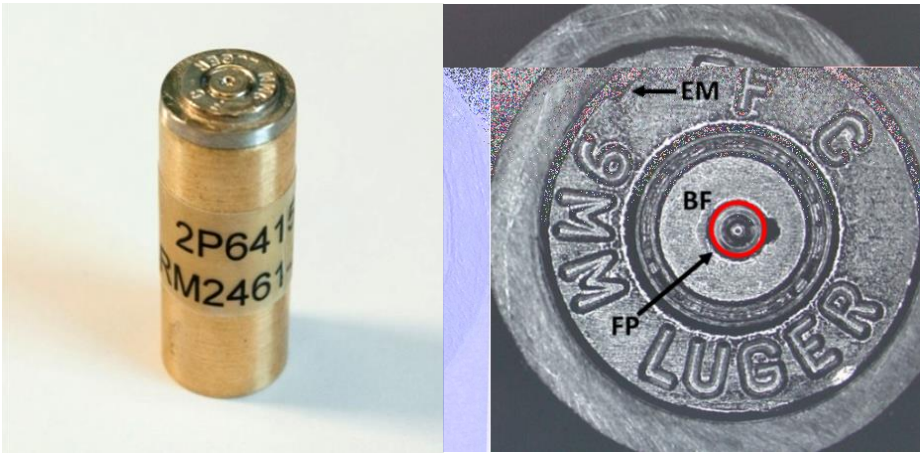

Fig.2-7. Left -- a NIST SRM 2461 Cartridge case mounted on a brass cylinder holder. Right -- optical micrograph shows the three certified areas of the SRM: breech face impression (BF), firing pin impression (FP), and ejector mark (EM).

2.3. NIST 2D/3D Ballistics Topography Measurement System

Visual comparisons of SRM Bullets and Cartridges showed that their ballistics signatures can be manufactured with high uniformity. However, minor differences on the 2D and 3D topography comparisons could be observed. It is therefore important to define a traceable

parameter to quantify the topography difference, and to develop a 2D/3D Topography Measurement System for measuring 2D/3D ballistics signature differences. This parameter is particularly important for the production, inspection and quality control of the SRM Bullets and Cartridges, as well as for the firearm evidence identification systems.

2.3.1. Cross correlation function maximum CCF_{max} and signature difference D_s

It was proposed to adapt the signal processing functions of auto-correlation and cross-correlation for the bullet signature comparisons [18,19]. Because the ballistics signatures can be considered as random profiles, their auto-correlation functions (ACF) decay with increase in the absolute value of the shift distance. This statistical property is very useful for ballistics signature comparisons to quantify the similarity of ballistics signatures. When two bullet profile signatures are compared with each other, one is taken as the reference signature A and the other is the compared signature B [18]:

- If the two profile signatures are exactly the same, A = B, their ACF achieves the maximum value (1.00) when the shift distance is zero (Fig.2-8 left).
- If two compared profile signatures A and B have essentially the same pattern but small differences in the profile details, then A ≈ B. For example, when two bullets are fired from the same gun, their profile signatures have the same pattern with strong correlation. With the shift distance set to the maximum correlation position, their CCF will have a maximum value but not as large as 1.00, because there are small differences between these two correlated profile signatures (Fig. 2-8 middle).

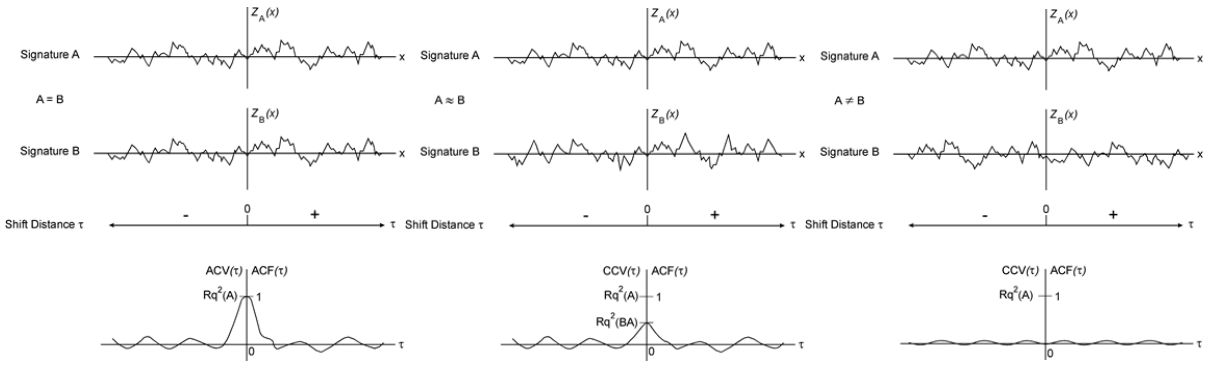

Fig.2-8. Bullet signature comparisons between identical bullet signatures B = A (left), between similar bullet signatures, B ≈ A (middle) and between dissimilar bullet signatures, B ≠ A (right).

- If signatures A and B come from bullets fired from different guns, there should be only small correlation between the two bullet signatures, B ≠ A. With the shift distance changing, only random variations appear on the CCF curve without a clear correlation peak (Fig. 2-8 right).

From the cross-correlation function (CCF) we calculate a parameter called CCF_{max}, which is the maximum value of the CCF when the two compared profiles are correlated at the maximum correlation position (or in phase). Although the CCF_{max} can be used for the profile signature comparison, it is not a unique parameter. Based on the definition of the cross-correlation function [41], if two compared signatures have the same shape but different vertical scales, their CCF_{max} is still 100 % even if they are two different signatures. Therefore, a unique parameter, signature difference D_s, is proposed for quantifying the profile signature differences [18,19]. It is calculated as follows:

- At the shift where the CCF_{max} between signature B and A occurs, construct a new profile $Z_{B-A}(X)$, which is equal to the difference of the compared profile signature $Z_B(X)$ and the reference profile signature $Z_A(X)$:

$$Z_{B-A}(X) = Z_B(X) - Z_A(X). \quad (2\text{-}1)$$

- Calculate the Rq value, root-mean-square roughness [10,11], for the new profile $Z_{B-A}(X)$. We call this parameter Rq(B - A).
- Calculate the signature difference D_s between signatures B and A defined as:

$$D_s = Rq^2(B-A) \; / \; Rq^2(A), \quad (2\text{-}2)$$

where $Rq^2(A)$ is the mean-square roughness of the reference signature $Z_A(X)$, used here as a comparison reference. From Eqs.2-1 and 2-2, it can be seen that when two compared profile signatures are exactly the same, $Z_{B-A}(X) = 0$, then $Rq^2(B-A) = 0$, and $D_s = 0$.

Since there is a liner relationship between D_s and CCF_{max}: $D_s = 2\,(1 - CCF_{max})$ [21], in most cases, only CCF_{max} is used for 2D and 3D ballistics signature comparisons.

2.3.2. 2D ballistics signature measurement system and measurement results for SRM bullets

Based on the proposed parameter and algorithm, the NIST Ballistics Signature Measurement System was developed for the measurement of SRM 2460 Standard Bullets [20,21]. The

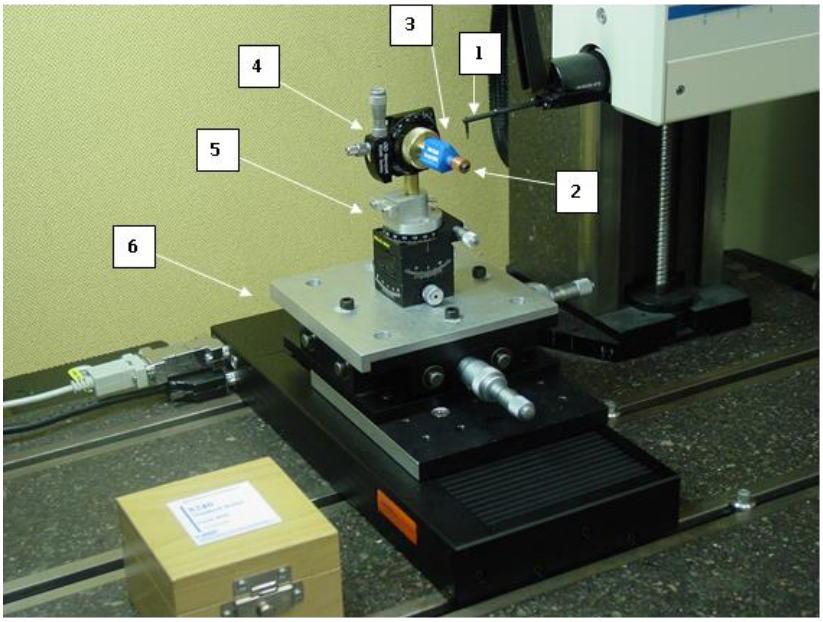

Fig.2-9. Measurement setup for the NIST Bullet Signature Measurement System. 1: Diamond stylus; 2: Standard Bullet; 3: Bullet holder; 4: Rotary stage; 5: Horizontal rotary stage; 6: X-Y stage.

measurement setup is shown in Fig.2-9. A commercial stylus instrument is used for bullet signature measurements. For each measurement, a diamond stylus (item 1 in Fig.2-9) traces a land impression of the standard bullet 2. The nominal value of tip radius of the diamond stylus is 2 μm. The nominal contact force is 0.001 N (about 100 mgf). The traversing speed is 0.5 mm/s. The vertical resolution is 0.01 μm, and the horizontal resolution is 0.25 μm.

The standard bullet 2 is set on a bullet holder 3, which is mounted on a rotary stage 4. The rotary stage is set on another horizontal rotary stage 5, which is rotated about 5° left around the vertical Z-axis, so that the bullet signature with a 5° right twist can be measured perpendicular to the land. Both the rotary stage 4 and the horizontal rotary stage 5 are set on an X–Y stage 6. This allows for the adjustment of the X–Y position of the bullet. After measuring the first land by scanning the diamond tip in the X-direction, the bullet 2 is rotated 60° by the rotary stage 4, so that the next land is measured. This is repeated for all six lands. Finally, the measurement profiles are input into the bullet signature measurement program for analysis.

The bullet signature measurement program is based on the proposed parameters and algorithm as discussed above [18,19]. A screen output of the bullet signature measurement program is shown in Fig.2-10. The top profile is the virtual bullet signature standard, or “Signature A”, which is one of the six modified surface profiles from the bullet signatures of the six master

bullets fired at ATF and FBI, as shown in Fig.2-3. The virtual signature standard is used to control the tool path of the numerically controlled diamond turning machine to produce the SRM bullets. It is also used as a reference standard for the measurements of the bullet signatures of the SRM bullets. The second profile in Fig.2-10 shows the measured bullet signature, or "Signature B", which in this case is a modified surface profile from the No. 1 land impression of the SRM 2460-001 Standard Bullet. At the maximum cross-correlation position of the two profiles, a correlation peak shows CCF_{max} = 99.55 % (see Fig. 2-10). At this position, a new signature, B – A (see the bottom profile in Fig.2-10), is constructed, which is equal to the difference between the two compared signatures B – A. Then the signature difference is calculated by Eq.2-2, D_s = 0.92 %. Detailed information on the measurement program can be found in Ref. 42.

Fig.2-10. User screen for bullet signature measurement between the land 1 of SRM 2460-001 Standard Bullet (Signature B, as shown on the second profile from the top) and the virtual standard (Signature A, as shown on the top). The cross-correlation function CCF_{max} = 99.55 %, the signature difference D_s = 0.92 %. The units of the top and bottom vertical scales are μm. The unites of the lateral scales are mm.

Measurement results show that the manufactured bullet signatures are very close to the virtual bullet signature standard. For example, Fig. 2-11 shows the histogram of CCF_{max} values from 240 signature measurements of 40 SRM Bullets, each measured at six lands with 2 mm width. All CCF_{max} values are higher than 95 %. Considering that CCF_{max} = 100 % (and D_s = 0) means that the measured bullet signature is exactly the same as the virtual bullet signature standard (point by point), the measurement results have demonstrated a high reproducibility for both the bullet signature measurement system and the manufacturing process of the SRM Bullets. Based on NIST Technical Note 1297 [43], an uncertainty analysis procedure was used for reporting the measurement results for both CCF_{max} and D_s values with 95 % confidence level [44].

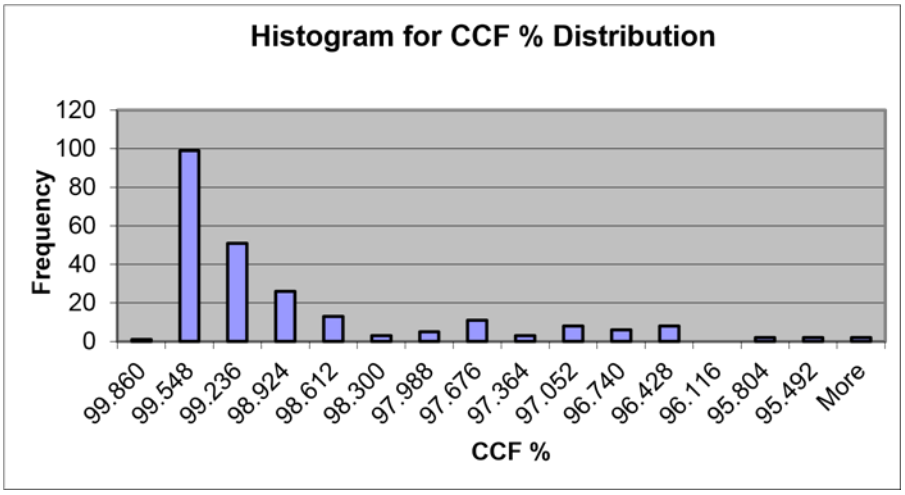

Fig.2-11. CCF_{max} distribution for 240 bullet signatures of 40 SRM Bullets. All CCF_{max} values are higher than 95 %, most are even higher than 99 %. CCF_{max} = 100 % means that the measured bullet signature is exactly the same as the virtual bullet signature standard (point by point).

2.3.3. 3D ballistic signature measurement system and measurement results for SRM cartridge cases

A 3D Topography Measurement System for the SRM Cartridge Cases was developed to calculate the 3D versions of the above parameters [18,19]. A Nanofocus confocal microscope was used for measurements of SRM Cartridge Cases (Fig.2-12). The measurement field is 1.6 mm and 0.8 mm using 10× and 20× lens; the X/Y resolution is about 3.13 µm and 1.56 µm and the Z resolution is 20 nm and 10 nm for 10x and 20x lens, respectively.

Fig.2-12. A Nanofocus confocal microscope was used for 3D measurements of SRM Cartridge Cases.

The areal cross-correlation function, ACCF [11,12], was used for quantitative measurement of the 3D topography differences of the SRM cartridges. Fig.2-13 shows a firing pin signature comparison between two prototype SRM Standard Cartridges S/N 001 and 002, which were electroformed replicas from the same master cartridge provided by the Bureau of Alcohol, Tobacco, Firearms and Explosives (ATF) and ideally should be identical. The firing pin signatures were imaged by a Nanofocus confocal microscope (Fig.2-12). The resulting 3D surface topographies from the two prototype Standard Cartridge Cases are shown on the top of Fig.2-13. These two surface topographies are Gaussian-filtered by λc = 0.25 mm long wavelength cutoff and registered along the X- and Y-directions and rotated around the Z-axis until the maximum correlation position is found, see bottom images left and center. This registration is accomplished via an affine and rigid (rotation and translation) image registration method, as described by Bergen, et al [45]. The multi-scale registration scheme was described further by Heeger [46] and implemented by Heeger as a suite of MATLAB functions [47] that were integrated into our 3D topography measurement software codes. Once registered, the 3D $CCF_{\max}$ is calculated to be 99.29 % (Fig.2-13). Meanwhile, a topography difference $Z_{(B-A)}$ is calculated at this position and shown in the bottom right in Fig.2-13. The signature difference between the two 3D topographies is calculated from Eq.2-2 (3D version) to be $D_s = Sq^2(B-A) \,/\, Sq^2(A)$, = 1.34 % (Fig.2-13).

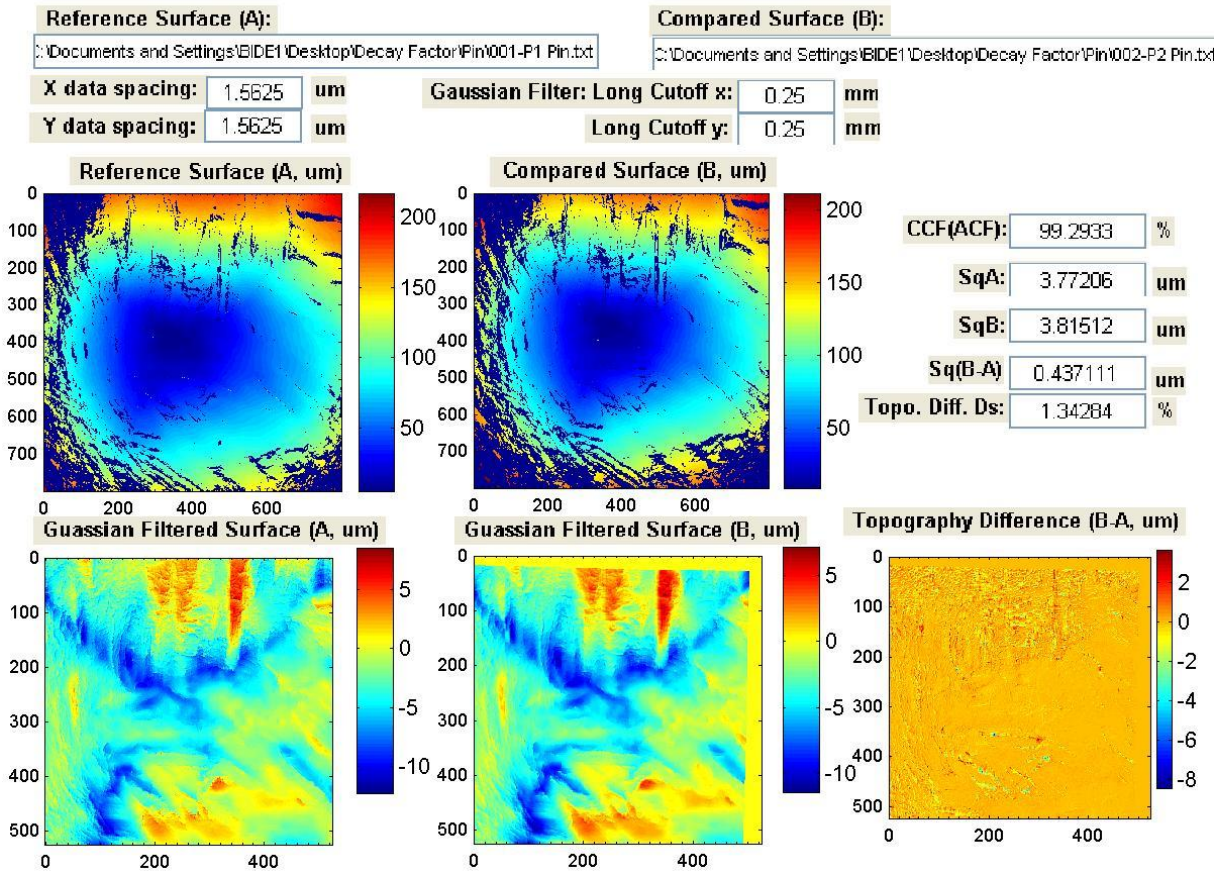

Fig.2-13. Topography correlation of firing pin images between prototype SRM Cartridge Cases #001 (top, left, used here as a reference) and #002 (top, right). The bottom row shows filtered and registered images for #001 (left) and #002 (middle) cartridges and the topography difference (right). CCF_{max} = 99.29 %, D_s =1.34 %.

2.3.4. Advantages of using CCF_{max} and D_s parameters for 2D/3D topography measurements in ballistics identifications and surface metrology

Based on the cross correlation function maximum CCF_{max}, a novel surface parameter called signature difference, D_s (or topography difference for 3D), is proposed for 2D and 3D ballistics signature measurements and comparisons. This parameter and algorithm can be generally used for 2D and 3D surface topography measurement and comparison in forensic science, surface metrology and other areas. These parameters for 2D and 3D topography measurement and comparison have several features [5,18,19]:

- They are easy to understand and use, and are traceable to the length standard.
- The same metric can be used for measurement and comparison of both 2D profiles and 3D topographies.

- Because surface information of all 2D or 3D data points is used for comparison, the parameters have high sensitivity, and can yield high repeatability and reproducibility.
- Although this parameter was developed for the NIST SRM Standard Bullets and Cartridge Case Project, it can be generally used for 2D profiles and 3D topographies measurement and comparisons in surface metrology and other areas.
- For the collection of all 2D profile and 3D topography measurements and comparisons, the minimum signature difference is $D_s = 0$, which occurs when, and only when, these two profiles or topographies are exactly the same. This means that when any two compared 2D profiles or 3D topographies have a signature difference of $D_s = 0$, these two profiles or topographies must be exactly the same (point by point).

2.4. Establish Traceability and Quality System for Nationwide Ballistics Measurements and Identifications

2.4.1. Establish traceability for nationwide ballistics measurements

NIST in collaboration with ATF has developed the SRM 2460 Standard Bullets and SRM 2461 Standard Cartridge Cases to support ballistics signature measurements and correlations for the National Integrated Ballistics Information Network (NIBIN) in the United States [5]. NIST has also developed a 2D and 3D Topography Measurement and Correlation System for ballistics signature measurements [5,18-21]. In 2008, NIST and ATF proposed to establish a National Ballistics Measurement Traceability and Quality System using these physical standards and measurement system.

According to the *International vocabulary of metrology -- Basic and general concepts and associated terms (VIM)* [9], *metrological traceability* is defined as

> *"property of a measurement result whereby the result can be related to a reference through a documented unbroken chain of calibrations, each contributing to the measurement uncertainty."*

From the above definition, three key steps for establishing metrological traceability for ballistics measurements are [25]:

- Establish a reference standard for ballistics signature measurements [5]. The NIST SRM Bullets and Cartridge Cases are used as a reference for both the topography measurements at NIST and the imaging correlations for NIBIN acquisitions at AFT.
- Establish an unbroken chain of calibrations from the national laboratories -- NIST and the National Laboratory Center of ATF -- to local laboratories and customers using the SRM Bullets and Cartridge Cases as reference standards. The unbroken chain of calibration covers both topography measurements at NIST and image correlations at ATF/NIBIN. For topography measurements, the measurement traceability is established using the virtual/physical SRM standard and the proposed parameters D_s and CCF_{max} [5,18,19]. For image correlation systems like IBIS, the traceability is established by image acquisitions of SRM Bullets and Cartridge cases at local IBIS sites, and correlations with the image standard, termed the "Golden Images" (see Figs.2-14 and 2-15) established at the National Laboratory Center of ATF [6,26].
- Evaluate measurement uncertainty and establish a control chart with control limits for quality control of both the topography measurements and imaging correlations [6].

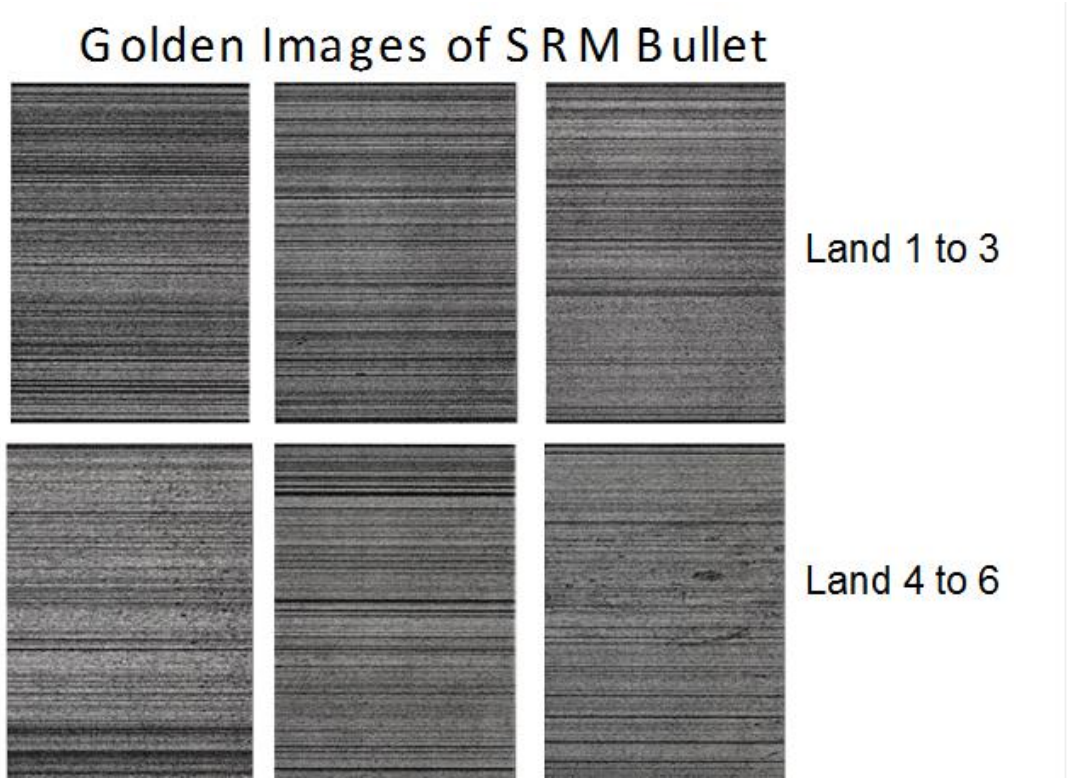

Fig.2-14. The "Golden Image" of six Land Engraved Areas (LEA) of the SRM 2460 Standard Bullet.

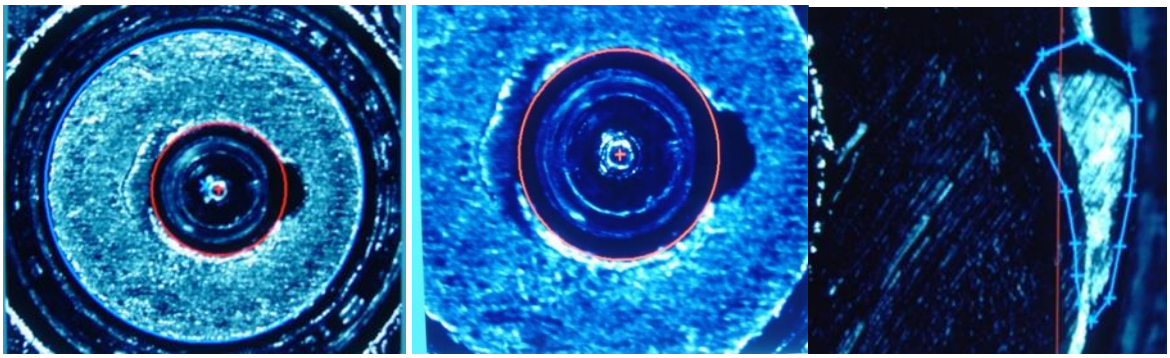

Fig.2-15. The "Golden Image" of the breech face (left), firing pin (middle) and ejector mark (right) of the SRM 2461 Standard Cartridge Case.

A flow diagram for the establishment of a traceability and quality system using the SRM bullets is shown in Fig.2-16 [6]. The six master bullets were profiled by NIST as shown by branch 1. The resulting set of six digitized 2D profile signatures was used as the virtual standard (see Fig.2-16 and Fig.2-3) that determined the tool path of a numerically controlled diamond turning machine at NIST to produce the physical standard of the SRM Bullets. One of them, numbered SRM 2460-001, was kept at NIST as a check standard for measurement quality assurance, as shown in branch 2 of Fig.2-16. Since 2003, this check standard has been routinely measured and correlated with the virtual standard more than 35 times and has demonstrated high measurement reproducibility: all the 2D correlation values $CCF_{\max}$ are higher than 99 % [6]. Fig.2-17 shows the control chart for 35 measurements of LEA 1 of the NIST check standard SRM 2460 Standard Bullet S/N 001. The top line shows the 35 correlation results of $CCF_{\max}$, the bottom line represents the specified (or the fixed) control limit of 95 %. The middle line is a "Dynamic Control Limit" based on the measured data, which was proposed by us and used at NIST for quality assurance of surface calibrations [2]. The Dynamic Control Chart will be discussed in Section 4.2.

Another SRM Bullet, numbered SRM 2460-002, was sent to the National Laboratory Center of ATF as a reference standard. After the topography measurements at NIST, all the SRM Bullets were imaged at the National Laboratory Center of ATF using their reference IBIS system [34] under standard operating conditions [44]. A set of the best images with the highest correlation scores was selected as the "Golden Image" (see Fig.2-14). By acquiring images of the SRM Bullets at local IBIS sites, and correlating the images with the Golden Image, differences in IBIS operating conditions and operators between the local IBIS sites and

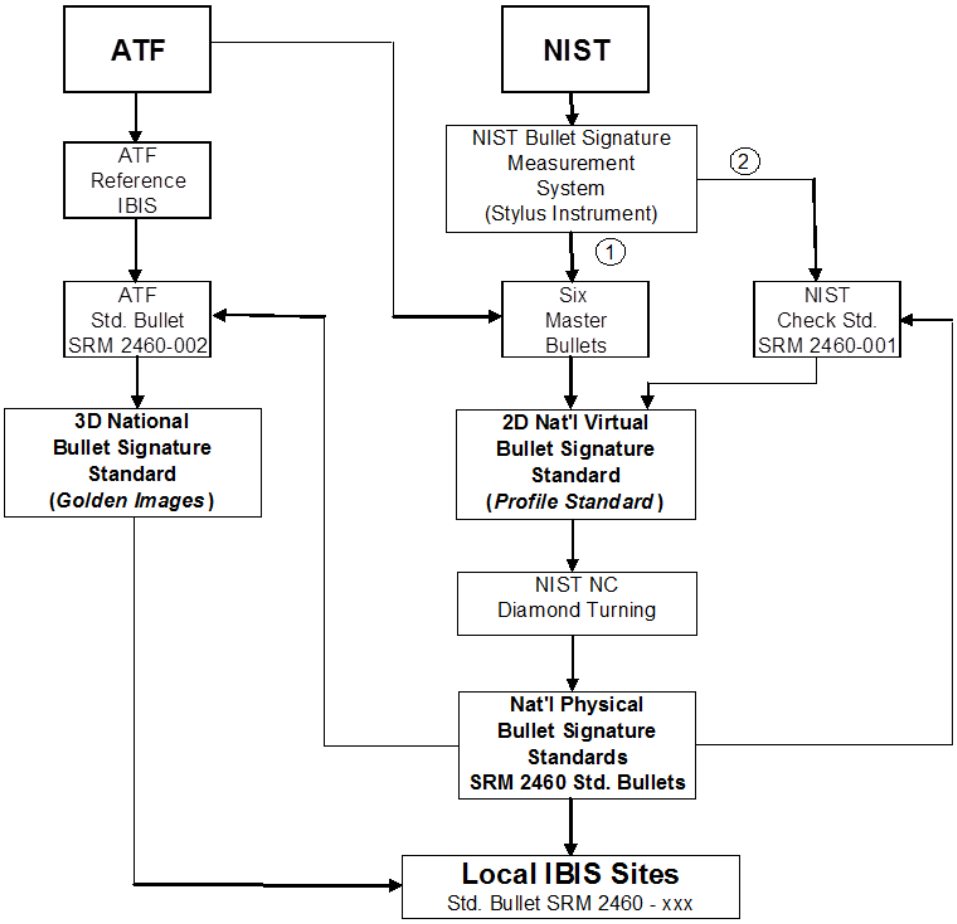

Fig.2-16. Establishment of a Traceability and Quality System for NIBIN acquisitions and correlations.

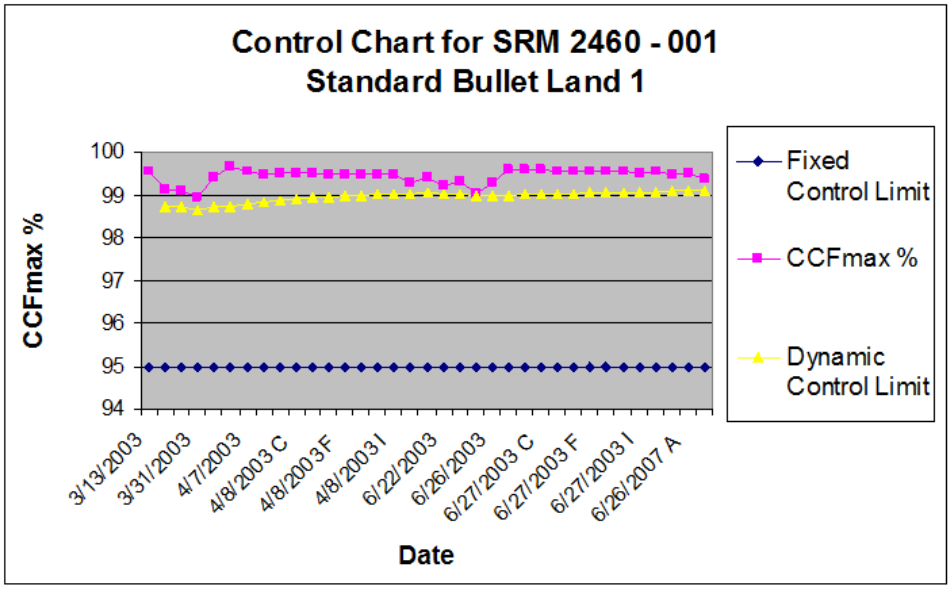

Fig.2-17. A control chart with fixed and dynamic control limits for NIST check standard SRM 2460 Standard Bullet #001 LEA #1.

the National Laboratory Center of ATF can be detected. This system, therefore, can enable both the topography measurements of ballistics signatures at NIST to be traceable to the virtual standard and the SI unit of length, and the image correlations at local IBIS sites to be traceable to the Golden Images of ATF's National Laboratory Center.

A similar approach is used for SRM Cartridge Cases. Fig.2-15 shows the Golden Image established at the ATF's National Laboratory Center for the breech face (left), firing pin (middle) and ejector mark (right) of the SRM Cartridge Cases. The proposed traceability and quality system for SRM Cartridge Cases also includes traceable 3D topography measurements at NIST and image acquisitions and correlations for NIBIN.

2.4.2. Establish a quality system for nationwide ballistics identifications -- The National Ballistics Imaging Comparison (NBIC) Project

During the 2008 NIBIN Users Congress held on June 17th and 18th in Orlando, FL, a protocol for the National Ballistics Imaging Comparison (NBIC) Project was initiated at the first NIST/ATF Workshop, and agreed upon by ballistics experts across the U.S. The project goal is to establish a Traceability and Quality System for ballistics signature correlations in U.S. crime laboratories within the NIBIN. NIST SRM 2460 Bullets and 2461 Cartridge Cases were used as reference standards. By repeating tests of the SRM Bullets and Cartridge Cases at local IBIS sites, and correlating the images with the Golden Images established at the ATF, control charts and control limits were developed for quality assurance of ballistics acquisitions and correlations in NIBIN. The quality assurance system can then be used for detecting and exploring any quality problems arising from operators' acquisition procedures, IBIS systems and correlation networks, as well as from the SRM standards themselves [6].

All participants agreed to use their IBIS for image acquisitions and correlations of their SRM Bullet and SRM Cartridge Case. These tests had three phases [6]:

- **Phase 1 --** Measurement repeatability tests: Ten repeat tests in one or two days on a single SRM Bullet and Cartridge Case by the same IBIS operator under the same measurement setup and the same instrument calibration. Detailed measurement setup and calibration procedure can be found in [6,40,44].

- **Phase 2** -- Short term measurement reproducibility tests: Four weekly tests (including one from the Phase 1 tests) on the same SRM Bullet and Cartridge Case by the same IBIS operator under multiple measurement setups and multiple instrument calibrations.
- **Phase 3** -- Long term measurement reproducibility tests: 12 monthly tests (including one from the Phase 1 tests) on the same SRM Bullet and Cartridge Case by the same IBIS operator under multiple measurement setups and multiple instrument calibrations.

In summary, the protocol called for 24 acquisitions of both a SRM Bullet and a Cartridge Case for each participant over the course of about a year. The correlation scores were entered on a spreadsheet designed by NIST for statistical analyses, from which control charts and control limits were developed for the proposed Traceability and Quality System [6].

19 ballistics examiners from 13 IBIS sites in the United States participated in this project from July 2008 to July 2009. The first set of test data was sent to NIST in September 2008. Based on the data analyses, a feedback report was sent to the participating examiners in October 2008, and discussed at the second NIST/ATF workshop held in New Orleans on January 8th, 2009. After October 2008, significant improvements were observed for some IBIS sites that previously had low IBIS scores before the feedback report.

The second set of test data was sent to NIST between February and March, 2009. The final set of test data was sent to NIST in September 2009. After statistical analyses, some control charts and control limits were developed for the proposed Traceability and Quality System.

The third NIST/ATF Workshop was held from March 23rd to 24th, 2010 in St. Louis to review the overall project and summarize the control charts and control limits [6]. A research paper summarizing this project was published in 2012 [6].

NIST SRM Bullets and Cartridge Cases [5], combined with the use of Control Charts and Control Limits developed by us [2], are powerful tools for quality assurance of NIBIN acquisitions and correlations. During the NBIC project, several quality problems related to the operator and acquisition procedure, the IBIS software and correlation network, as well as the SRM Cartridges themselves, have been successfully identified and corrected. Detailed information can be found in Ref. 6.

2.5. Congruent Matching Cells (CMC) Method -- Theory and Application in Forensic Evidence Identification and Error Rate Estimation

2.5.1. Background

Side-by-side toolmark image comparisons for firearm identification have more than a century's history [27]. However, the scientific foundation of firearm and toolmark identification has been challenged by recent court decisions. As stated in the 2008 and 2009 National Academies Report [28,29]: "*The validity of the fundamental assumptions of uniqueness and reproducibility of firearms-related toolmarks has not yet been fully demonstrated…*" and "*Since the basis of all forensic identification is probability theory, examiners can never really assert a conclusion of an 'identification to exclusion of all others in the world,' but at best can only assert a very small (objective or subjective) probability of a coincidental match…*"

The legal standard for the acceptance of scientific evidence contained in the U.S. Supreme Court decision, called the *Daubert* standard [28], "*places high probative weight on quantifiable evidence that can be tested empirically and for which known or potential error rates may be estimated, such as identification using DNA markers.*" [28] However, as stated in the 2009 National Academies Report [29], "*But even with more training and experience using newer techniques, the decision of the toolmark examiner remains a subjective decision based on unarticulated standards and no statistical foundation for estimation of error rates…*"

Since 1980's, estimates for the probability of a coincidental match have been used for supporting DNA identifications [29]. "*The courts already have proven their ability to deal with some degree of uncertainty in individualizations, as demonstrated by the successful use of DNA analysis (with its small, but nonzero, error rate)*" [29]. It is therefore a fundamental challenge in forensic science to establish a scientific foundation and a statistical procedure for quantitative error rate reports to support firearm identifications, in the same way that reporting procedures have been established for forensic identification of DNA evidences [29].

Our project team has been working on the topography measurement methods and physical standards for ballistic surface characterization [5,6,18-21]. I invented a novel analytical approach in 2013, known as the Congruent Matching Cells (CMC) method [7,31] for ballistic identifications. Basic concepts of the CMC method are discussed in the following sections.

2.5.2. Basic concepts for the CMC method

(A) Valid and invalid correlation region

The correlated surfaces of fired bullets and ejected cartridge cases include "valid" and "invalid" correlation regions [7,31]. The valid correlation region contains individual characteristics [27] of the ballistics signature that can be used effectively for identification. The invalid correlation region does not contain individual characteristics of the ballistics signature, and therefore, should be eliminated from ballistics identification [7,31]. Invalid correlation areas can occur, for example, due to insufficient contact between the firearm surface and the bullet or cartridge case during firing.

Fig.2-18 demonstrates a correlation of two surface topographies A and B originating from the same firearm. The valid correlation region is represented by the superscript ($^{+}$); the invalid correlation region is represented by ($^{-}$). In Fig.2-18, the union symbol "∪" [48] is used to represent the union of two sets of images; the intersection symbol "∩" [48] is used to

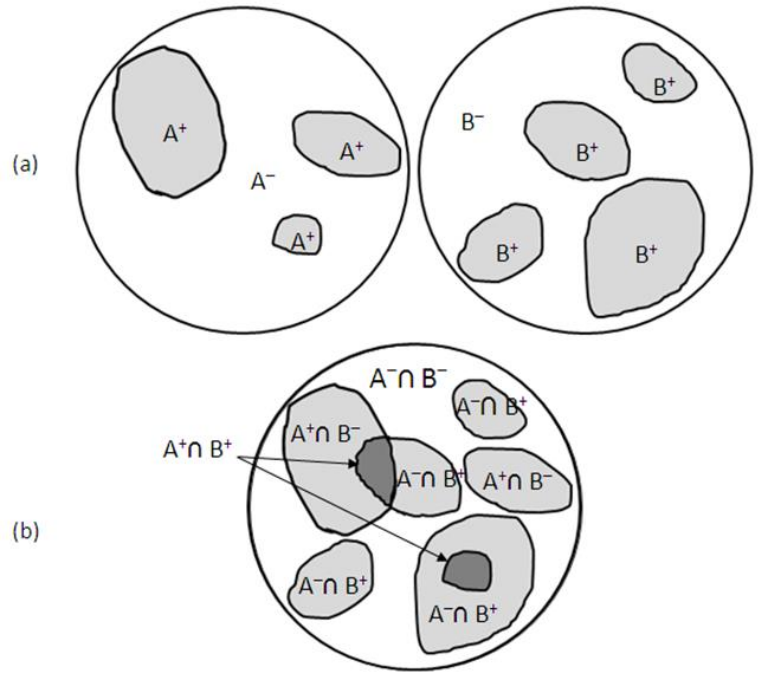

Fig.2-18a shows the valid correlation regions (A+ and B+) and invalid correlation regions (A– and B–) for individual topographies A and B originating from the same firearm. Fig.2-18b shows the common valid correlation regions $[\mathbf{A}^{+} \cap \mathbf{B}^{+}]$ and invalid correlation regions $[(\mathbf{A}^{+} \cap \mathbf{B}^{-}) \cup (\mathbf{A}^{-} \cap \mathbf{B}^{+}) \cup (\mathbf{A}^{-} \cap \mathbf{B}^{-})]$ for a pairwise correlated topography $[\mathbf{A} \cap \mathbf{B}]$.

represent the intersection (or overlap) of two sets of images. For the individual topography A and B, each contains both the valid and invalid correlation regions (Fig.2-18a):

$$A = A^{+} \cup A^{-},$$
$$B = B^{+} \cup B^{-}. \qquad (2\text{-}3)$$

For a pair-correlated topography $[A \cap B]$ (Fig.2-18b):

$$[A \cap B] = [A^{+} \cap B^{+}] \cup [(A^{+} \cap B^{-}) \cup (A^{-} \cap B^{+}) \cup (A^{-} \cap B^{-})], \qquad (2\text{-}4)$$

where $[A^{+} \cap B^{+}]$ represents the common valid correlation region, $[(A^{+} \cap B^{-}) \cup (A^{-} \cap B^{+}) \cup (A^{-} \cap B^{-})]$ represents the invalid correlation region.

(B) Correlation cells

The correlation cell is designed for accurate ballistic identifications of 3D topography signatures. A correlation cell is a basic correlation unit with 1) a "sufficiently small" cell size so that a mosaic of cells can effectively represent the valid correlation region and separate it from the invalid correlation region; and 2) a "sufficiently large" cell size to contain a significant number of peaks and valleys for accurate topography correlations. Both are important for effective and accurate ballistic identifications. By using the correlation cells, the valid correlation region can be identified and the invalid correlation region can be eliminated from correlation. Thus, the correlation accuracy can be increased (see Section 2.5.4).

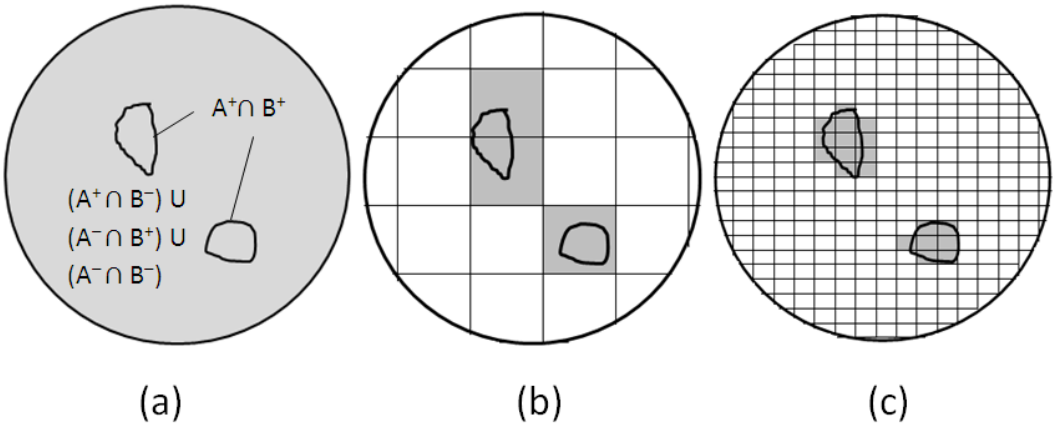

Fig.2-19a shows a pair of topographies $[A \cap B]$ correlated over the whole region including both the valid and the invalid correlation regions. Fig.2-19b shows that the use of correlation cells can eliminate part of the invalid correlation region and increase correlation accuracy. Fig. 2-19c shows the use of smaller correlation cells that can further eliminate the invalid correlation region and increase correlation accuracy.

Fig.2-19a shows a pairwise correlated topography $[A \cap B]$ including both valid correlation regions $[A^+ \cap B^+]$ (as shown by two inside demarcated regions) and an invalid correlation region $[(A^+ \cap B^-) \cup (A^- \cap B^+) \cup (A^- \cap B^-)]$ (as shown by the remaining region). If the correlation is conducted over the whole region, the correlation accuracy represented by the cross correlation function maximum CCF_{max} [18] is likely to be low, because of the large invalid correlation region involved into correlation (see Fig.2-19a). If the correlation region can be divided into correlation cells (see shadowed regions in Fig.2-19b), the cell correlations can be used to identify the valid correlation regions and eliminate the invalid correlation region; the correlation accuracy can thus be increased. If the cell size can be further reduced to a "sufficiently small" but still contains "sufficiently large" topography information for ballistics identification (see shadowed regions in Fig.2-19c), the correlation accuracy can be further increased [7,31].

(C) Cell size

As stated previously, a correlation cell must be "sufficiently small" for high correlation accuracy; but must be "sufficiently large" to contain enough topography features for accurate ballistics identification. In practice, the cell size is experimentally optimized -- not too small and not too large, either may result in low correlation accuracy.

The cell size also depends on the size and shape of the correlated topographies. If the correlation region is large and flat, such as the breech face impression of the cartridge cases, the cell size may be relatively large. If the correlation region is small and contains curvatures, such as the firing pin impression; or if the correlated region contains complex shapes, such as some ejector mark impressions, the cell size may necessarily be smaller.

As a starting point for test of the 9 mm caliber cartridge cases, it is suggested that the cell size for breech face correlations be in the range of (0.25 mm × 0.25 mm) to (0.5 mm × 0.5 mm). Those estimates imply that the number of cells is in the range of about 50 to 200 for the correlations of breech face of 9 mm cartridge cases [7,31].

(D) Identification of the valid and invalid correlation regions using correlation cells

If topographies A and B, originating from the same firearm, are registered at their maximum correlation position (Fig.2-20), the registered cell pairs located in their common valid

correlation regions (as shown by the solid cell pairs A_1, A_2, A_3… and B_1, B_2, B_3…) are necessarily characterized by [7,31]:

- High pairwise topography similarity quantified by the cross correlation function maximum CCF_{max} [18];
- Similar registration angles θ for all correlated cell pairs in topography A and B; and
- A "congruent" *x*-*y* spatial distribution pattern for the correlated cell arrays A_1, A_2, A_3… and B_1, B_2, B_3… or nearly so.

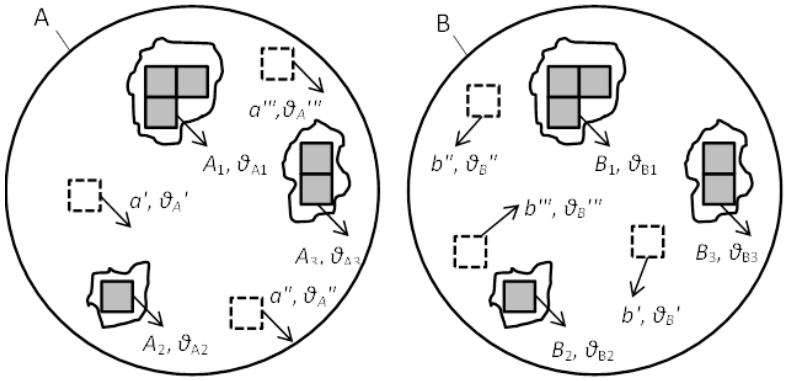

Fig.2-20. Assuming that A and B originate from the same firearm, there are three sets of correlation cells A_1, A_2, A_3 and B_1, B_2, B_3 located in three valid correlation regions $[\mathbf{A}^+ \cap \mathbf{B}^+]$ (as shown by three inside enclosed regions). The other cell pairs *a'*, *a''*, *a'''*… and *b'*, *b''*, *b'''*… are located in the invalid correlation region $[(\mathbf{A}^+ \cap \mathbf{B}^-) \cup (\mathbf{A}^- \cap \mathbf{B}^+) \cup (\mathbf{A}^- \cap \mathbf{B}^-)]$ (as shown by the remaining region). Correlation cells in topography A are used as reference cells for correlation with cells arrays in topography B.

On the other hand, if the registered cell pairs come from the invalid correlation regions of A and B (such as the dotted cells *a'*, *a''*, *a'''*… and *b'*, *b''*, *b'''*… in Fig.2-20), or if the samples originated from different firearms, their cross correlation function values CCF_{max} are likely to be low, and their cell arrays are likely to show significant difference in *x*-*y* distribution patterns and registration angles θ.

2.5.3. The proposed "Congruent Matching Cells (CMC)" method

Congruent matching cell pairs, or CMCs, are therefore determined by three sets of identification parameters: cross correlation value CCF_{max}, registration angle θ, and translation distances in *x* and *y* with corresponding thresholds T_{CCF}, T_θ, T_x and T_y. The correlated cell pairs are considered CMCs -- that is, part of a congruent matching cell pattern -- when their correlation value CCF_{max} is greater than a chosen threshold T_{CCF} and their registration angle θ

and *x*, *y* registration positions, relative to a common reference position, are within the chosen threshold limits T_θ, T_x and T_y.

How many CMC pairs are required so that the overall surface topographies can be identified as matching? As a starting point, we use a numerical identification criterion *C* equal to 6, taking a lead from the method of Consecutively Matching Striae (CMS) developed by Biasotti and Murdock for identification of bullet striation signatures [49-51]. This method has been used internationally for bullet and striated toolmark identifications since 1984 [50].

As a start point for test, the numerical criterion for Consecutively Matching Striae (CMS) method, $C = 6$, is adopted for the proposed Congruent Matching Cells (CMC) method [7,31]:

> *At least C (assuming C = 6 as a start point for test) Congruent Matching Cell (CMC) pairs show high correlation values represented by* $CCF_{max} > T_{CCF}$*; show the "congruent" distribution pattern represented by the same spatial x-y registration positions within the threshold* T_x *and* T_y*; and show the same registration phase angle* θ *within the threshold* T_θ.

2.5.4. Validation tests for the proposed CMC method

An initial validation test of the CMC method was conducted using a set of cartridge cases that had achieved prominence in the firearms identification community when it was produced for a study of visual firearm identifications by ballistics examiners initiated by Fadul *et al.* at the Miami-Dade Crime Laboratory [52]. The set contains 40 cartridge cases ejected from handguns with 10 consecutively manufactured pistol slides (3 slides were used to fire 3 cartridge cases each, 4 slides were used to fire 4 cartridge cases each, and 3 slides were used to fire 5 cartridge cases each). The slide is a component of a semi-automatic pistol firing mechanism that absorbs the recoil impact of the cartridge case onto its breech face. Thus, the surface topography of the slide is impressed onto the breech face of the cartridge case upon impact. Ballistics correlations involving a population of consecutively manufactured gun parts represent the most challenging scenario for testing the capability to accurately identify bullets or cartridge cases as being fired or ejected from the same firearm, because of the increased possibility of the firearm's matching-characteristics of the persistent manufacturing gun parts that could be the basis for false identifications [52]. The surfaces of the slides were finished by sand blasting, a process

used by some firearm manufacturers which produces highly random 3D surface topographies [53]. The objective then for topography measurement and analysis is to distinguish the individual characteristics of the surface impressions from any underlying similarities in consecutively manufactured slides resulting from earlier phases of the manufacturing process, and therefore, yielding a correct conclusion of identification or exclusion with error rate estimation.

The breech face impression topographies on the cartridge cases were measured by a disk scanning confocal microscope (Fig.2-12) and were correlated using the CMC method. A total of 780 correlations (= (40 × (40 – 1)) / 2) were performed, comprising 63 (= 3×3 + 4×6 + 3×10) known matching (KM) and 717 (= 780 – 63) known non-matching (KNM) image pair comparisons [8,32]. Note that these correlations are not completely independent because each image of the 40 cartridge cases may correlate with KM and KNM images with different sample sizes, but the total sample size is same.

The original images have a nominal pixel spacing of 3.125 μm, but the pixel spacing is increased to 6.25 μm for fast correlation tests. The root mean square instrument noise in the vertical direction was approximately 3 nm. Before correlating, the images were trimmed to extract the breech face impression of interest. The images were bandpass filtered to reduce noise with short wavelengths cutoff λs = 0.016 mm and to remove surface form and waviness with long wavelengths cutoff λc = 0.25 mm, thus highlighting individual characteristics. The cell size for the set of correlation tests was chosen to be 470 μm by 470 μm, and the range of relative cell registration angles was restricted to ±30° with respect to their initial orientation [8].

One set of validation test results is shown in Fig.2-21. The nominal number, N_{nom}, of compared cell pairs for each topography correlation equals 49 (for a 7 × 7 cell array). The number N of compared effective cell pairs for each correlation, i.e. cell pairs containing a reasonable number of pixels, depends on the common domain of each topography pair. On average for this study, 26 cell pairs were correlated for each image correlation. The cell size a, the pixel spacing, and the thresholds T_{CCF}, T_{θ}, T_x and T_y are shown on the upper right side of Fig.2-21. The number of congruent matching cell pairs (CMCs) for the 63 KM topography pairs ranges from 9 to 26; while the number of CMCs for all 717 KNM topography pairs ranges from 0 to 2.

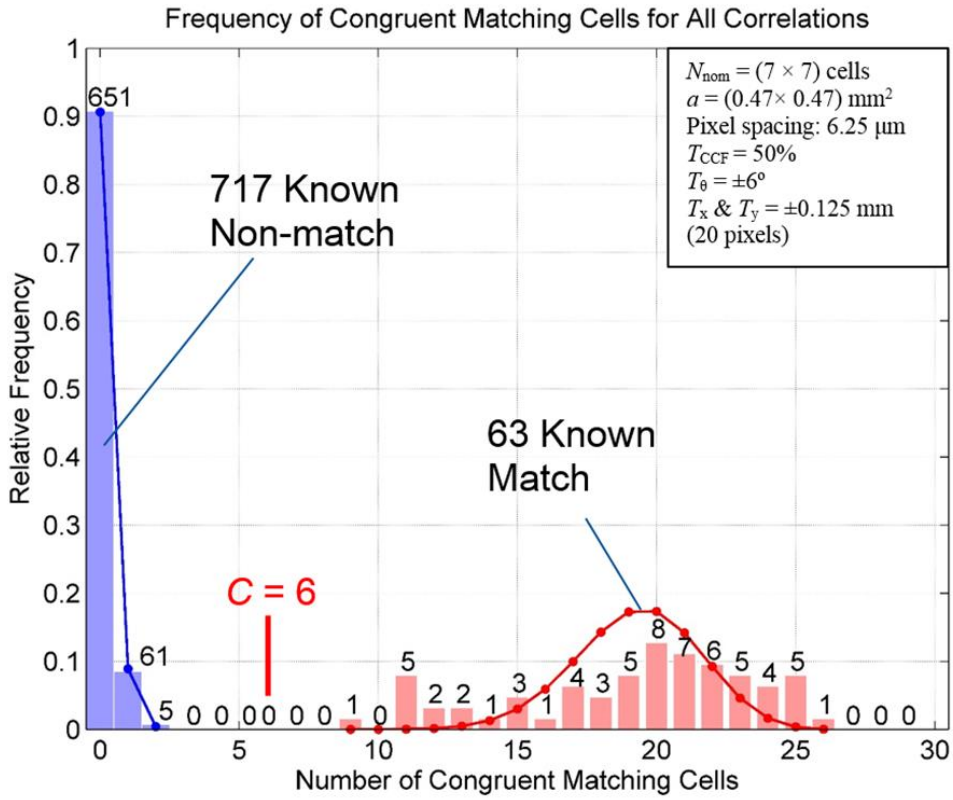

Fig.2-21. Relative frequency distribution of CMC numbers for KM and KNM image pairs. For the 63 KM cartridge pairs, the CMC ranges from 9 to 26. For the 717 KNM cartridge pairs, the CMC ranges from 0 to 2. The curves represent the statistical fitting of theoretical binomial distributions Ψ_{CMC} (blue) calculated by Eq.2-6 and the values of Φ_{CMC} (red) calculated by Eq.2-8. Note that the distribution models are discrete histograms, with the connecting lines drawn for visualization.

Of the 717 KNM image pairs, 651 pairs have CMC = 0 (no congruent matching cells). There are only five non-matching topography pairs that have two congruent matching cells, i.e. CMC = 2 (Fig.2-21), one of them is shown in Fig.2-22A. For the 63 KM topography pairs, only one topography pair has CMC as low as 9 (Fig.2-21), this topography pair is shown in Fig.2-22B. All the other KM topography pairs have CMC number ranging from 11 to 26 (Fig.2-21) [8].

There is a significant separation between the KM and KNM distributions without an overlap (Fig.2-21). Additional tests using different correlation parameters and slightly different versions of correlation software also show similar results without an overlap [32,33]. In standard binary classifier terms the results indicate both high sensitivity and specificity [54] and suggest the feasibility of using the CMC method for firearm identifications. The identification accuracy can likely be improved further by optimizing the image processing, cells size, parameter threshold values, and by using finer registration intervals [8,32,33].

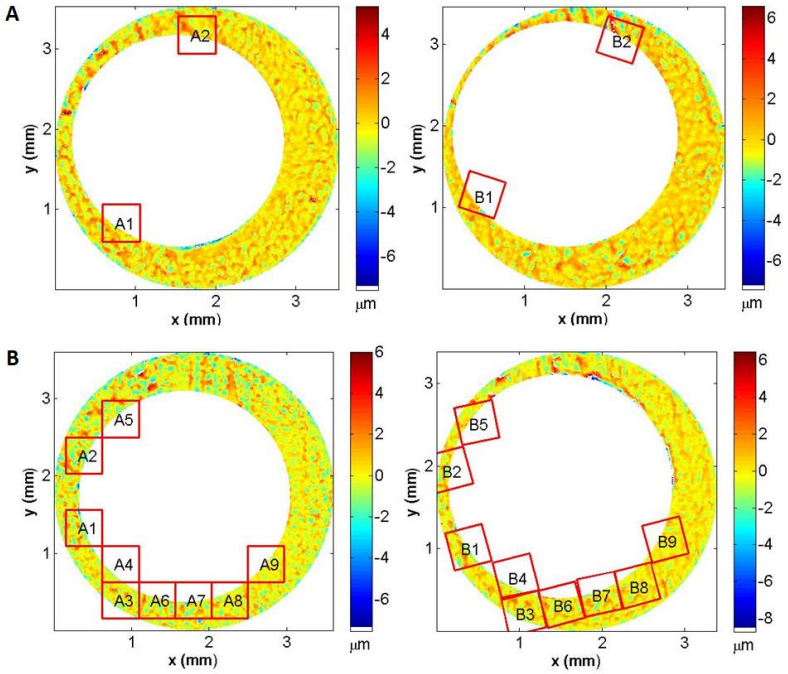

Fig.2-22. Depiction of congruent matching cells for two sets of correlated topography pairs: for the 717 KNM topography pairs, only five pairs have a CMC value as high as 2, one of these image pairs is shown in (A). For the 63 KM topography pairs, only one has a CMC value as low as 9, that pair is shown in (B).

2.5.5. Error rate estimation using the CMC method

The large number of correlation cells associated with the multiple correlation parameters for each correlated cell pair of the CMC method lead to a statistical approach to calculating error rates, that is, the probability that a positive identification is actually false (false positive) and the probability that an exclusion from identification is actually false (false negative). Two types of error rates are of interest. The cumulative error rate represents the expected error rate for a large number of statistical samples with similar characteristics. The individual error rate represents the probability of a coincidental conclusion for a particular comparison result, for example, the probability of a correlation of CMC = 15 yielding "match" conclusion is actually originated from a non-matching image pair [7,8].

The initial approach proposed to estimate error rates was to make the approximation that the probability of a false positive (P_1) is the same for all non-matching cell pairs, and that the probability of a false negative (P_2) is the same for all matching cell pairs [8]. P_1 and P_2 are estimated from experimental distributions of correlated cell pairs of KM and KNM topographies [7,8]. Fig.2-23 shows the experimental frequency distributions of correlated cell

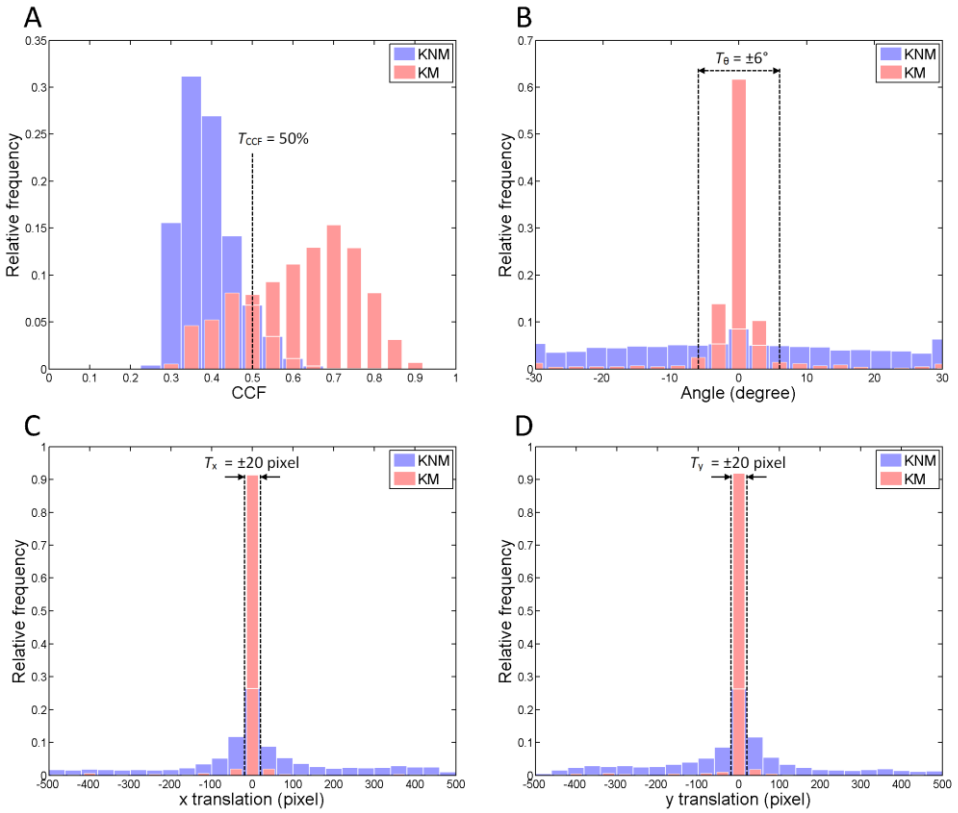

Fig.2-23. Experimental relative frequency distributions of the correlated cell pairs for the KM (pink) and KNM (blue) topographies with respect to different identification parameters: A) CCF_{max} with a threshold T_{CCF} = 50%; B) θ with T_θ = ±6°; C) x with T_x = ±20 pixels (or ±0.125 mm); and D) y with T_y = ±20 pixels (or ±0.125 mm). The KM (63 pairs) and KNM (717 pairs) distributions are each scaled to their particular sample size.

pairs for KM (pink) and KNM (blue) topographies with respect to four specification parameters CCF_{max} (Fig.2-23A), registration angle θ (Fig.2-23B) and registration distances in x and in y (Fig.2-23C and D) [8]. The thresholds T_{CCF}, T_θ, T_x, and T_y are also shown. Although there are large overlaps between the KM and KNM cell distributions for each parameter CCF_{max}, θ, x and y, combining all four parameters yields a significant separation between the CMC distributions of KM and KNM image pairs (Fig.2-21).

The combined false positive and false negative probabilities, P_1 and P_2, for each correlated cell pair can be estimated by a combination of the experimental false positive and false negative identification probabilities associated with each of the four identification parameters (CCF_{max}, θ, x and y), taking into account of any cross-correlations between them. For the finite 40 cartridge data set here, P_1 and P_2 can be estimated by conditional probabilities one parameter at a time [7,8]. First, the number of KNM cell pairs that pass the T_{CCF} threshold (CCF_{max} >

50%) are counted and compared with the total number of correlated cell pairs to derive the individual probability $P_{1(CCF)}$ (see Tab.2-1). Then only the cell pairs passed the T_{CCF} test are included in the probability distribution for the next test of parameter θ, from which the conditional probability $P_{1(\theta|CCF)}$ is estimated, and so on. The individual false positive and false negative identification probabilities associated with all thresholds estimated in this way are shown in Tab.2-1.

Tab.2-1. The combined false positive and false negative identification probabilities, P_1 and P_2, for each correlated cell pair are estimated from the individual false positive and false negative identification probabilities of each identification parameter, which are estimated from the experimental distributions of the correlated cell pairs of the KM and KNM topographies by a conditional probability test method.

Correlation parameters and thresholds		**Individual false positive and false negative identification probabilities**	
CCF_{max}, T_{CCF} > 50%		$P_{1(CCF)}$ = 0.0782	$P_{2(CCF)}$ = 0.2322
θ, T_θ <	±6°	$P_{1(\theta\|CCF)}$ = 0.2673	$P_{2(\theta\|CCF)}$ = 0.0200
X, T_x <	±125 μm (±20 Pixels)	$P_{1(x\|CCF,\theta)}$ = 0.3604	$P_{2(x\|CCF,\theta)}$ = 0.0098
Y, T_y <	±125 μm (±20 Pixels)	$P_{1(y\|CCF,\theta,x)}$ = 0.5000	$P_{2(y\|CCF,\theta,x)}$ = 0.0049
Combined false positive and false negative identification probability P_1 and P_2		**P_1 = 0.003765**	**P_2 = 0.2586**

The overall identification probabilities P_1 and P_2 can be estimated by combining the conditional probabilities described above. The combined false identification probability P_1 for each KNM cell pair is the probability that all four individual identification parameters are positive, that is, the CCF_{max} result is above the threshold and the three spatial parameters are within the chosen threshold limits. P_1 can be estimated by:

$$P_1 = \prod_{i=1}^{i=4} P_{1(i)} = P_{1(CCF)} \times P_{1(\theta|CCF)} \times P_{1(x|\theta,CCF)} \times P_{1(y|x,\theta,CCF).} \qquad (2\text{-}5a)$$

Conversely, the combined false exclusion probability P_2 for each KM cell pair is the probability that any of the four individual identification parameters (and/or their combinations) incorrectly yields a non-matching result:

$$P_2 = 1 - \prod_{i=1}^{i=4}\left[1 - P_{2(i)}\right]$$
$$= 1 - \left[\left(1 - P_{2(CCF)}\right)\times\left(1 - P_{2(\theta|CCF)}\right)\times\left(1 - P_{2(x|\theta,CCF)}\right)\right.$$
$$\left.\times\left(1 - P_{2(y|x,\theta,CCF)}\right)\right] \qquad \text{(2-5b)}$$

The probabilities, P_1 and P_2, for individual cells are then inserted into a binomial distribution model to estimate the cumulative false positive and false negative error rates for the entire set of cartridge cases. Fig.2-24 shows a schematic diagram of a conceptual model for two CMC distribution density (probability mass) functions, Φ_{CMC} and Ψ_{CMC}, for KM and KNM topography pairs, respectively. The distribution density Ψ_{CMC} for KNM correlations with CMC variable h can be modeled with the binomial distribution (N, P_1) [55], with probability mass function:

$$\psi_{(CMC=h)} = C_N^h \cdot (P_1)^h \cdot (1 - P_1)^{N-h}\,, \qquad \text{(2-6)}$$

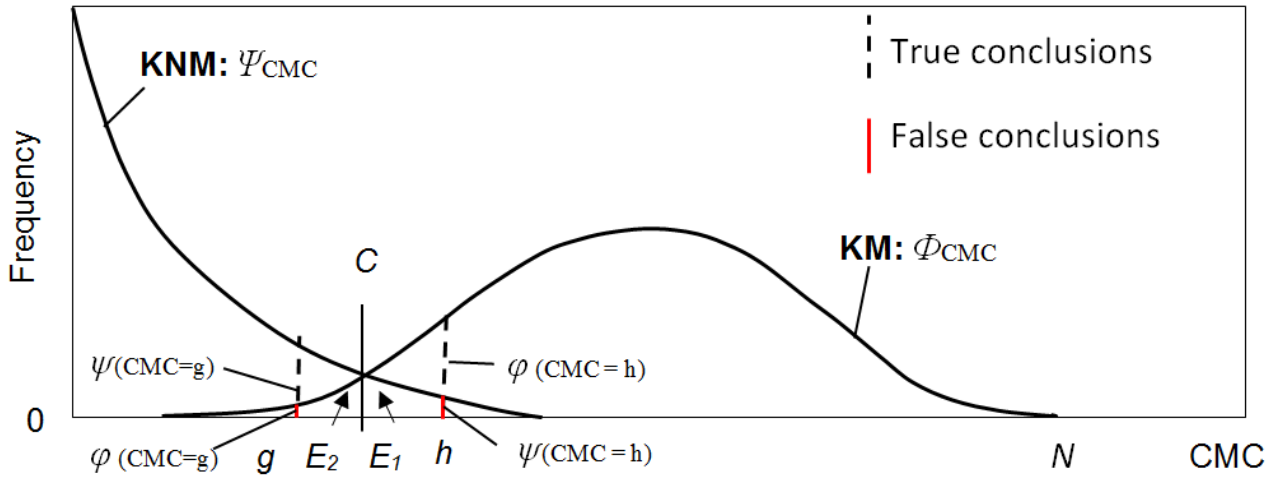

Fig.2-24. Schematic diagram of the CMC distribution functions for correlated KM and KNM topographies, Φ_{CMC} and Ψ_{CMC}. The regions E_1 and E_2 under the curves represent cumulative false positive (false identification) and false negative (false exclusion) error rates. For each individual "matching" identification determined by $h \geq C$ and each "non-matching" exclusion determined by $g < C$, there are likelihoods for both "True" and "False" conclusions as demonstrated by the black dotted bars and the red bars, respectively.

where $C\,{}_N^h = N!/((N-h)!\,h!)$ is the number of combinations of h out of N elements. For the P_1 value estimated earlier, the Ψ_{CMC} distribution curve is plotted in Fig.2-21 (blue line with CMC ranging from 0 to 2).

The cumulative false positive error rate E_1 is given by the sum of the probability mass function Ψ_{CMC} for CMC values between C and N:

$$E_1 = \sum_{CMC=C}^{CMC=N} \psi_{(CMC)} = \psi_{(CMC=C)} + \psi_{(CMC=C+1)} + \cdots + \psi_{(CMC=N)}$$
$$= 1 - \left(\psi_{(CMC=0)} + \psi_{(CMC=1)} + \cdots + \psi_{(CMC=C-1)}\right), \qquad (2\text{-}7)$$

where the cumulative false positive error rate E_1 is determined by three factors: the effective number of correlation cells N in a correlation; the numerical identification criterion C of the CMC method (C = 6); and the combined false positive identification probability P_1 of each correlated cell pair estimated from Eq.2-5a.

Similarly, the distribution of Φ_{CMC} for KM images (Fig.2-24) with CMC variable g can also be modeled with the binomial distribution (N, $1 - P_2$) [7,8,55], with probability mass function

$$\varphi_{(CMC=g)} = C_N^g \cdot (1-P_2)^g \cdot (P_2)^{N-g}. \qquad (2\text{-}8)$$

For the P_2 value estimated earlier, the Φ_{CMC} distribution curve is plotted in Fig.2-21 (red line with CMC ranging from 9 to 26). The cumulative false negative error rate E_2 is the sum of the discrete probability mass function Φ_{CMC} for CMC values between 0 and (C – 1):

$$E_2 = \sum_{CMC=0}^{CMC=C-1} \varphi_{(CMC)} = \varphi_{(CMC=0)} + \varphi_{(CMC=1)} + \cdots \varphi_{(CMC=C-1).} \qquad (2\text{-}9)$$

Based on Eqs.2-7 and 2-9, the cumulative false positive and false negative error rates E_1 and E_2 are estimated using the average effective cell number N = 26 and the combined false positive and false negative identification probabilities P_1 and P_2 (Tab.2-1). The results are shown in Tab.2-2. For the 717 KNM comparisons, the cumulative false positive error rate is $E_1 = 6.2\times 10^{-10}$, which represents the sum of φ_{CMC} values between 6 and N. The cumulative false negative error rate is $E_2 = 7.4\times10^{-09}$, which represents the sum of the ψ_{CMC} values between 0 and 5.

Tab.2-2. Estimated cumulative false positive and false negative error rates E_1 and E_2 based on the set of 780 cartridge image pairs with average effective cells N = 26. Also shown are the individual identification probabilities R_1 at selected CMC values of 9 and 26 and the individual exclusion probabilities R_2 at selected CMC values of 0 and 2. The maximum individual identification (false positive) probability is $R_{1\,(CMC\,=\,9)} = 2.3\times10^{-10}$.

CMC	E_1	E_2	$\varphi_{(CMC)}$	$\psi_{(CMC)}$	$R_{1(CMC)}$	$R_{2(CMC)}$
0			5.3×10^{-16}	0.91		5.2×10^{-17}
2			1.4×10^{-12}	4.2×10^{-03}		3.0×10^{-11}
CMC < 6		7.4×10^{-09}				
9			2.2×10^{-05}	4.5×10^{-16}	2.3×10^{-10}	
26			0.00042	9.3×10^{-64}	2.5×10^{-59}	
CMC ≥ 6	6.2×10^{-10}					

2.5.6. Surface and topography metrology support firearm evidence identification

The field of firearms identification is more than 100 years old and the field of surface metrology is at least 80 years old, but the combination of the two -- using surface topography measurements and correlations for identification of fired bullets and cartridge cases -- has only been around for about 15 years. The combined field is so new that current firearm identifications at crime labs for bullets or cartridge cases are still performed manually by experts in optical (side-by-side) comparison microscopes, and the conclusion of a “match” or ‘non-match” is mainly based on experts’ experience. Nevertheless, this interdisciplinary field brings a vision that one day firearm related investigations and identifications might be accomplished or affirmed through database searches using topography data of the ballistics evidence and automated correlation programs. Further, a conclusion that certain firearm evidence is a match or a non-match could include an uncertainty (or error rate) report.

Reporting error rate for firearm identification is a fundamental challenge in forensic science [28,29]. NIST researchers have developed for the first time a statistical foundation and a practical method to estimate an error rate [7,8], demonstrated on a set of cartridge cases ejected from handguns with consecutively manufactured pistol slides [8,32,33]. Although small, this type of sample presents a challenging and pioneer test for firearms identifications and experts.

The CMC method has been tested by a different set of consecutively manufactured firearms with large sample size (95 slides with 4465 image pairs) with good correlation results [8].

It must be emphasized that the estimated error rate numbers are specific to the particular set of firearms and are not meant to be applicable to other firearm scenarios. However, the error rate assessment procedures can be adapted, with refinements and model adjustments for specific situations, to provide scientific support and error rate estimates for other firearm identification scenarios [8], including large scale databases, in a manner similar to the Coincidental Match Probability (CMP) procedures developed for DNA identifications [29].

The CMC method may also serve as a foundation for manufacturers to develop the Next Generation Ballistic Identification Systems characterized by high accuracy and error rate reporting, which would represent a decided advance over current automated ballistic identification systems. In September 2013, a U.S. manufacturer, Leeds Forensic Systems, Inc. located in Minneapolis, MN, sent an email to NIST: "***We feel, the Error Rate Software based on the Congruent Matching Cell theory could revolutionize the science of firearms comparison, and we wanted a license to sell it…***" [56]. Based on the NIST invented CMC method, the Leeds Forensic Systems, Inc. has developed the next generation ballistics identification system called ***CaseHitter*™,** which has been demonstrated at the 2015 Association of Firearm and Tool-mark Examiners (2015 AFTE) meeting in May 2015, Dallas, TX. At the cover page of the software, it shows: "***This software is based on the CMC (Congruent Match Cells) method and Error Rate Procedure invented by NIST.***"

It can be expected when ballistic examiners input topography or optical intensity images into a program that automatically conducts correlations using the CMC method, and displays the correlation conclusion (matching or non-matching) with an error rate report [8]. The NIST invented CMC method and statistical procedure can provide a scientific foundation and a practical method to estimate error rates for ballistic identifications in court proceedings. An error rate procedure could also be used for laboratory assessment and accreditation in accordance with the ISO 17025 standard [57] and ASCLD/LAB procedures [58].

Chapter 3. Other Applications of 2D and 3D Topography Measurements

Besides firearm evidence identifications, 2D and 3D topography measurements can also be used in other fields such as instrument characterization and production quality control. This chapter introduces my work using 2D topography measurements for instrument comparison of four surface instruments based on different techniques, and 3D topography measurements for determining the "decay factor" of the electro-forming technique for surface duplication and for production quality control of SRM Standard Cartridge Cases.

3.1. 2D Topography Metrology for Instrument Characterization

A traditional question in surface metrology is: when different surface instruments are used to measure the same surface, do they get the same results? And if not, why? [1]

Fig.3-1 shows signature profiles of the No. 1 land impression on the SRM 2460-001 Standard Bullet measured by four instruments with different techniques (profile 2 to 5), and compared with the profile of the virtual standard traced on the ATF's master bullet by a stylus instrument (profile 1) [22]. Profile 2 is traced by a stylus instrument, and correlated with the virtual standard (profile 1). The correlation result is $CCF_{\max}$ = 99.6 %. Profile 3 is traced by an interferometric microscope; the correlation result is $CCF_{\max}$ = 92.1 %. Profile 4 is traced by a Nipkow disk confocal microscope, the correlation result is $CCF_{\max}$ = 99.0 %. Profile 5 is traced by a laser scanning confocal microscope, the correlation result is $CCF_{\max}$ = 95.3 %. The $CCF_{\max}$ differences came from many factors [22], of which the instrument noise and image stitching technique of different instruments were certainly important factors for instrument characterization.

It was suggested that the reference standards, comparison parameter and measurement system developed from the NIST Standard Bullets and Cartridge Cases project could be generally used in surface metrology for 2D and 3D topography comparisons and instrument characterization. However, it must be noted that the repeatability and reproducibility tests mentioned above were performed by three different operators at three different laboratories. The method divergence and environment variations are certainly among the factors which affect the test results [22].

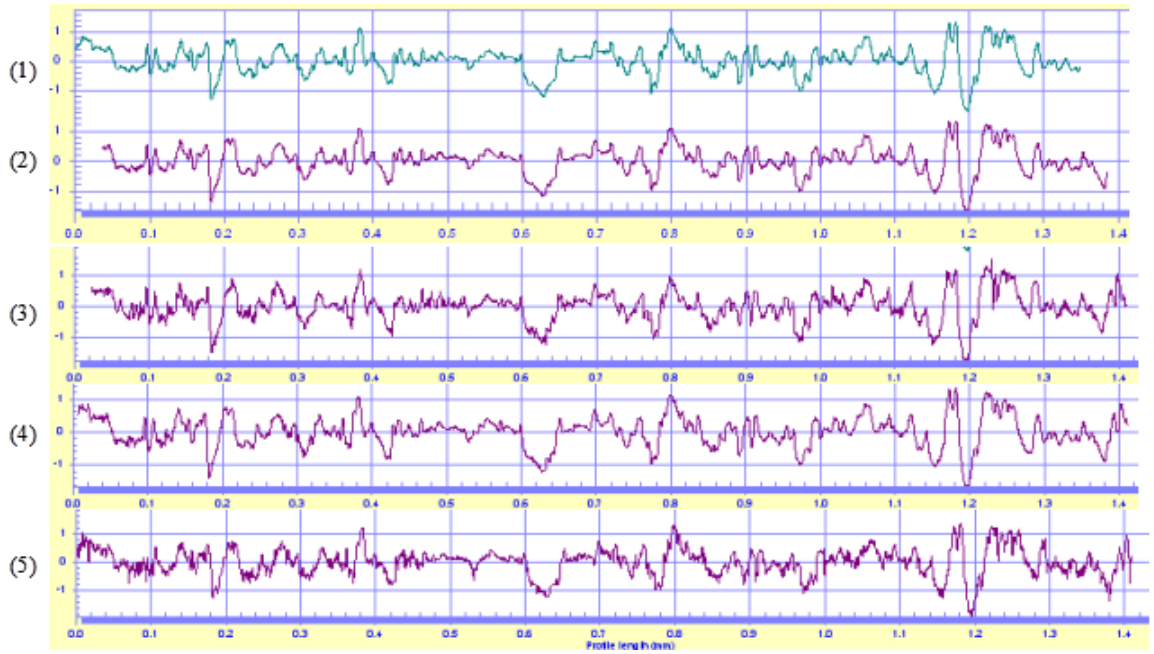

Fig.3-1. The signature profile of the #1 land impression of SRM 2460-001 Standard Bullet was measured by four techniques (profile 2 to 5) and correlated with the profile of the virtual standard traced by a stylus instrument on the ATF's master bullet (profile 1). Profile 2 was traced by the stylus instrument, CCF_{max} = 99.6 %. Profile 3 was traced by an interferometric microscope, CCF_{max} = 92.1 %. Profile 4 was traced by a Nipkow disk confocal microscope, CCF_{max} = 99.0 %. Profile 5 was traced by a laser scanning confocal microscope, CCF_{max} = 95.3 %.

3.2. 3D Topography Measurements for Determination of the Decay Factor for Surface Duplication Using Electro-Forming Technique

In order to ensure that the SRM Cartridge Cases are produced with virtually the same surface topography as the master, it is necessary to test the decay factors of the replication process, and design an optimum plan for the production of a large amount of SRM Cartridges with maximum uniformity of surface topography [23].

Two decay factors, called the horizontal and vertical decay factors α and β, are defined and tested. The horizontal decay factor α is defined for quantifying topography decay among specimens replicated one after the other from the same master. The vertical decay factor β is defined for quantifying topography decay among specimens produced from one generation to the next [23].

Twenty-six replica cartridge cases were replicated from the same master cartridge provided by ATF. 17 of these cartridges (#001 to #017) were replicated from the same negative replica, and

were used for the tests of the horizontal decay factor α (Fig.3-2). The remaining nine positive replica cartridges (#019 to #035) were nine successive generations from the same master, and were used for the tests of the vertical decay factor β (Fig.3-2) [23].

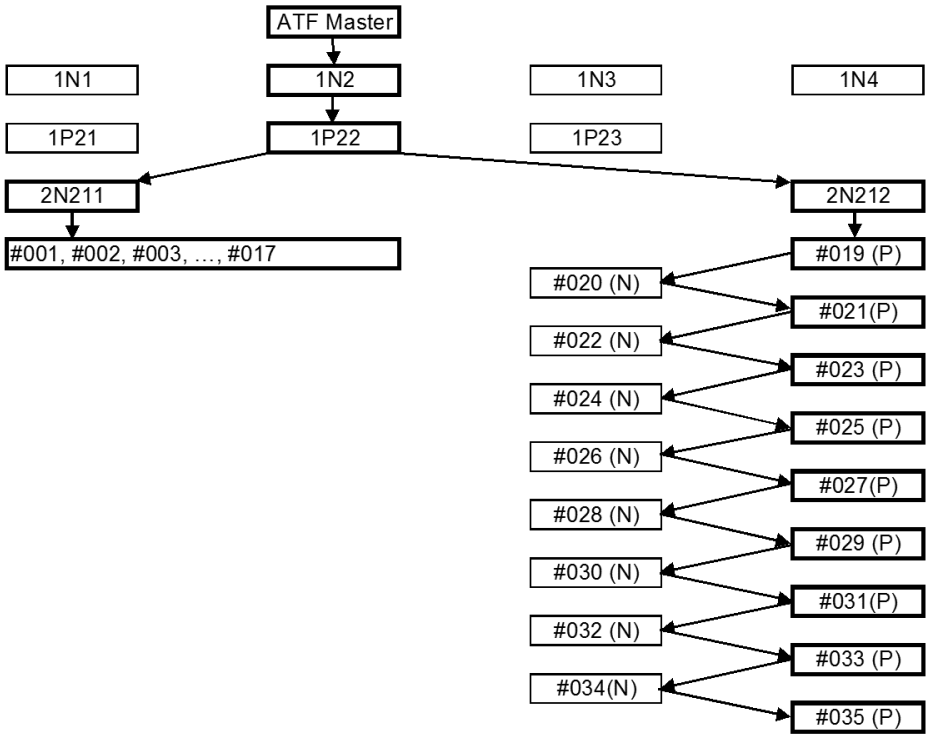

Fig.3-2. Design for horizontal and vertical decay factor tests.

Fig.3-3(a) shows the test result for the horizontal decay factor α. The No. 1 replica was used as a reference, against which the successive 16 casings were correlated. A linear least squares fitting was used for approximating the exponential decay function. The resulting horizontal decay function is [23]:

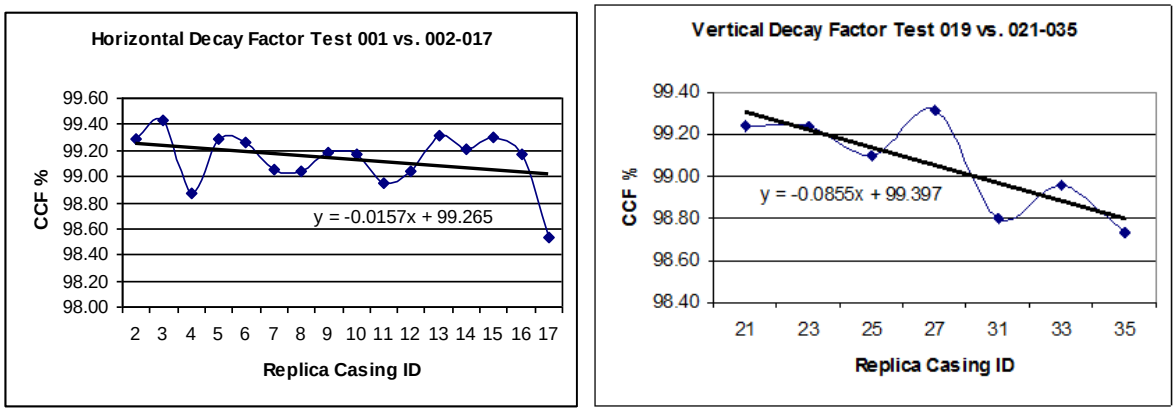

Fig.3-3. Horizontal (a) and vertical (b) decay factor test results.

$$H_d\,(i) = -\,0.0157\ \% \times (i-1) + 99.26\ \%\ CCF_{\max}\ (i = 2 \text{ to } 17). \qquad (3\text{-}1)$$

Where i represents the number of the replica casing (from 2 to 17); α is 0.0157 % $CCF_{\max}$ per replication. The term 99.26 % $CCF_{\max}$ approximates the pre-exponential factor which biased slightly from the perfect topography with 100 % $CCF_{\max}$. The cross correlation function maximum, $CCF_{\max}$, is used here as a quantitative parameter for the similarity of topography comparisons [18,19].

Fig.3-3(b) shows the test result for the vertical decay factor β of the nine generations of replica cartridges. The first replica (No. 19) was used as a reference, against which the successive eight generation cartridges were correlated. There was a damage shown on the surface of the sixth-generation replica (No. 29). Thus, the $CCF_{\max}$ value ($CCF_{\max}$ = 96.84 %, see Fig.3-4) had significant difference from the others. This data was considered as flawed data and was removed from the tests. The remaining seven cartridges are correlated with the reference. After linear least squares fitting, the vertical decay function is [23]:

$$V_d\,(j) = -\,0.0855\ \% \times (j-1) + 99.40\ \%\ CCF_{\max}\ \ (j = 2 \text{ to } 8). \qquad \mathbf{(3\text{-}2)}$$

Where j represents the generation number of the replica casings (from 2 to 8); β is 0.0855 % $CCF_{\max}$ per generation.

From Eqs.3-2 and 3-3, it can be seen that the vertical decay factor, β = 0.0855 %, is more than five times as large as the horizontal decay factor, α = 0.0157 %. Therefore, it is important to reduce the generation-to-generation replications as much as possible during the production process.

For the NIST SRM 2461 Standard Cartridge Case project, it was planned to produce 256 SRM casings from the same ATF master casing with $CCF_{\max}$ higher than 95 %. Based on the decay factors, we estimated the topography decays for two production plans. The first one, called "16 × 16", uses the ATF master to make 16 negative replicas, and then, uses each negative replica to make 16 SRM casings. The $CCF_{\max}$ for the last SRM casing is estimated as (97.37 ± 0.20) % [23]. The uncertainty (k = 1) is a Type A standard uncertainty derived from the parameter fitting to the data of Fig.3-3. The second plan, called "4 × 4 × 4 × 4", uses the ATF master to produce 4 negative replicas; and then, uses each negative replica to make 4 positive replicas; again, uses each positive replica to make 4 negative replicas; and finally, uses each negative replica to

make 4 SRM casings. The CCF_{max} for the last SRM casing is calculated as CCF_{max} = (96.01 ± 0.25) % (also k = 1) [23]. Both plans can produce 256 SRM casings with CCF_{max} values higher than 95 %.

Based on the production plan, 137 SRM 2461 cartridge cases were produced so far and certified for forensics / crime scene investigations [40]. Fig.2-7 (left) shows a SEM 2461 standard cartridge case which is mounted on a brass cylinder holder. Fig.2-7 (right) shows a SRM cartridge case (left) and three certified areas (right) of the breech face impression (BF), firing pin impression (FP), and ejector mark (EM).

3.3. 3D Topography Measurements for Production Quality Control of SRM Cartridge Cases

When the 3D topography measurement system was used for determining the "decay factors" of the replication process of the SRM Standard Cartridge Cases, it was found that there was one set of correlation data from the #29 replica showed questionable results (see Fig.3-4). For the No. 29 replica, the CCF_{max} value (96.84 %) showed significant difference (out of ±2σ range) from the others, because there was a damage showing on the surface of the No. 29 replica. This data was considered as flawed data and was removed from the tests. Fig.3-5 shows a comparison between the No. 29 replica's image and the reference image of the No. 1 cartridge.

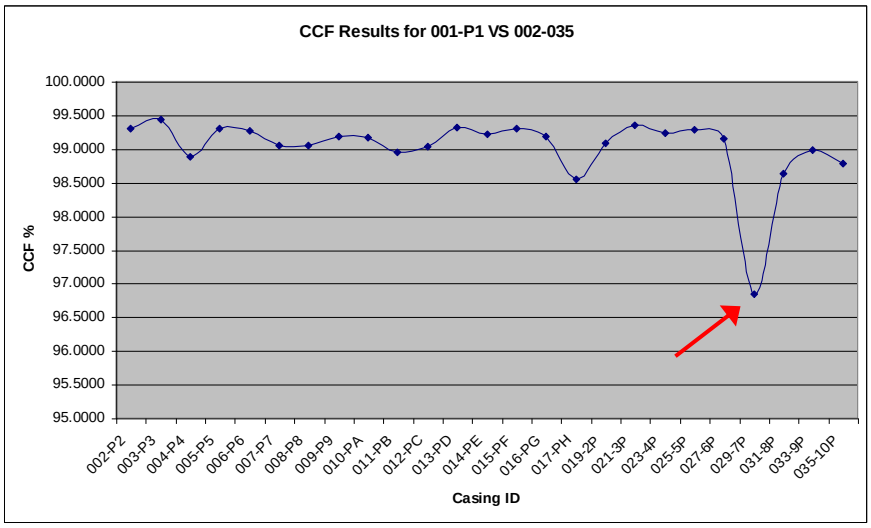

Fig.3-2. The No. 29 replica showed significant difference from the others, the CCF_{max} value is 96.84 %.

There is a surface defect on the surface of No. 029 replica casing, as shown at the middle and right images of the bottom row, resulting the $CCF_{\max}$ value dropping to 96.84 %.

When comparing Fig.3-5 with Fig.2-13 which shows a comparison of No. 2 vs. No. 1 cartridges with $CCF_{\max}$ = 99.29, it can be seen that the CCF_{max} value is very sensitive to the surface defect, and therefore, this suggests that the CCF_{max} parameter and the topography measurements can be used for test of surface defects for quality control of production lines [19].

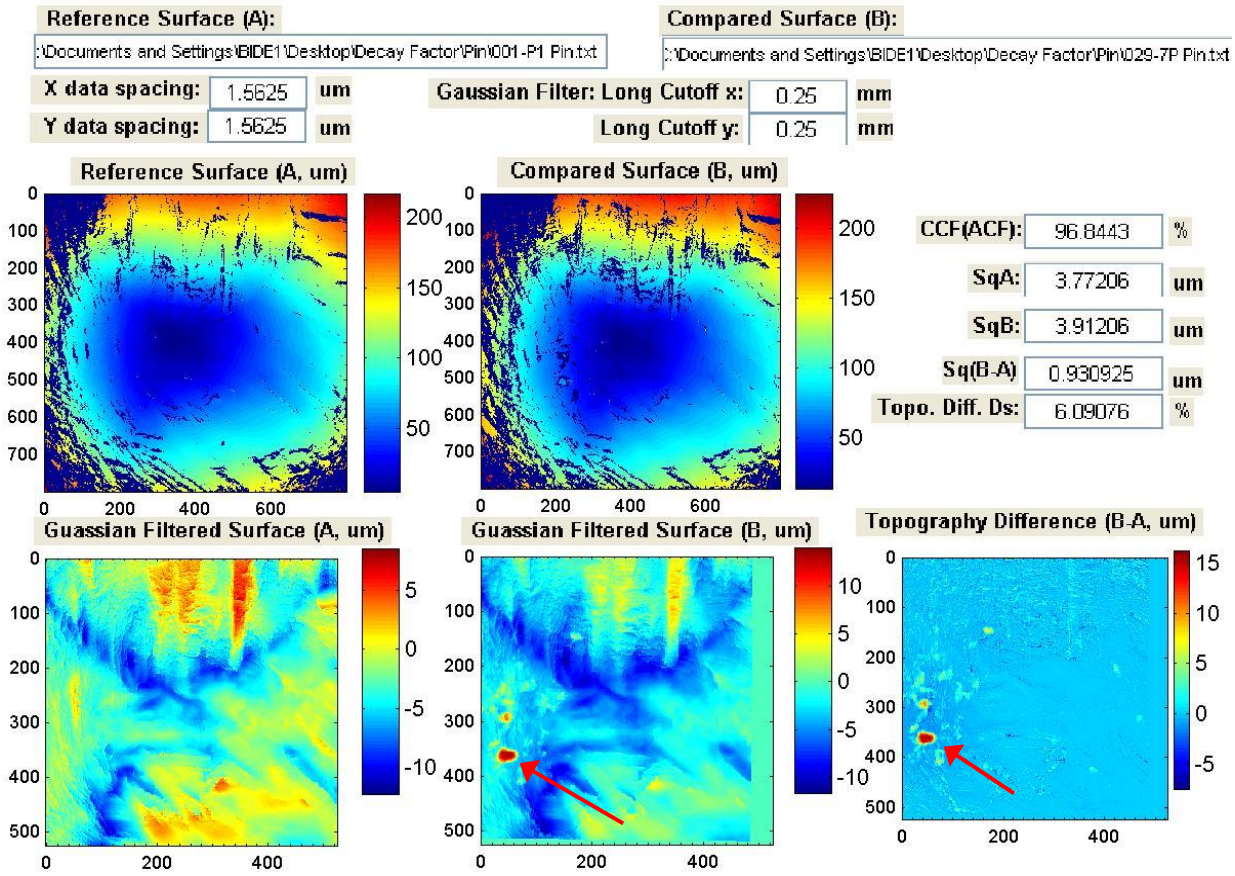

Fig.3-3. Topography correlation of firing pin images between prototype SRM Cartridge 001 (top, left, used here as a reference) and 029 (top, right). The bottom row shows filtered images for 001 (left) and 029 (middle) cartridge and the topography difference (right). A surface defect on 029 cartridge can be seen in the bottom row of middle and right images. Thus, $CCF_{\max}$ decreased to 96.84 %, and D_s increased to 6.09 %.

Chapter 4. Surface Metrology for Engineering Surface Quality Control

Surface metrology bridges manufacturing process and functional performance of engineering surfaces. Engineering surface quality control involves a control loop consisting of surface manufacturing, surface texture measurements, and engineering function [59,60]. The function of engineering surfaces could be optimized by designing their surface texture and specifying characteristic parameters and control values through controlled experiments, and selecting material, manufacturing processes, and quality procedures to meet the optimized engineering function [12,13]. Both the surface calibration standards and measurement control procedure play an important role in engineering surface quality control.

This chapter introduces my contributions in engineering surface quality control:

- Designed and manufactured the Precision Random Profile Roughness Specimens for quality control of smooth engineering surfaces [1]. These specimens were made with roughness *R*a values ranging from 0.015 μm to 0.1 μm -- less than 1/10 of the *R*a values of the similar specimens developed by PTB in Germany. These specimens were included in the ASME B46 [62] surface standard in 1995.
- Proposed a Dynamic Control Chart for measurement quality control of engineering surfaces [2].

4.1. Design, Manufacture and Test of the Precision Random Profile Roughness Specimens

4.1.1. Background

Many engineering surfaces, especially those of smooth engineering surfaces manufactured by grinding, lapping, polishing, honing *et al*. with *R*a $\leq$ 0.1 μm, have random profiles or with random components on their surface profiles. Random profiles have wide amplitude distributions (usually Gaussian) and wide spatial frequency distributions [1,13]. As a result, measurements of these surfaces with different instruments could produce varying results if the spectral responses of the instruments differ significantly [1,13]. In 1965, Häsing at PTB (Physikalisch-Technische Bundesanstalt, Germany) developed the random profile roughness specimens to represent these types of surfaces [14]. These specimens are made with a

measuring area having a unidirectional random profile manufactured by a grinding process. The random profile is repeated every 4 mm, a period equal to the evaluation length of the measurement. Therefore, the measured random profile is always essentially constant within the measuring area, irrespective of the measuring positions on the specimen [14]. These specimens consist of a set of three pieces, with *R*a values of 1.5 μm, 0.5 μm, and 0.15 μm, which could be used for the quality control of medium machined engineering surfaces within the same *R*a range. The PTB specimens were written into the International Standard ISO 5436 [61] and the U.S. National Standard ASME B46 [62].

4.1.2. PTB random profile specimens for engineering surface quality control

With PTB random profile roughness specimens, stylus instruments can be subjected to a summary test covering all stages from the stylus tip to the indication of the measured value. These roughness specimens play an important role in getting agreement for engineering surface measurement among various instruments. Hillmann [63] reported that "*a couple of years ago* (before 1989), *differences in measured surface parameters of 40% and more were ascertained in national and international comparison measurements. Now* (in 1989), *the differences between measurements carried out within the framework of the German Calibration Service amount to only a few percent; in an audit of the European Communities less than 15% was attained.*" Hillmann's recommendations included the use of both the well-defined measurement conditions and well characterized roughness specimens [63].

4.1.3. The precision random profile roughness specimen

The PTB standards are limited to *R*a values > 0.15 μm. However, smooth engineering surfaces with *R*a ≤ 0.1 μm play an increasingly important role both in industry and research. With the development of modern science and technology, the quality control for smooth engineering surfaces (*R*a ≤ 0.1 μm) becomes increasingly important, not only because of their important engineering functions, but also the high production costs [1,13]. NIST's Surface and Nanostructure Metrology Group of the Engineering Physics Division frequently received requests from U.S. industry to provide Standard Reference Material (SRM) Precision Random Profile Roughness Specimens to support smooth surface measurements for U.S. industry. In 1985, I developed the Precision Random Profile Roughness Specimens in Beijing with *R*a ranging from 0.01 μm, 0.05 μm to 0.1 μm, these specimens were written into the U.S. National Standard ASME B46-1995 [62] in 1995.

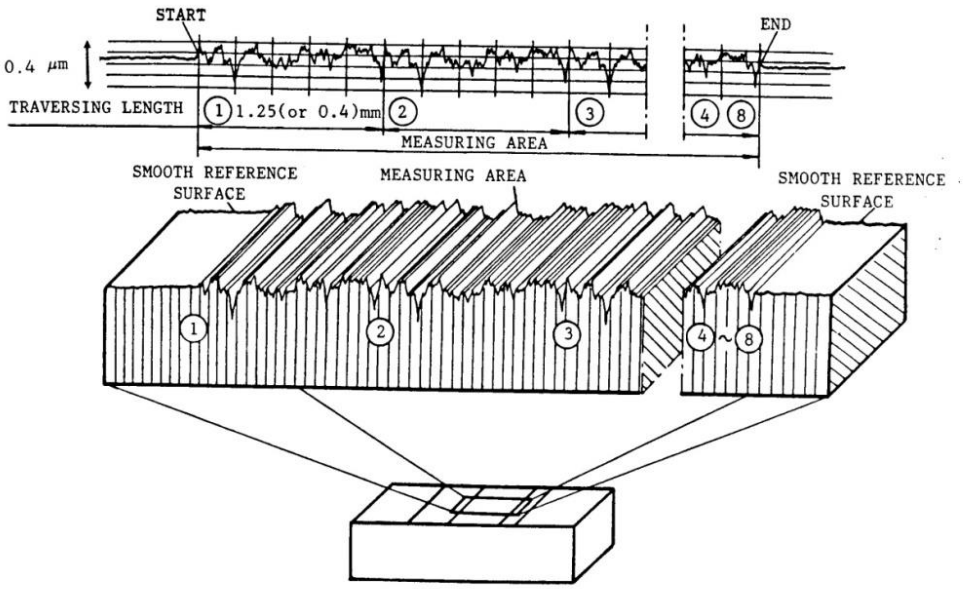

Fig.4-1. The Precision Random Profile Roughness Specimen.

The Precision Random Profile Roughness Specimens were designed with the following characteristics (see Fig.4.1) [1]:

a) The profile repetition is 0.4 mm and 1.25 mm; the roughness average *R*a range is from 0.01 μm, 0.05 μm to 0.1 μm, which is less than 10 % of the *R*a range of PTB specimens.
b) A smooth reference surface with *R*a less than 0.005 μm is located on the mean lines of the random profiles (see Fig.4-1), which can provide a reference datum for roughness measurements and profile comparisons for smooth engineering surfaces [1,13].
c) The micro hardness (HV ≥ 800) [1] is higher than the PTB specimens (HV ≥ 700) [14]. That is helpful for the high precision measurements and long term of use of these specimens.

The prototype Precision Random Profile Roughness Specimens were initially designed, patented and manufactured by myself in 1985 using a guided-lapping process, and was published in 1988 [1] (see Fig4-1). Those specimens are similar to PTB random profile roughness specimens but have small values of *R*a roughness. The measuring areas are composed of several (4-8) identical unidirectional random profile surfaces side by side, and their profile repetitions -- 0.4 mm and 1.25 mm -- are equal to the recommended evaluation lengths for measuring them [62]. The specimens are a set of four pieces having *R*a values of

0.1 μm, 0.05 μm, and 0.025 μm (these three with profile repetition of 1.25 mm) and 0.012 μm (with profile repetition of 0.4 mm). There are also two smooth reference surfaces located at opposite ends of the measuring area (see Fig.4-1). The smooth reference surfaces were made to be situated on the mean lines of the random roughness profiles with the surface finish roughness *R*a ≤ 0.005 μm and flatness ≤ 0.01 μm [1]. The reference surfaces provide a mechanical measuring datum for a skid to move on. By this means, the mechanical noise of the stylus instrument can be reduced [1]. Lines of intersection between the smooth reference surfaces and the measuring area also provide a datum for the start and end positions of the random profiles. It makes the comparison possible between the profile graphs obtained with various instruments [1].

PTB roughness specimens, with their relatively longer peak spacing do not yield *R*a results that are sensitive to the stylus size [63]. However, my specimens, with mean peak spacing less than 10 μm, are very sensitive to the stylus size [1,13], and therefore, could be used for checking stylus condition in surface measurements. To obtain agreement between results on my specimens measured with various instruments, the reference conditions, especially the stylus size, should be carefully adhered to. Like the PTB specimens, my specimens simulate the situation of measuring smooth engineering surfaces and provide a means of exposing the problems and obtaining agreement when stylus and other instruments are used for measuring smooth engineering surfaces [1,13].

4.1.4. The replica of the precision random profile roughness specimen

The replicas of my specimens were made by the electro-forming technique which showed almost identical surface topography between the replicas and the master specimens [38]. Those replica specimens have been used in U.S. and internationally for smooth engineering surface quality control. In 2009, an engineer of GE Aviation sent an email to NIST [64]:

"*In September 2005 GE Aviation received 4 surface finish calibration samples from NIST -- with surface Ra's between 0.5 micro-inches* (about 0.0125 μm) *to 3.9 micro-inches* (about 0.0975μm). *These samples were used to perform a gauge R&R* (repeatability and reproducibility) *study within GE engineering between a Mitutoyo profilometer, a Taylor Hobson profilometer, and a Wyko optical profiler and verified that all devices gave equivalent results. The samples were used as calibration for verifying measurements taken on deep roller*

burnished compressor hardware with single digit micro-inch Ra finishes. The NIST samples were used to perform a gauge R&R study between Cincinnati-based GE engineering surface finish measurement devices (Mitutoyo profilometer and Wyko optical profiler), Wilmington, NC-based surface finish measurement devices (Mitutoyo profilometer with standard stylus length, Mitutoyo profilometer with 3X stylus length ("daddy long-legs"), and Hooksett, NH-based surface finish measurement devices (Hommel profilometer)." [64]

"*Using the surface finish calibration samples provided by NIST gave GE engineering confidence that we could measure surface finishes down in the single digit micro-inch Ra range (about 0.025 μm), and allowed us to verify that we could measure the surface finish on the same part at 3 different locations and report the same result at all locations. The NIST samples allowed GE engineering to expand our measurement capabilities and eliminate gauge R&R issues between various manufacturing shops, and* ***I would like to say thanks to NIST for donating these samples as they were invaluable for helping us to clear up surface finish measurement issues we were having at the time***." [64]

Besides smooth engineering surface quality control, the Precision Random Profile Roughness Specimens have also been used in other research projects including "Stylus profiling at high resolution and low force" [65]; "Stylus flight in surface profiling" [66]; "NIST virtual/physical random profile roughness calibration standards" [39] and "Experimental test of blind tip reconstruction for scanning probe microscopy" [67], all received significant results. It has been frequently referred by literatures including **Prof. T.R. Thomas' renowned book "*Rough Surfaces*" in 1999** [68].

4.2. Development of a Dynamic Control Chart for Engineering Surface Quality Control

4.2.1. Uncertainty for NIST surface roughness and step height calibrations

Reporting measurement uncertainty is usually the last step in a measurement procedure. It is a time-consuming process, and mistakes for either over- or under-estimated uncertainties may occur. In the Surface and Nanostructure Metrology Group of the Engineering Physics Division of NIST, a standardized procedure for reporting uncertainty of measurements for NIST surface roughness and step height calibrations was developed in the early of 1990's, and revised in

2010 [15,69]. A set of check standards covering a range of step heights from 0.02937 µm to 22.90 µm and roughness values, *R*a, ranging from 0.3 µm to 3 µm was repeatedly measured for measurement quality control. We have analyzed the historical control charts using dynamic control limits [2]. The analyzed results support the uncertainty procedure and provide useful information for future revision.

4.2.2. Proposed dynamic control chart

The upper and lower dynamic control limits, $\mu \pm 2\sigma$, are calculated from the updated mean, μ, and the updated standard deviation, σ, using the measurement history for a check standard. These values are then compared with the upper and lower fixed control limits, $y \pm CL$, which are calculated from the reference value, y, assigned to the check standard, and the control limits, CL, which are calculated using the uncertainty components of both the calibration and the check standard, which affect the variation of repeated measurements of the check standard [15, 69]. When the dynamic control limits are close (but not over) to the fixed control limits, it indicates that the measurement reproducibility for the check standard supports the estimated uncertainty estimation of the uncertainty budget. Otherwise, the specific components of the uncertainty budget may be either over- or under-estimated, and they may need to be revised [2].

A dynamic control chart with both fixed and dynamic control limits is shown in Fig.4-2. This was developed for NIST step-height calibrations using a stylus instrument [15,69]. A 0.09065 µm step (expanded uncertainty of 0.00044 µm, $k = 2$) was used as a calibration standard for instrument calibration, and a 0.02937 µm step (expanded uncertainty of 0.00042 µm, $k = 2$) was used as a check standard for measurement quality control. There are 28 control measurements of the check standard carried out from 1993 to 2004. The fixed upper and lower control limits, $y \pm CL$, are calculated from the equation:

$$y \pm CL = y \pm 2\, u_{(CL)} \qquad (4\text{-}1)$$

where y is the reference value of the step height, 0.02937 µm, determined by interferometric and stylus measurements, and $u_{(CL)}$ is the combined standard uncertainty of the fixed control limits which is calculated from the relevant, mostly random, components of uncertainty budget for the measurement process [69], which include uncertainty components from instruments and

standards -- both the calibration standard (0.09065 µm step) and the check standard (0.02937 µm step) -- which affect the variation range of the check measurements. For the report of uncertainty for NIST step height calibrations, four sources of standard uncertainty are included in the uncertainty budget [15,69]:

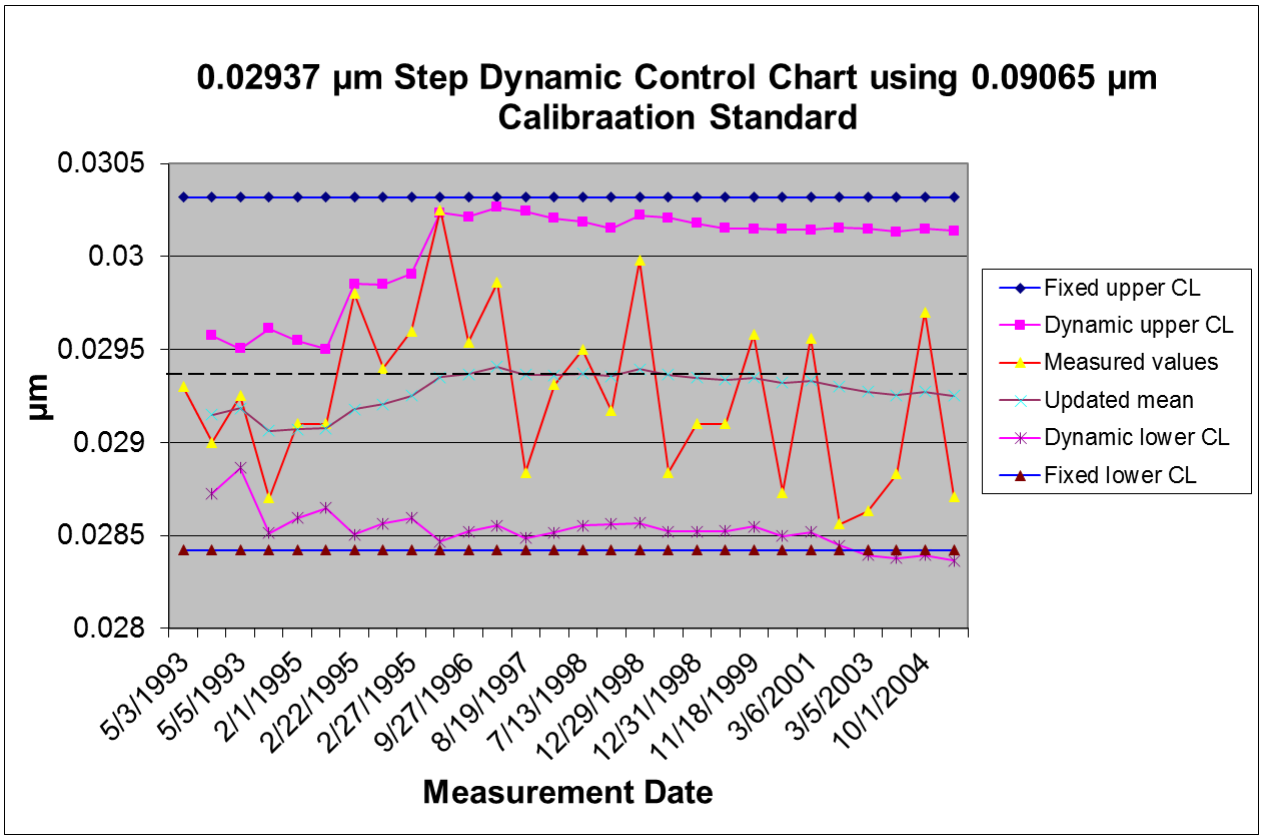

Fig.4-2. A dynamic control chart shows both fixed and dynamic control limits (*CL*). The 0.02937 µm step check standard was repeatedly measured by a stylus instrument calibrated by a 0.09065 µm calibration standard. The dashed line represents the reference value of 0.02937 µm of the check standard.

(1) Geometrical nonuniformity and surface finish of the step-height or calibration ball master used to calibrate the instrument. This leads to an uncertainty in stylus measurements of the master to obtain the calibration constant(s) for the instrument.

(2) Variations in the calibration constant(s) due to (a) noise in the stylus instrument transducer, (b) surface topography in the reference datum of the stylus instrument, (c) sampling and digitizing processes in the controller, and (d) round-off in the software computations.

(3) Variations in the measured *R*a values due to nonlinearity in the instrument transducer.

(4) Uncertainty in the average height of the step-height master or in the radius of the calibration ball as determined from interferometric and other measurements of those objects.

Fig.4-2 shows a dynamic control chart of 0.02937 μm step height check standard using 0.09065 μm step height as a calibration standard. Both the fixed and dynamic control limits (CL) are shown. The 0.02937 μm step check standard was repeatedly measured by a stylus instrument calibrated by a 0.09065 μm calibration standard. The dashed line represents the reference value of 0.02937 μm check standard.

A dynamic control chart with both fixed and dynamic control limits is a useful tool for promoting the process of developing and refining the uncertainty budget and verifying the measurement uncertainty. It can also be used for monitoring the long-term variation for measurement quality control. When a draft uncertainty procedure is first developed, the Type A and Type B uncertainty components may not be carefully investigated, and their sensitivity coefficients may not be well established. Thus, the measurement uncertainty may be either over- or under-estimated. By repeatedly measuring a check standard from time to time, a dynamic control chart with both fixed and dynamic control limits can be established (Fig.4-2). If the upper and lower dynamic control limits $\mu \pm 2\sigma$ are close to but still within that of the fixed control limits $y \pm 2u_{(CL)}$, that indicates the measurement reproducibility for the check standard supports the estimated components of the uncertainty procedure. Otherwise, if the dynamic control limits are too small or too large -- larger than the fixed control limits, that indicates the uncertainty procedure may need to be revised.

The measurement reproducibility obtained from the measurements of the check standard may take days, months or even years -- if it is necessary to monitor the long-term variations for a measurement system including the calibration and check standard, measurement instrument, measurement environment and operators. During that period, the uncertainty procedure may have been continually revised [2].

From Fig.4-2, it can be seen that after about ten measurements, the dynamic control limits, $\mu \pm 2\sigma$, are getting stable and are close to but still within the fixed control limits, $y \pm 2u_{(CL)}$. This indicates that the check measurements support the estimated components of the uncertainty procedure [15,69]. The dynamic control limits also show a small trend of downward drift after

the year of 2001. It may be just a random variation, because the results of check measurements are still within the range of the fixed control limits. On the other hand, it may show the beginning stage of a long-term downward drift, which needs to be continually monitored, and possibly corrected. After the initial draft of this paper in 2006 [2], this check standard was re-measured for three times. Measurement results have confirmed that there is a downward drift for the 0.02937 μm step height check standard. As a temporary step of correction, we have expanded the uncertainty component $u_{(c)1}$ to reflect the change of the 0.02937 μm check standard. For the long run, we plan to replace it with a new check standard.

The Dynamic Control Charts have also been successfully used in the National Ballistics Imaging Comparison (NBIC) Project for establishing a Traceability and Quality System for nationwide ballistics identifications in the United States, and received significant results [6].

Chapter 5. Microform Metrology for Rockwell Hardness Standardization

Rockwell Hardness C (HRC) is the most widely used mechanical testing method for metal products. However, HRC scales in different countries were not unified, which was evolved an international "Technical Barrier to Trade" (TBT). Since 1980's, three NMIs in EC countries -- Italy, Germany and France established an "EC Common HRC Scale" by averaging and correction of three different national scales [70-72]. The unified EC HRC scale challenged HRC tests in the United States. However, the EC HRC common scale couldn't be adapted as a US national standard, since the unified EC HRC scale lacks metrological traceability, stability, reproducibility and transparency [4].

The development of ISO 9000 quality standards [73] provided a strong motivation to establish a worldwide unified Rockwell hardness C (HRC) scale. Before 1990's. there were no national standards for HRC tests in the U.S. In 1993, NIST initialized a new project for Rockwell hardness standardization. In 1995, I proposed a "Metrological Approach" to unifying international HRC scales based on the precision calibrations of the influence quantities for HRC tests -- including those from the testing machine, diamond indenter and testing cycle, and to ensure the calibration of all influence quantities traceable to three base unites -- length, mass and time [4].

My major contributions in this NIST project are:

- Established a Microform Calibration System at NIST with the lowest calibration uncertainties in the world for calibration of the Rockwell diamond indenters [3]; developed an uncertainty procedure [3] and calibrated the microform geometry of National Standard Rockwell Diamond Indenters for five National Metrology Institutes (NMIs) [4].
- Proposed a "Metrological Approach" to unifying international Rockwell hardness C tests based on the precision calibration of the influence quantities traceable to base unite, instead of the "Performance Approach" used at that time in EC countries based on performance comparisons and corrections of different national hardness scales [4].

- Conducted international comparisons on microform measurements of Rockwell indenters and HRC hardness tests in five NMIs in U.S., Italy, Germany, China and Japan, which strongly supported the Metrological Approach to unifying international Rockwell hardness tests. I drafted a research paper entitled "Establishing a Worldwide Rockwell Hardness Scale with Metrological Traceability" which was published it at the *Metrologia* **34,** 1997 in Paris [4].

5.1. Challenges to Establishing a Worldwide Unified HRC Scale

5.1.1. Background

Rockwell hardness scales are empirical, and as such are defined by reference standards (standard testing machines and standard Rockwell hardness diamond indenters) and reference testing conditions. A Rockwell scale is established by the performance of a standard diamond indenter with a nominal geometry as shown in Fig.5-1 (for HRC, HRD, HRA, HR45N, HR30N and HR15N scales) using a standard testing machine and a standardized testing cycle. For many years, efforts in Rockwell hardness standardization have mainly concentrated on three aspects [4]:

(A) To develop standard machines and direct verification techniques;

(B) To develop standard diamond indenters and calibration techniques;

(C) To control the testing cycle and to develop a standardized common testing cycle.

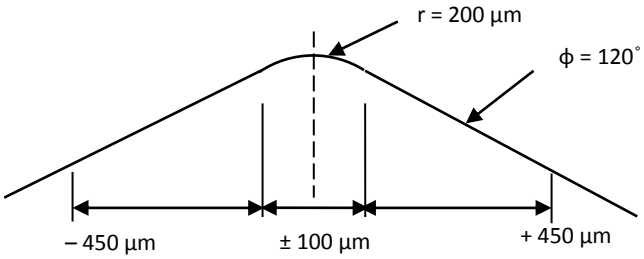

Fig.5-1. Rockwell diamond indenter with a nominal geometry of 200 µm tip radius and 120° cine angle (for HRC, HRD, HRA, HR45N, HR30N and HR15N scales).

(A) Standard hardness machine

Since the 1940's, standard hardness machines have been developed at different laboratories [74-77]. More recently deadweight and laser-type standard machines, developed at IMGC (Italy) [76], NIM (China) [77], and NIST (U.S., a new version of IMGC machine), have shown measurement repeatability better than ± 0.1 HRC (± 2σ) [76,77].

(B) Standardized testing cycle

Different testing cycles result in significant differences in Rockwell hardness tests [78]. Currently used testing cycles show large variations among National Metrology Institutes (NMIs) and between NMIs and industries [78]. To establish a worldwide unified HRC scale, it is necessary that the NMIs use a standardized common testing cycle, including the standardized loading velocity and holding times with narrow, but acceptable tolerances.

(C) Standard diamond indenters

From the 1950's to the 1980's, different measurement techniques were developed for the geometric measurements of the diamond indenters [79-82]. However, the expanded measurement uncertainties for the 200 μm tip radii were reported to be in the range of micrometers [79,80,82], or sometimes even larger [81]. Significant differences in geometry and hardness performance existed among different national indenters [71]. In addition, many complex features of the diamond indenters, such as surface roughness and form errors, could not be explored and quantified. International comparisons of HRC tests using national indenters showed a variation range of ±0.9 HRC [70]. The non-unified testing cycles along with the non-unified microform geometries of the national indenters are largely responsible for these differences. The former is mainly a standardization issue; the solution would be an international agreement on a standardized common testing cycle for worldwide unified HRC scales. The latter is a metrology issue; the solution is based on precision metrology to establish high quality standard Rockwell indenters [4,83]. Ideally, these standard indenters should be characterized by high geometric uniformity, high hardness performance uniformity, interchangeability and reproducibility [4,84].

5.1.2. Previous standardization efforts

Since the 1950's, the influences of indenters' geometry in Rockwell hardness tests were analyzed theoretically and empirically [85-88]. After the work of Yamamoto, Yano *et al.* [80,88], a systematic correction method based on geometry measurements was implemented at NRLM (Japan) for hardness measurements using a set of collective national indenters. This system has been used in Japan for the control of the uniformity of the national hardness scale since the 1960's [88].

Since the 1980's, HRC scales have been locally unified in European Community countries by averaging national scales based on three national hardness machines with their indenters [72]. Although the national indenters were chosen on the basis of geometrical measurements and the machines were of the metrological type, the inter-comparisons showed bias among three national scales which were averaged and unified as an EC common HRC scale [72].

In China, a laser deadweight standard machine was established at NIM in 1980 [77]. Since 1986, the national HRC scale was established through performance comparisons traceable to the established EC common scale [89].

In the U.S., private companies have maintained their own internal scales using "historical" hardness blocks [90], probably with unknown biases between these scales and an ideal scale. As these "historical" blocks were used up, they were replaced by new blocks, possibly compromising the consistency of these scales over time. To remedy this state of affairs, development of a standard testing machine for Rockwell hardness was undertaken and completed at NIST in the 1990's, with ongoing development of Standard Rockwell Diamond Indenters and metrological traceability which was completed in the late of 1990's.

5.1.3. Requirements for a worldwide unified Rockwell scale

Ideally, a worldwide unified Rockwell scale should be characterized by [4]:

(A) **Metrological traceability:** The reference standards are established traceable to basic unites with tightly controlled tolerances and acceptably small measurement uncertainties. These include the force and displacement calibrations for the standard hardness machines, and the microform calibrations for the standard diamond indenters. The Rockwell scale established in accordance with these references standards will show metrological traceability without significant bias to an ideal scale.

(B) **Stability and reproducibility:** Stability and reproducibility of the reference standards and Rockwell scales are ensured by traceable measurements. Each standard (machine or indenter) can be replaced by other qualified standards. The reproduced reference standards can perform the same function as the original ones without causing the common scale to drift outside the certification range.

(C) **Transparency and independency:** The procedures, techniques and reference standards used for establishing the common scale should be well known and could be

independently reproduced by another laboratory to create and maintain the same HRC hardness scale without systematical bias.

5.1.4. Establishing a worldwide unified HRC scale using geometrically calibrated standard indenters

The worldwide unified scale could be achieved by establishing the reference standards (standard machines and standard indenters) through traceable measurements, and standardizing the testing cycles. High accuracy standard machines were developed based on force and displacement calibrations [76,77]. Stylus and laser interferometry techniques have been used for the microform measurements of diamond indenters. These techniques have largely reduced the measurement uncertainties. By using a laser interferometer with a tailored wavefront, expanded measurement uncertainties of ±1.5 μm for the tip radii and ±0.018° for the cone angles were reported at MPA NRW [91]. By using a commercial stylus instrument with a set of calibration and check standards, expanded measurement uncertainties of ±0.4 μm for the tip radii and ±0.01° for the cone angles were reported at NIST [3,4,92,]. The complex geometric features of Rockwell diamond indenters, including the profile deviations from the least-squares radii, the cone flank straightness, the holder axis alignment error, the surface roughness and surface defects, can also be explored and quantified [3,4,92,].

It is possible to establish a worldwide unified scale based on these newly developed measurement techniques, instead of on performance comparisons and corrections to offset the significant differences of diamond indenters. The key point is to prove that geometrically calibrated standard indenters could significantly improve the hardness measurement consistency to an acceptable degree; and that these standard indenters could be produced by different manufacturers and calibrated by different measurement techniques.

A joint study by five National Metrological Institutes (NMIs) responsible for national Rockwell standards at that time was conducted [4]. The inter-comparison results showed that: with closely controlled geometries, the hardness tests for these indenters showed a performance variation range of approximately ±0.2 HRC [4].

A general conclusion is that the use of geometrically calibrated and performance verified standard indenters in different national standard machines with a standardized testing cycle

could enable the establishment of a common HRC scale within an expanded uncertainty of approximately ±0.2 HRC (±2σ). This common scale could be independently established in different NMIs with metrological traceability and reproducibility and without significant bias to the ideal scale [4].

5.2. Characteristics of Working Grade, Calibration Grade, and the Proposed Standard Grade Rockwell Diamond Indenters

5.2.1. Geometric properties of Rockwell hardness diamond indenters

The Rockwell hardness diamond indenter is a diamond cone with 120° cone angle blended in a tangential manner with a spherical tip of 200 μm radius (Fig.5-1). The geometric properties affect the hardness performance of the indenters. The geometric parameters of the Rockwell diamond indenters include [4]:

(A) The parameters for the spherical tip surface, which include:
- the mean radius;
- the maximum and the minimum radius in different measurement sections;
- the form errors of the spherical tip, which can be characterized by the maximum profile peak and profile valley deviations from the least-squares shape.

(B) The parameters for the cone surface, which include:
- the mean cone angle;
- the maximum and the minimum cone angle in different measurement sections;
- the form errors of the cone surface which can be characterized by the maximum cone flank straightness error.

(C) The holder axis alignment error.

(D) The surface roughness and surface defects.

5.2.2. Proposed standard grade Rockwell diamond indenters

Technical requirements for geometric tolerances and performance uniformities of the standard indenters have been proposed by NIST [84]. The geometric tolerances of the proposed standard indenters are designed for a hardness performance variation range of ±0.15 HRC to an ideal scale [84].

The performance variation range of ±0.15 HRC discussed above is close to the combined random variation range of the standard machine and standard blocks [84]. Any performance tests of the diamond indenters must include the random variations of the standard machine, as well as the random non-uniformity of the standard blocks. For the standard machines, the random repeatability has been reported as no more than ±0.1 HRC (±2σ) [76,77,83]. For the standard blocks, the non-uniformity tested at NIST showed a total range of less than ±(0.15) HRC in seven indentations. Therefore, if geometrically qualified standard indenters show a performance variation range within ±0.15 HRC (including random variations of standard machine and standard blocks), it is reasonable to conclude that the hardness performances of these standard indenters would have been unified without significant systematic bias among them. The Rockwell scale established using these standard indenters in a standard machine with a standardized testing cycle would then have metrological traceability and reproducibility without significant bias to the ideal scale. Following this approach, the expanded uncertainty of the common Rockwell hardness C scale calculated by a quadratic sum between different national laboratories could be expected to be about ±0.2 HRC [4].

5.3. Hardness Comparison Tests between a Common Indenter and Five Different National Indenters

A key point is to demonstrate that geometrically calibrated and qualified standard indenters, which could be produced by different manufacturers and calibrated by different measurement techniques, can enable hardness measurement consistency to an acceptable degree. First, as a baseline, we estimate the existing hardness variation range among five NMIs' national indenters in U.S., Italy, Germany, Japan and China with respect to a common indenter. Then, we compare the geometry measurements and hardness tests of 16 diamond indenters made by two different manufacturers. The geometric parameters of these indenters are measured by two different techniques, and are close to meeting the technical requirements for the proposed Standard Rockwell Hardness Diamond Indenters [4].

A common indenter and a single set of hardness blocks with nominal hardness values of (30, 40, 50 and 60) HRC were tested by five Rockwell hardness machines in five NMIs using the same nominal testing cycle [4]. At each laboratory, each block was first tested by four indentations using a common indenter. The mean values of the four indentations are compared

in Fig.5-2. The zero line comes from the average of the five national laboratories. In this report [4], the total variation range of hardness tests in the whole testing scale is reported, rather than the ranges at different hardness levels. The testing results show good agreement with a total range of (–0.19 to +0.16) HRC. This is because the national hardness machines were directly verified by traceable measurements of the force and displacement, and all national laboratories used similar testing cycles for this study [4]. The small variations shown in Fig.5-2 mainly represent the small differences among five NMIs' national standard machines and testing cycles, as well as the possible non-uniformity of the standard blocks.

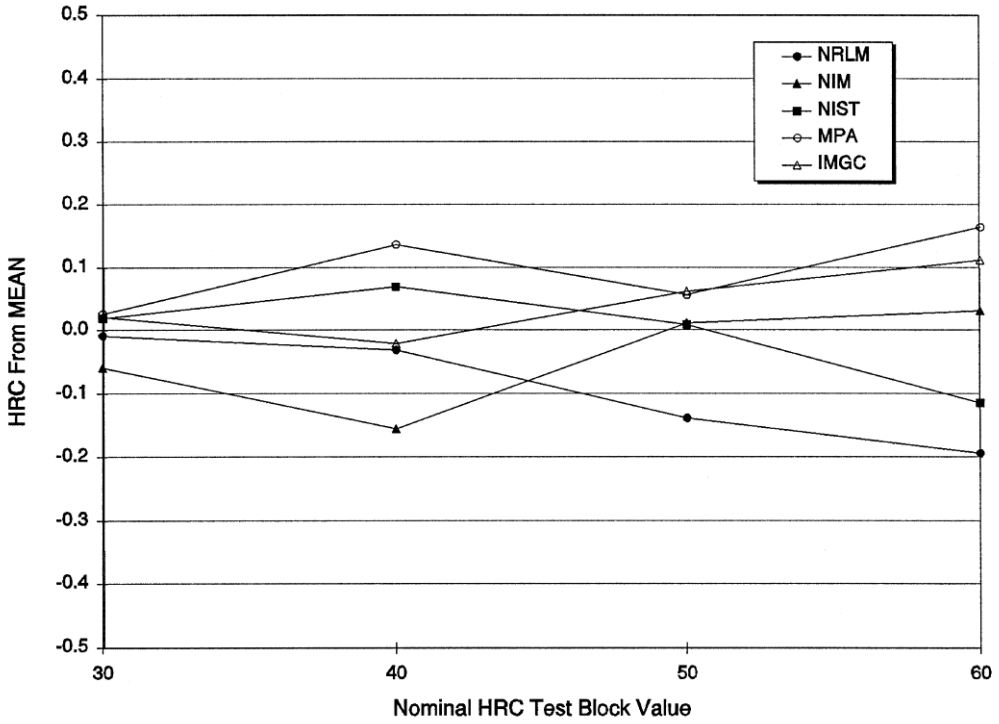

Fig.5-2. A common indenter was tested by five national machines using similar testing cycles, the variation range is (-0.19 to +0.16) HRC.

The hardness tests were repeated using the five NMI's national indenter. The variation range increased to (-0.29 to +0.38) HRC (see Fig.5-3), which represents the combined variation range of five different national indenters, national machines and testing cycles, which mainly represents the performance differences of the existing five national indenters augmented somewhat by the random errors arising from the subtraction of two sets of measurements.

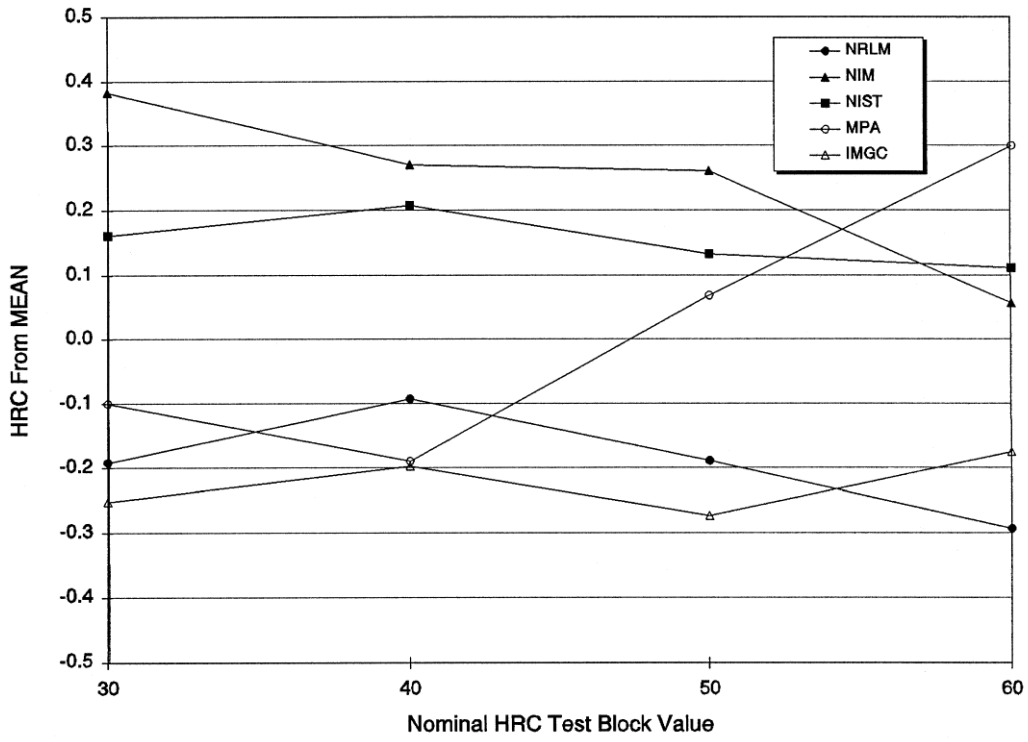

Fig.5-3. Five national indenters were tested by five national machines using similar testing cycles, the variation range is (-0.29 to +0.38) HRC.

5.4. Comparisons of Geometric Measurements and Hardness Performance Tests

Nine Rockwell diamond indenters made by diamond manufacturer A were measured both by a stylus instrument at NIST [4,92] and by a laser interferometer at MPA NRW [91]. The window size is ± (450 to 100) μm for cone angle calibrations and ± 100 μm for tip radius calibrations. The geometric measurement results for the mean tip radii and the mean cone angles are compared for the two instruments as shown in Tab.5-1 [4]. NIST's expanded uncertainty is a combination of geometrical non-uniformity of the measured indenter and the expanded measurement uncertainty, which is ±0.4 μm for the tip radius and ±0.01° for the cone angle [3,4]. The NIST expanded uncertainty represents a 95% confidence interval. For the MPA NRW results, the combined expanded uncertainties reported are ±2 μm for the mean radii and ±0.067° for the mean cone angles, which include the expanded measurement uncertainties of ±1.5 μm and ±0.018° respectively, both are with a coverage factor of k = 2 [4,91].

Tab.5-1. Measurement comparisons using a stylus instrument at NIST and a laser interferometer at MPA NRW

Indenter No.	Components		(a) Stylus Instrument	(b) Laser Interferometer	δ = (a) - (b) U = (Comb. Unc'ty)	Significant difference?
3309	Tip Radius	Mean	198.34 µm	198.39 µm	-0.05 µm (δ)	
		Unc'ty (±)	2.04 µm	2 µm	2.86 µm (U)	
	Cone Angle	Mean	119.98 °	120.00 °	-0.02 ° (δ)	
		Unc'ty (±)	0.03 °	0.067 °	0.07 ° (U)	
3581	Tip Radius	Mean	199.06 µm	198.64 µm	0.42 µm (δ)	
		Unc'ty (±)	1.97 µm	2 µm	2.81 µm (U)	
	Cone Angle	Mean	120.00 °	120.01 °	-0.01 ° (δ)	
		Unc'ty (±)	0.02 °	0.067 °	0.07 ° (U)	
3513	Tip Radius	Mean	199.17 µm	199.22 µm	-0.05 µm (δ)	
		Unc'ty (±)	1.54 µm	2 µm	2.52 µm (U)	
	Cone Angle	Mean	120.01 °	119.99 °	0.02 ° (δ)	
		Unc'ty (±)	0.03 °	0.067 °	0.07 ° (U)	
3302	Tip Radius	Mean	200.39 µm	200.20 µm	0.19 µm (δ)	
		Unc'ty (±)	2.49 µm	2 µm	3.19 µm (U)	
	Cone Angle	Mean	119.94 °	119.93 °	0.01 ° (δ)	
		Unc'ty (±)	0.07 °	0.067 °	0.10 ° (U)	
3488	Tip Radius	Mean	200.55 µm	201.13 µm	-0.58 µm (δ)	
		Unc'ty (±)	0.75 µm	2 µm	2.14 µm (U)	
	Cone Angle	Mean	120.07 °	120.06 °	0.01 ° (δ)	
		Unc'ty (±)	0.02 °	0.067 °	0.07 ° (U)	
3313	Tip Radius	Mean	200.82 µm	201.68 µm	-0.86 µm (δ)	
		Unc'ty (±)	2.22 µm	2 µm	2.99 µm (U)	
	Cone Angle	Mean	120.07 °	120.07 °	0.00 ° (δ)	
		Unc'ty (±)	0.06 °	0.067 °	0.09 ° (U)	
3366	Least Sq. Radius	Mean	202.02 µm	204.88 µm	-2.86 µm (δ)	
		Unc'ty (±)	2.80 µm	2 µm	3.44 µm (U)	
	Cone Angle	Mean	120.01 °	119.99 °	0.02 ° (δ)	
		Unc'ty (±)	0.05 °	0.067 °	0.08 ° (U)	
3307	Tip Radius	Mean	202.65 µm	207.56 µm	**-4.91** µm (δ)	***Yes***
		Unc'ty (±)	1.14 µm	2 µm	2.30 µm (U)	
	Cone Angle	Mean	119.97 °	119.97 °	0.00 ° (δ)	
		Unc'ty (±)	0.05 °	0.067 °	0.08 ° (U)	
3312	Tip Radius	Mean	202.90 µm	206.77 µm	**-3.87** µm (δ)	***Yes***
		Unc'ty (±)	1.59 µm	2 µm	2.56 µm (U)	
	Cone Angle	Mean	119.98 °	119.96 °	0.02 ° (δ)	
		Unc'ty (±)	0.05 °	0.067 °	0.08 ° (U)	

Two other indenters measured at NIST previously [84] were added to the set of nine. One of them was made by a different manufacturer B from the other ten indenters made by manufacturer A. The total of 11 indenters showed a range of mean radii from 198.34 µm to 202.90 µm, and a range of mean cone angles from 119.94° to 120.07° (Tab.5-1), according to the measurement results with the stylus instrument. These indenters nearly meet the technical requirements for the proposed standard indenters [84].

All 11 indenters were tested by the NIST standard deadweight machine using the same testing cycle. Four HRC hardness blocks with nominal hardness values of (25, 35, 50 and 60) HRC

were used for the tests. For each hardness test, four indentations were made on the same block. The mean values of the four indentations are compared in Fig.5-4. The zero line comes from the average of the 11 indenters. The total performance variation range is (–0.17 to +0.23) HRC from (25 to 60) HRC for all 11 indenters, including the variation of the testing machine and the non-uniformity of the hardness blocks. These results suggest that the improved standard indenters could produce a hardness measurement uniformity of ±0.2 HRC. Another set of tests using nine indenters made by two manufacturers also showed similar results [4]. That suggests that standard indenters could be produced by different manufacturers with sufficient consistency both in geometry parameters and hardness performance.

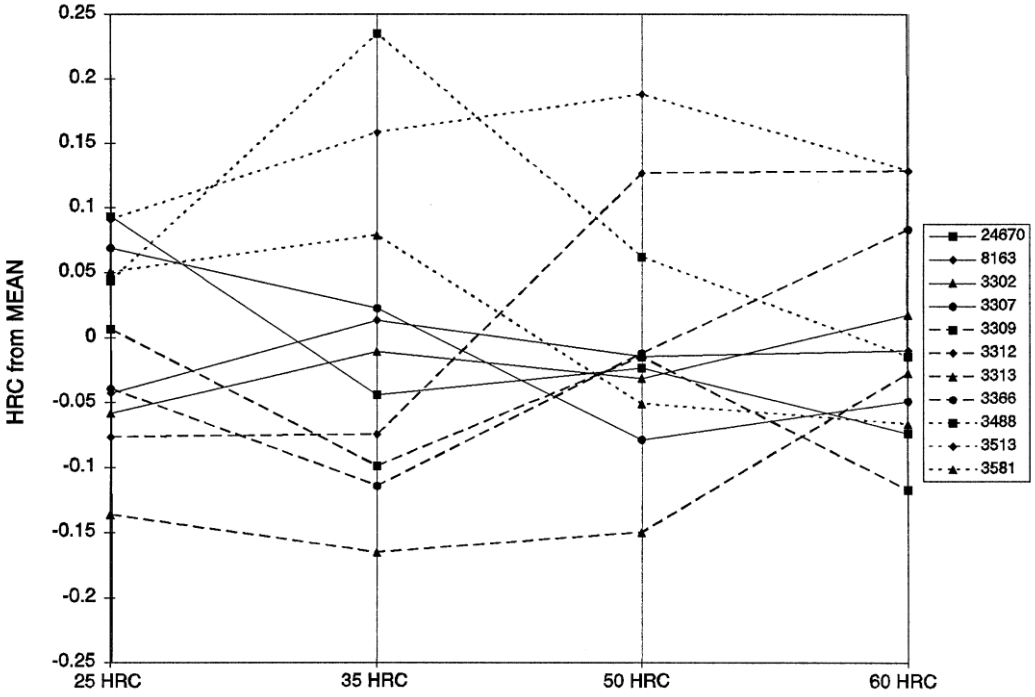

Fig.5-4. Performance comparisons of 11 indenters, the variation range is (-0.17 to +0.23) HRC.

5.5. Establishing a Worldwide Unified Rockwell Hardness Scale with Metrological Traceability

A worldwide unified Rockwell scale should be characterized by metrological traceability, stability and reproducibility [4]. It could be achieved by establishing the reference standards (standard machines and standard indenters) through traceable measurements and by unifying the reference testing conditions. The standard machines and standard indenters could be

independently established in different NMIs. Different direct verification techniques with tightly-controlled tolerances and measurement uncertainties could be used to ensure the metrological traceability and reproducibility for these reference standards and reference conditions [4].

Standard Rockwell Diamond Indenters have high uniformity in both microform geometry and hardness performance, and to be interchangeable and reproducible. Standard indenters could be produced by different manufacturers and calibrated by different measurement techniques. Stylus and laser interferometry techniques have shown significantly improved measurement agreements over previous techniques. In order to achieve a higher measurement agreement, the window sizes of the two approaches need to be unified [4].

Geometric measurements and hardness tests among five NMIs show that a common indenter used in five national standard machines to test a common set of hardness blocks yielded a hardness variation range of (–0.19 to +0.16) HRC. Five NMI's national indenters exhibited a hardness performance variation range of (–0.33 to +0.44) HRC [4]. A set of 11 indenters was measured by a stylus instrument; nine of them were also measured by a laser interferometer. These indenters show consistent geometry and are close to meeting the technical requirements of the proposed standard indenters. The hardness tests for the 11 indenters show a variation range of (–0.17 to +0.23) HRC. These results suggest that the proposed standard indenters could possibly obtain a performance uniformity range of approximately ±0.2 HRC [4]. A worldwide unified scale requires a standardized common testing cycle which could produce a hardness measurement reproducibility range of approximately ±0.2 HRC when using a common indenter in different national standard hardness machines [4].

By using the geometrically calibrated and performance verified standard indenters in different national standard machines with a standardized common testing cycle, it can be expected to establish a worldwide common HRC scale with an expanded uncertainty of approximately ±0.2 HRC. Unlike the EC common HRC scale established by performance comparisons and corrections on different national HRC scales [72], the proposed worldwide common scale would have metrological traceability and reproducibility without significant bias with respect to the ideal scale [4]. The proposed approach can also be used for unifying other HR scales using conical diamond indenters (HRD, HRA, HR45N, HR30N, and HR15N) [4].

Note: The project entitled Establishing a Metrological Approach to Unifying International Rockwell Hardness Scales has celebrated three NIST awards, in which Song and his collogues were recognized "***For development of a metrology-based Rockwell C Hardness Scale which will reduce trade barriers and has made the U.S. a world leader in the field***."

Chapter 6. Summary, Impact and Outlook

As a concluding part of the thesis, this chapter is intended to sumarize my contributions in surface and topographuy metrology in different fields of firearm evidence identificaiton, enginering surface quality control and Rockwell hardness standardization. In each field, the major projects and accomplishments, delieveables and impacts are conclusively reviewed, followed by a discussion of the outlook and future work using surrfce and topography metrology in the new challinging projects at NIST.

The Ph.D. thesis summarizes my 30-year's research work at the National Institute of Standards and Technology -- it emphasizes on how to use the general knowledge and fundamental principles in surface metrology to support engineering surface quality control and firearm evidence identifications. This includes how to define a measurable quantity and develop a reference standard; how to establish a measurement system; how to construct a traceability and quality system; and how to evaluate measurement uncertainty for engineering surface control and firearm evidence identification. The thesis also presents a review on some of the state-of-the-art technologies used in National Metrology Institutes (NMI) and measurement institutions in surface and topography metrology. It compares the advantages and limitations of some techniques and provides case studies and applications in R&D related industries that will be beneficial to different fields in precision engineering and metrology, advanced manufacturing, and firearm evidence identification.

6.1. Major Research Projects, Accomplishments and Deliverables

6.1.1. Topography metrology for firearm evidence identification and error date estimation

Since 1997, as a Project Lead, I have been working with my Project Team of Forensic Topography and Surface Metrology at NIST. We have completed important research projects to provide support in measurements and standards for U.S firearm evidence identification. My major accomplishments and deliverables are:

- Designed the NIST SRM 2460 Standard Bullet and SRM 2461 Standard Cartridge Cases and the manufacturing process [5], led the team and completed the manufacturing

and delivered 40 SRM 2460 Standard Bullets [44] and 135 SRM 2461 Standard Cartridge Cases [40].

- Proposed a unique parameter, Topography Difference D_s, for 2D/3D topography comparisons [18,19], led the team and developed NIST 2D/3D Topography Measurement System for firearm evidence identifications [5,20,21].
- Proposed and led a National Ballistics Imaging Comparison (NBIC) project, formulated a Traceability and Quality System for National Integrated Ballistics Information Network (NIBIN) in the United States [6].
- Invented a Congruent Match Cells (CMC) method for accurate firearm evidence identification and error rate estimation [7,8], led the team and conducted programming, initial validation tests [32,33] and initial error rate estimation [8].
- Proposed the usages of 2D topography comparisons for instrument characterization [22] and 3D topography comparisons for production quality control [19,23].

6.1.2. Surface metrology for engineering surface quality control

My major accomplishments and deliverables from the surface metrology projects for engineering surface quality control include:

- Designed and manufactured the Precision Random Profile Roughness Specimens with *R*a ranging from 0.01 μm to 0.1 μm for quality control of smooth engineering surfaces [1].
- Designed the Dynamic Control Chart with dynamic control limits for quality control of surface and topography measurements [2].

6.1.3. Microform metrology for establishing a worldwide unified Rockwell hardness C scales with metrological traceability

My major accomplishments and deliverables from the microform metrology project include:

- Proposed a "Metrological Approach" based on the precision calibration of the microform geometry of Rockwell diamond indenters for establishing a worldwide unified Rockwell C hardness scales with metrological traceability [4].
- Established the NIST Microform Calibration System with calibration and check standards [3], developed calibration and uncertainty procedures for the microform calibration of Rockwell diamond indenters [3].

- Conduced microform geometry and hardness performance measurement comparisons at five National Metrological Institutes (NMI's) in U.S., Italy, Germany, Japan and China. The comparison results strongly supported the NIST proposed Metrological Approach for establishing a worldwide unified Rockwell hardness C scales with metrological traceability [4].

6.2. Impacts

6.2.1. Topography metrology supports firearm evidence identification

The scientific foundation of firearm and toolmark identification has been challenged by recent court decisions and by the 2008 and 2009 National Academies Report [28,29], "*The validity of the fundamental assumptions of uniqueness and reproducibility of firearms-related toolmarks has not yet been fully demonstrated…*" and "*Since the basis of all forensic identification is probability theory, examiners can never really assert a conclusion of an 'identification to exclusion of all others in the world,' but at best can only assert a very small (objective or subjective) probability of a coincidental match…*"

The Forensic Topography and Surface Metrology Project at NIST established in 1997 addressed this challenge by using their expertise in surface and topography metrology to support firearm evidence identification in the United States. We developed SRM Bullets and Cartridges Cases [5,40,44], which have been used as reference standards in forensic laboratories of U.S. and other eight countries. We proposed a unique parameter to quantify 2D/3D topography comparisons [5,18]. We developed a 2D/3D ballistics correlation program [20,21] and formulated a nationwide Traceability and Quality System for firearm evidence identifications in the U.S. [6,25,26].

Based on the Congruent Match Cells (CMC) method invented by me [7,31], I led our team and developed correlation programs for accurate firearm evidence identifications [32,33]. We have also developed an error rate procedure and conducted the first set of error rate estimation [7,8]. The proposed CMC method and error rate procedure can serve as a foundation for manufacturers to develop Next Generation Ballistic Identification Systems characterized by high correlation accuracy and error rate reporting, which would represent a decided advance over current automated ballistic identification systems. An error rate procedure could also be

used for laboratory assessment and accreditation in accordance with the ISO 17025 standard [57] and ASCLD/ LAB procedures [58].

Based on the CMC method, our research team is working with U.S. manufactures to develop the Next Generation Ballistics Identification System characterized by high correlation accuracy and correlation speed, and by directly providing a correlation conclusion (identification or exclusion) with error rate report. A U.S. manufacture, Leeds Forensic Systems, Inc., located in Minneapolis, MN, sent an email to NIST on September 30th, 2013:

"*We feel the Error Rate Software based on the Congruent Matching Cell theory could revolutionize the science of firearms comparison, and we wanted a license to sell it…*" [56]

At the exhibition booth of 2015 Association of Firearm and Tool-mark Examiners annual meeting (2015 AFTE) held in Dallas, TX, two U.S. companies Leeds Forensic Systems, Inc. and X-wave Innovation Inc. (XII) have demonstrated their commercial product called "*CaseHitter*" for Next Generation Ballistics Identification System which used the NIST invented CMC method for firearm evidence identification and error rate reporting. At the cover page of the *CaseHitter* program, it stated that:

"*This software is based on the CMC (Congruent Match Cells) method and the Error Rate Procedure invented by NIST.*"

6.2.2. Surface metrology supports engineering surface quality control

I developed the Precision Random Profile Roughness Specimens for quality control of smooth engineering surfaces [1]. The replicas of my specimens were made by the electro-forming technique which showed almost identical surface topography between the replicas and the master specimens [38]. Those replica specimens have been used in U.S. and internationally for smooth engineering surface quality control. In 2009, an engineer of GE Aviation sent an email to NIST [64]:

"*…Using the surface finish calibration samples provided by NIST gave GE engineering confidence that we could measure surface finishes down in the single digit micro-inch Ra range (about 0.025 μm), and allowed us to verify that we could measure the surface finish on the same part at 3 different locations and report the same result at all locations. The NIST samples allowed GE engineering to expand our measurement capabilities and eliminate gauge R&R*

issues between various manufacturing shops, and ***I would like to say thanks to NIST for donating these samples as they were invaluable for helping us to clear up surface finish measurement issues we were having at the time.***" [64]

Besides smooth engineering surface quality control, the Precision Random Profile Roughness Specimens have also been used in other research projects including "Stylus profiling at high resolution and low force" [65]; "Stylus flight in surface profiling" [66]; "NIST virtual/physical random profile roughness calibration standards" [39] and "Experimental test of blind tip reconstruction for scanning probe microscopy" [67], and received significant results. It has been frequently referred by literatures including **Prof. T.R. Thomas' renowned book "*Rough Surfaces*" in 1999** [68].

I proposed to develop the Dynamic Control Chart [2] which has been used for NIST step height and surface roughness calibrations for many years and for establishing a traceability and quality system for NIBIN (National Integrated Ballistics Information Network) in the United States [6].

6.2.3. Microform metrology supports international Rockwell hardness standardization

I proposed a Metrological Approach to unifying international HRC scales [4]. I led a team at NIST and established a Microform Calibration System for precise calibration of the microform geometry of Rockwell diamond indenters [3,4,16,17], which holds the highest calibration accuracy in the world for the microform calibration of Rockwell diamond indenters. A group of Standard Rockwell Diamond Indenters were calibrated at NIST, by which international comparisons in fine NMIs (National Metrology Institutes) were conducted. The comparison results strongly support the NIST proposed Metrological Approach to unifying the international Rockwell hardness scale. A joint report of the five NMI's entitled "Establishing a worldwide unified Rockwell hardness scale with metrological traceability" was published in the journal of *Metrologia* [4].

Based on the calibration results for the microform geometry of Rockwell diamond indenters, we proposed to revise the technical specification of ISO standard for the straightness of cone flank of Rockwell diamond indenters which has been accepted in the newly issued ISO 6508-3:2015(E) standard entitled "*Metallic materials — Rockwell hardness test — Part 3: Calibration of reference blocks.*" [93] Since 1990's, we initialized a SRM Rockwell Diamond

Indenters project to support U.S. manufacturing industries. we cooperated with the best diamond indenter manufacturers in U.S. and internationally, received and calibrated more than 70 Rockwell diamond indenters. However, since the old ISO standard initially published in 1986 (ISO 715-1986) and revised in 2005 (ISO/ 6508-3-2005) specified a very tight tolerance for the cone flank straightness (0.5 μm for maximum), few of the NIST calibrated indenters can meet this specification. Since the late 1990's, based on the microform calibrations and finite element simulations, we suggested to relax the tolerance range for cone flank straightness from "0.5 μm for maximum" to "0.5 μm for average and 0.7 μm for maximum", and specifying the window size and location for calibration of Rockwell indenters [94-96]. We continually presented our research results at the CIPM Working Group for Hardness (WGH) and the ISO TC 164 committee meetings, as well as by conference presentations and journal publications [94-96]. Our suggestions have been adapted by the newly issued ISO standard in 2015 [93]. We are working on microform calibrations and hardness performance tests and considering the initiation of a new project to develop SRM Rockwell Hardness Diamond Indenters in conformance with the revised ISO standard to support U.S. manufacturers.

This project progress was frequently reported by NIST Monthly Highlights [97] and Material Matters [98]. Based on the significant contributions to U.S. and international Rockwell hardness standardization, the project team has celebrated three NIST awards, in which Song and his colleagues were recognized [99]:

"…***for development of a metrology-based Rockwell C Hardness Scale which will reduce trade barriers and has made the U.S. a world leader in the field.***"

6.3. Future Work

I'm currently leading the NIST efforts in the future research projects in the fields of firearm evidence identifications, engineering surface quality control and Rockwell hardness standardization which include:

6.3.1. Proposed future projects for firearm evidence identifications

- **Develop a new identification criteria for the Congruent Match Cells (CMC) method**

Current CMC identification criterion is based on the Consecutively Matching Striae (CMS) method developed by Biasotti and Murdock [49-51]. It is proposed to include a weighting function to correlations cells based on the effective correlation pixels, and to develop a Normalized Congruent Match Area (NCMA) method and identification criteria to increase the correlation accuracy.

- **Develop other congruent match methods for forearm evidence identification and error rete estimation**

  That includes the Congruent Match Cross-sections (CMX) method for firing pin correlations [100,101]; the Congruent Match Profile Segments (CMPS) method for bullet signature identifications [102,103]; and the Congruent Match Features (CMF) method for breech face, firing pin and ejector mark image correlations.

- **Develop a procedure for reporting Likelihood Ratio (LR) for ballistics identifications**

  Based on the error rate procedure for ballistics identifications invented at NIST [7,8,31], develop a procedure for reporting Likelihood Ratio (LR) for ballistics identifications, thus emulating methods used for forensic identification of DNA evidences.

6.3.2. Proposed NIST Small Business Innovation Research (SBIR) project for development of precision random profile roughness specimens

In 2012, the NIST Small Business Innovation Research (SBIR) project was proposed for development of Precision Random Profile Roughness Specimens to support engineering surface quality control for smooth engineering surfaces [104]. The proposed SBIR project aims to develop NIST SRM Precision Random Profile Roughness Specimens, which are intended for use as calibration and check standards for stylus and optical instruments to measure smooth engineering surfaces. From this SBIR project, the proposed NIST SRM 2076-2078 Precision Random Profile Roughness Specimens will be developed for quality control of smooth engineering surfaces, which will greatly support U.S. manufacturing industry.

6.3.3. Proposed NIST SRM 2809 standard Rockwell hardness diamond indenters

Since 1990's, NIST initialized a SRM Rockwell Diamond Indenters project to support U.S. manufacturing industries. Researchers of NIST are now working on microform calibrations and hardness performance tests and considering the initiation of a new project to develop SRM

Rockwell Diamond Indenters in conformance with the revised ISO standard to support U.S. manufacturers.

REFERENCES: (* Eight key publications submitted with my Ph.D. thesis for review)

*1. Song J, "Random profile precision roughness calibration specimens," *Surface Topography*, 1988, **1**: p29-40.

*2. Song J, Vorburger T V, "Verifying measurement uncertainty using a control chart with dynamic control limits," *MEASURE* (Journal of NCSL-International), NCSL-International, 2007, **2**(3): p76-80.

*3. Song J, Rudder F Jr, Vorburger T V, Smith J, "Microform calibration uncertainties of Rockwell diamond indenters," *Journal of Research of NIST*, 1995, **100**(5): p543-561.

*4. Song J, Low S, Pitchure D, Germak A, DeSogus S, Polzin T, Yang H, Ishida H, Barbato G, "Establishing a worldwide unified Rockwell hardness scale with metrological traceability," *Metrologia*, BIPM, Paris, 1997, **349**(4): p331-342.

*5. Song J, Whitenton E, Kelley D, Clary R, Ma L, Ballou S, "SRM 2460/2461 standard bullets and casings project," *J. Res. Natl. Inst. Stand. Technol*., 2004, **109**(6): p533-542.

*6. Song J, Vorburger T V, Ballou S, Thompson R, Yen J, Renegar T B, Zheng A Silver R, Ols M, "The national ballistics imaging comparison (NBIC) project," *Forensic Science International*, 2012, **216**: p168-182. http://dx.doi.org/10.1016/j.forsciint.2011.09.016.

*7. Song, J., "Proposed Congruent Matching Cells (CMC) method for ballistics identification and error rate estimation," *AFTE Journal*, 2015, **47**(3): p177-185.

*8. Song J, Vorburger T V, Chu W, Yen J, Soons J A, Ott D B, Zhang N-F, *"Estimating error rates for firearm evidence identifications in forensic science,"* passed NIST review, to be submitted to *Forensic Science International* for publication.

9. BIPM, IEC, IFCC, ILAC, ISO, IUPAC, IUPAP and OIML, *International vocabulary of metrology -- Basic and general concepts and associated terms (VIM)*, JCGM 200, ISO, Geneva, 2008.

10. ISO 11562-1998, *Geometrical Products Specifications (GPS) -- Surface texture: Profile method -- Metrological characteristics of phase correct filters*, ISO, Geneva, 1998.

11. ASME B46.1-2012, *Surface Texture -- Surface Roughness Waviness and Lay*, ASME, New York, 2012.

12. Song J, Vorburger T V, "Surface Texture," *ASM Handbook (Vol. 3) -- Friction, Lubrication and Wear Technology*, ASM, PA, 1992, p334-345.

13. Song J, Vorburger T V, "Standard reference specimens in quality control of engineering surfaces," *Journal of Research of NIST*, 1991, **96**(3): p. 271-289.

14. Häsing J, "Herstellung und eigenschaften von referenznormalen für das einstellen von oberflachenmessgeraten," *Werkstattstechnik*, 1965, **55**(Jahrg): p380-383.

15. Song J, Vorburger T V, "Uncertainty procedure for NIST surface finish and microform calibrations," in *Proc. 1996 Measurement Science Conference* (MSC), CA, 1996, p403-417.

16. Song J, Rudder F Jr, Vorburger T V, Hartman A, Scace B, Smith J, "Microform calibrations in surface metrology," *Int. J. Mech. Tools Manufact.* 1995, **35**(2): p301-310.

17. Song J, Low S, Zheng A, "NIST microform calibration system for Rockwell hardness standardization," in *Proc. SPIE -- The 4th International Symposium on Precision Mechanical Measurements (ISPMM)*, **SPIE 7130**, Bellingham, WA, 2008, p1-7.

18. Song J, Vorburger T V, "Proposed bullet signature comparisons using autocorrelation functions," in *Proc. 2000 NCSL*, National Conference of Standards Laboratories International (NCSL), Toronto, Canada, 2000.
19. Song J, Vorburger T V, "A novel parameter proposed for 2D and 3D topography measurements and comparisons," in *Proc.* **SPIE 6672**: 0M1-0M8, SPIE, Bellingham, WA, 2007.
20. Song J, Ma L, Whitenton E, Vorburger T V, "2D and 3D surface texture comparisons using autocorrelation functions," *Key Engineering Materials,* Trans. Tech. Publications, Swaziland, 2005, **295**: p437-440.
21. Ma L, Song J, Whitenton E, Zheng A, Vorburger T V, "NIST bullet signature measurement system for SRM (standard reference material) 2460 standard bullets," *Journal of Forensic Sciences,* ASTM International, PA, 2004, **49**(4): p649-659.
22. Song J, Vorburger T V, Renegar T B, Rhee H, Zheng A, Ma L, Libert J, Ballou S, Bachrach B, Bogart K., "Correlations of topography measurements of NIST SRM 2460 standard bullets by four techniques," *Measurement Science and Technology*, London, 2006, **17**(2): p500-503. DOI:10.1088/0957-0233/17/3/S07.
23. Song J, Rubert P, Zheng A, Vorburger T V, "Topography measurements for determining the decay factors in surface replication," *Measurement Science and Technology*, London, UK, 2008, **19**(8): p1-4. DOI:10.1088/0957-0233/19/8/084005.
24. Song J, Chu W, Vorburger T V, Thompson R, Yen J, Renegar T B, Zheng A, Silver R, "Development of ballistics identification -- From image comparison to topography measurement in surface metrology," *Measurement Science and Technology*, 2012, **23**(4): p1-6. http://stacks.iop.org/0957-0233/23/054010.
25. Song J, Vorburger T V, Ballou S, Ma L, Renegar T B, Zheng A, Ols M, "Three steps towards metrological traceability for ballistics signature measurements," *Measurement Science Review*, 2010, **10**(2): p19-21. DOI: 10.2478/v10048-010-0004-8.
26. Song J, Vorburger T V, Ballou S, Ma L, Renegar T B, Zheng A, Ols M, "Traceability for ballistics signature measurements in forensic science," *Measurement*, 2009, **42**(10): p1433-1438. DOI: 10.1016/j.measurement.2009.07.006.
27. Scientific Working Group for Firearm and Toolmarks (SWGGUN), *The foundations of firearm and toolmark identification*. http://www.swggun.org.
28. The National Research Council, *Ballistic imaging*, 2008, p3, p20, p82.
29. The National Research Council, *Strengthening forensic science in the United States -- A path forward*, 2009, p153-154, p155, p184.
30. Association of Firearm and Tool-marks Examiners (AFTE), *The theory of identification, range of striae comparison reports and modified glossary definitions -- An AFTE criteria for identification committee report, AFTE Journal*, 1992, **24**(3): p337.
31. Song J, "Proposed NIST ballistics identification system (NBIS) based on 3D topography measurements on correlation cells," *AFTE Journal*, 2013, **45**(2): p184-194.
32. Chu W, Tong M, Song J, "Validation tests for the congruent matching cells (CMC) method using cartridge cases fired with consecutively manufactured pistol slides," *AFTE Journal*, 2013, **45**(4): p361-366.
33. Tong M, Song J, Chu W, Thompson R, "Fired cartridge case identification using optical images and the congruent matching cells (CMC) method," *Journal of Research of NIST*, 2014, **119**(023): p575-582. http://dx.doi.org/10.6028/jres.119.023.
34. *Integrated Ballistics Identification System (IBIS),* Forensic Technology Inc., Montreal, Canada. www.fti-ibis.com.

35. Office of Firearms, Explosives and Arson, ATF: *ATF's NIBIN Program*, 1998 AFTE (Association of Firearm and Tool Mark Examiners) Workshop, July 12-17, 1998, Tampa, FL. Also see ATF's NIBIN Program at http://www.nibin.gov/nibin.pdf, 2005.
36. Teaque E C, Scire F, Vorburger T V, "Sinusoidal profile precision roughness specimens", *Wear*, 1982, **83**: p61-74.
37. Vorburger T V, Song J, Giauque C, Renegar T B, Whitenton E, Croarkin M, "Stylus-laser surface calibration system," *Precision Engineering*, 1996, **19** (2): p157-163.
38. Song J, Vorburger T V, Rubert P, "Comparison between precision roughness master specimens and their electro-formed replicas," *Precision Engineering*, 1992, **14**(2): p84-90.
39. Song J, Evans C, McGlauflin M, Whitenton E, Vorburger T V, Yuan Y, "NIST virtual/physical random profile roughness calibration standards," *Proc. SPIE'98, Scattering and Surface Roughness*, 1998, **SPIE 3426**: p213-221.
40. National Institute of Standards and Technology (NIST) Certificate -- *Standard Reference Material 2461 Standard Cartridge Case,* NIST, 2012, http://www.nist.gov/pml/div683/grp02/sbc.cfm.
41. Jenkins G, Watts D, *Spectral analysis and its applications*, Holden-Day, San Francisco, 1968, p171.
42. Song J, Whitenton E, Ma L, Zheng A, Vorburger T V, "Initial measurement results for 20 NIST SRM 2460 standard bullets," in *Proc. Measurement Science Conference (MSC)*, CA, 2004.
43. Taylor B, Kuyatt C, *Guidelines for evaluation and expressing the uncertainty of NIST measurement results*, NIST Technical Note **1297**, National Institute of Standards and Technology, Gaithersburg, MD, 1994.
44. National Institute of Standards & Technology (NIST) Certificate -- *Standard Reference Material 2460 Standard Bullets*, NIST, 2006. http://www.nist.gov/pml/div683/grp02/sbc.cfm.
45. Bergen J R, Anandan P, Hanna, K, Hingorani R, "Hierarchical model-based motion estimation," in *Proceedings of Second European Conference on Computer Vision*, Springer-Verlag, 1992, p237-252.
46. Heeger D, *"Notes on motion estimation,"* prepared by Prof. David J. Heeger for Courses Psych 267/CS 348D/EE 365, New York University, Oct. 20, 1996.
47. Heeger D, "MATLAB™ Software for image registration," Copyright 1997, 2000 by Stanford University.
48. ISO 80000-2, *Qualities and units -- Part 2: Mathematical signs and symbols to be used in the natural sciences and technology*, ISO, Geneva, 2009.
49. Biasotti A, "A statistical study of the individual characteristics of fired bullets," *J. Forensic Sci.* 1959, **4**: p34-50.
50. Biasotti A, Murdock J E, "Criteria for identification or state of the art of firearm and toolmark identification," *AFTE Journal*, 1984, **16**(4): p17-34.
51. Biasotti A, Murdock J E, "Firearms and toolmark identification: legal issues and scientific status," in *Modern Scientific Evidence: The Law and Science of Expert Testimony*, ed. by Faigman D L, Kay D H, Saks M J, Sanders J, St Paul: West Publishing Co., 1997, p124-151.
52. Fadul T G Jr, Hernandez G A, Stoiloff S, Gulati S, *National Institute of Justice Project Report*, Document 2012, No. 237960.
53. Williamson J B P, "The shape of solid surfaces," *Sec. 1.2 in Rough Surfaces*, Thomas T R ed., first edition, Longman, Harlow, Essex, UK 1982.

54. Thibodeau L A, "Sensitivity and specificity," in *Encyclopedia of Statistical Sciences*, Kotz S and Johnson N L eds., 1st edition, John Wiley, New York, 1988, p370-372.
55. Ross S, *A first course in probability*, MacMillan, New York, 1976.
56. Boulay K., Leeds Forensic Systems, Inc. Minneapolis, MN, "An email communication with NIST," September 30, 2013.
57. ISO 17025, *General requirements for the competence of testing and calibration laboratories*, ISO, Geneva, 2005.
58. American Society of Crime Laboratory Directors / Laboratory Accreditation Board (ASCLD/LAB). http://www.ascld.org.
59. Whitehouse D J, "The parameter rash -- is there a cure?" *Wear*, 1982, **83**: p75-78.
60. BS 1134, *Method for the assessment of surface texture,* Part 2, London, British Standards Institution, 1972.
61. ISO 5436-1995, *Calibration specimens -- stylus instruments -- types, calibration and use of specimens*, ISO, Geneva, 1995.
62. ASME B46-1995, *Surface texture: roughness waviness and lay,* ASME, New York, 1995.
63. Hillmann W, *Comparison of roughness measurements in the European community*, Commission of the European Communities, Community Bureau of Reference, BCR. Report, EUR 12 180 EN, 1989.
64. NIST, *Monthly Highlight*, NIST, July, 2009.
65. Song J, Vorburger T V, "Stylus profiling at high resolution and low force," *Applied Optics,* OSA, 1991, **30** (1): p42-50.
66. Song J, Vorburger T V, "Stylus flight in surface profiling," *J. Manufacturing Science and Engineering*, ASME, 1996, **118** (2): p188-198.
67. Dongmo S, Villarrubia J, Jones S, Renegar T B, Postek M, Song J, "Experimental test of blind tip reconstruction for scanning probe microscopy," *Ultramicroscopy,* 2000, **85**: p141-153.
68. Thomas T R, *Rough Surfaces (Second Edition),* Imperial College Press, London, 1999, p28-29.
69. Appendix A: *Measurement Conditions and Sources of Uncertainties for NIST Surface Roughness and Step Height Calibration Reports*, last revised in June 2010, at the NIST website www.mel.nist.gov/div821/webdocs-13/surfcalib.htm.
70. OIML/SP19/SR/4, *Comple rendu de la comparison international des echelles de durete Rockwell C et Vickers HV 30,* OIML, Paris, 1984.
71. Peggs G, "Synthesis report on the intercomparison of hardness measurements for the Community Bureau of Reference (BCR)," NPL, UK, 1988.
72. Barbato G, DeSogus S, Germak A, "Report on the results obtained in the comparison of the HRC scales maintained at ETCA, IMGC and MPA NRW, IMGC," Torino, Giugno, Rapporto Techico Ieterno, 1994, **R382**.
73. ISO 9000: 2015, *Quality management systems -- Fundamentals and vocabulary*, ISO Geneva, 2015.
74. Meyer K, "Das Erreichen der Vergleichbarkeit der Härtemesswerte -- ein Problem der Werkstoff-Prüftechnik von Internationaler Bedeuturg," *VDI Berichte*, 1957, **11**: p103-122.
75. Marriner R S, "Standard hardness testing machine," *Acta Imeka*,1964. **3**(2): p235.
76. Barbato G, DeSogus S, Levi R, "Design studies and characteristic description of the standard dead-weight hardness tester of the IMGC," *VDI Berichte*, 1978, p308.

77. Tsai C, Li F, *et al*., "The design of the NIM laser type national deadweight standard Rockwell and Rockwell superficial hardness machine," National Institute of Metrology (NIM), Beijing, China, 1981.
78. Petik E, "The effect of a change of loading cycle parameters in hardness testing," *Bulletin OIML*, 1988, **113**: p35-40.
79. Tolmon F R, Wood J G, "Precision measurement of Rockwell diamond penetrators," *Engineering*, 1951, **172**: p89-90.
80. Yamamoto K, Yano H, "Studies on determination of standard Rockwell diamond indenters," *Bulletin of the NRLM*, 1967, **14**, NRLM.
81. Nash P G, "A new method for the measurement of Rockwell diamond indenters," *NPL Report*, NP (UK), 1978, MOM**33**.
82. Barbato G, DeSogus S, "Measurement of the spherical tip of Rockwell indenters," *J. Testing & Evaluation*, 1988, **16** (4): p369-374.
83. Song J, Smith J H, Vorburger T V, "A metrology approach to unifying Rockwell C hardness scales," in *Proceedings of 9th International Symposium of Hardness Testing in Theory and Practice*, VDI Berichte, Dusseldorf, Germany, 1995, **1194**: p19-31.
84. Song J, Vorburger T V, "Standard grade Rockwell diamond indenters -- A key to a worldwide unified Rockwell hardness scale," in *Proceedings of 1996 National Conference of Standard Laboratories*, NCSL, CA, 1996, P403-417.
85. Hild K, "Der einfluss der toleranzen des messverfahrens nach Rockwell C auf die hartwerte," *Zeitschrift fur Instrumentenkunde*, 1958, **66**.
86. Bochmann G, Hild H, "Der einfluss von abweichungen des eindring korpers von der soliform auf die hartewerte bei dem messverfahrennach Rockwell C," *Zeitschrift fur Instrumentenkunde*, 1960. **68** (6).
87. Barbato G, DeSogus S, Levi R, "The meaning of the geometry of Rockwell indenters," *Rapp. Tec. Int.*, Sept. 1978, R**128**.
88. Yano H, Ishida H, Kamoshita T, "Characteristics of standard Rockwell diamond indenters and method of establishing standard indenters," in *Proceedings of the Round-Table Discussion on Hardness Testing*, 7th IMEKO World Congress, London, 1976.
89. Barbato G, DeSogus S, Li, F, Wang Q, "Comparison of hardness measurements between China (NIM) and Italy (IMGC)," *Bulletin OIML*, December, 1986, **105**.
90. Tobolski E L, "Origin and past development of the Rockwell hardness standards," in *Proceedings of 1992 Measurement Science Conference*, MSC, CA, 1992.
91. Polzin T, Schwenk D, "Measuring of Rockwell indenters by means of a laser interferometric instrument," in *Proceedings of 9th International Symposium of Hardness Testing in Theory and Practice*, VDI Berichte, Dusseldorf, Germany, 1995. **1194**: p. 265-273.
92. Song, J, Rudder F Jr, Vorburger T V, Hartman A W, Scace B R, Smith J H, "The geometric characterization of Rockwell diamond indenters," in *Proceedings of the XIII IMEKO World Congress*, Torino, Italy, 1994, p779-784.
93. ISO 6508-3:2015(E): *Metallic materials -- Rockwell hardness test -- Part 3: Calibration of reference blocks.* ISO Geneva, 2015.
94. Song J, Low S, Ma L, "Tolerancing form deviations for NIST standard reference material (SRM) 2809 Rockwell diamond indenters," in *Proc. International Symposium on Advances in Hardness Measurement (HARDMEKO 2007),* NMIJ, Tsukuba, Japan, 2007, p97-102.

95. Song J, Low S, Ma L, "Tolerancing form deviations for Rockwell diamond indenters," in *Proc. IMEKO TC3/TC5/TC20 Joint International Conference,* IMEKO, Celle, Germany, 2002.
96. Ma L, Low S, Zhou J, Song J, DeWit, R, "Simulation and prediction of hardness performance of Rockwell diamond indenters using finite element analysis," *Journal of Testing and Evaluation,* ASTM International, PA, 2002, **30**(4): p265-273.
97. Low S, Song J, "NIST proposed significant change to the ISO Rockwell hardness test method standard to increase availability of calibration grade hardness indenters," *NIST Monthly Highlights,* August/September, 2015, p4.
98. Low S, Song J, "NIST's changes to the ISO Rockwell hardness test method standard increase availability of calibration-grade hardness indenters," *Material Matters*, Fall 2015, MML, NIST, p13.
99. Edward Bennett Rasa Award of the National Institute of Standards and Technology, December, 1996.
100. Song J, Zhang H, "Proposed Congruent Match Cross-sections (CMX) method for firing pin correlations," presented at the 2016 AAFS conference, February 2016, Los Vegas.
101. Zhang H, Song J, Tong M, Chu W, "Correlation of firing pin impressions based on the congruent matching cross-sections (CMX) method", *Forensic Science International,* **263**, 2016, p186-193.
102. Song J, Chu W, "Proposed Congruent Match Profile Segments (CMPS) method for bullet signature identifications," presented at the 47th AFTE conference, New Orleans, May 29th, 2016.
103. Chu W, Song J, "Initial validations tests for the Congruent Match Profile Segments (CMPS) method for bullet signature identifications," to be submitted to the *Journal of Forensic International*.
104. Song J, "Development of SRM precision random profile roughness specimens," a proposal for 2012 NIST Small Business Innovation Research (SBIR) project, NIST, 2012.

Appendix A: Biography with a publication list
See attached file A

Appendix B: Eight key publications
See attached files B

1. Song J, "Random profile precision roughness calibration specimens," *Surface Topography*, 1988, **1**: p29-40.
2. Song J, Vorburger T V, "Verifying measurement uncertainty using a control chart with dynamic control limits," *MEASURE* (Journal of NCSL-International), NCSL-International, 2007, **2**(3): p76-80.
3. Song J, Rudder F Jr, Vorburger T V, Smith J, "Microform calibration uncertainties of Rockwell diamond indenters," *Journal of Research of NIST,* 1995, **100**(5): p543-561.
4. Song J, Low S, Pitchure D, Germak A, DeSogus S, Polzin T, Yang H, Ishida H, Barbato G, "Establishing a worldwide unified Rockwell hardness scale with metrological traceability," *Metrologia*, BIPM, Paris, 1997, **349**(4): p331-342.
5. Song J, Whitenton E, Kelley D, Clary R, Ma L, Ballou S, "SRM 2460/2461 standard bullets and casings project," *Journal of Research of NIST*, 2004, **109**(6): p533-542.
6. Song J, Vorburger T V, Ballou S, Thompson R, Yen J, Renegar T B, Zheng A Silver R, Ols M, "The national ballistics imaging comparison (NBIC) project," *Forensic Science International*, 2012, **216**: p168-182. http://dx.doi.org/10.1016/j.forsciint.2011.09.016.
7. Song, J., "Proposed Congruent Matching Cells (CMC) method for ballistics identification and error rate estimation," *AFTE Journal*, 2015, **47**(3): p177-185.
8. Song J, Vorburger T V, Chu W, Yen J, Soons J A, Ott D B, Zhang N-F, *"Estimating error rates for firearm evidence identifications in forensic science,"* passed NIST review, to be submitted to *Forensic Science International* for publication.

Appendix A:
Biography with a publication list
For J. Song's PhD by published work, Engineering School of University of Warwick
Submitted on June 5th, 2016 (See attached files)

Junfeng (John) Song

Engineering Physics Division (EPD)
Physical Measurements Laboratory (PML)
National Institute of Standards and Technology (NIST)

100 Bureau Drive, Stop 8212, Gaithersburg, MD 20899
song@nist.gov; 301 975-3799 (phone); 301 975-4396 (fax)

A. Formal Education:

M.S. Mechanical Engineering, Harbin Institute of Technology (HIT), Harbin, China, 1982

B. Professional Employment History:

1997 – Present
Mechanical Engineer,
Project Lead for NIST's Forensic Topography and Surface Metrology Project,
Post Doc. Research Advisor for NRC/NAS.

1994 – 97
Mechanical Engineer, NIST.

1987 – 94
Guest Researcher, NIST.

1981 – 87,
Engineer, Senior Engineer and Group Lead, Changcheng Institute of Metrology and Measurement (CIMM), Beijing, China.

C. Awards:

NIST Judson C. French Award, 2002.
NIST E. B. Rosa Award, 1996.
NIST Director's "Certification of Appreciation" for Guest Researcher, 1994.

D. Recent research projects:

Project Lead for:

- NIST SRM 2460 standard bullets project, completed in 2007;
- NIST SRM 2461 standard cartridge cases project, completed in 2012;
- NIST National Ballistics Imaging Comparison (NBIC) project, completed in 2011;
- Establish the "National Ballistics Evidence Search Engine (NBESE)" using 3D topography measurements on correlation cells: 2012-present.
- Development of a Congruent Match Cells (CMC) method for firearm evidence identification and error rate estimation., 2013-present.

E. A publication list

(* Eight key publications, see attached files)

A. **Topography Metrology for Firearm Evidence Identification and Error Rate Estimation in Forensic Science**

[1]* **Song, J.,** Whitenton, E., Kelley, D., Clary, R., Ma, L., Ballou, S., "SRM 2460/2461 standard bullets and casings project," *J. Res. Natl. Inst. Stand. Technol.,* **109,** 6 (2004), 533-542, NIST.

[2] **Song, J.,** Vorburger, T., Clary, R., Whitenton, E., Ma, L., Ballou, S., "Standards for bullets and casings," *Materials Today,* November 2002, 26-31, Elsevier Science Ltd, UK, 2002.

[3] **Song, J.,** Vorburger, T., Ols, M., "Establishment of a virtual/physical standard for bullet signature measurements," in Proc. 2001 NCSL, National Conference of Standards Laboratories International, Washington DC, 2001.

[4] **Song, J.,** Vorburger, T., Ballou, S., Renegar, T., Ma, L., Whitenton, E., Kelley, D., Clary, R., Zheng, A., Ols, M., "NIST standard bullets and casings project," in Proc. 2007 ASPE Conference, America Society for Precision Engineering (ASPE), Dallas, 2007.

[5] **Song, J.**, Vorburger, T., Clary, R., Ma, L., Whitenton, E., "NIST standard reference material (SRM) 2460/2461 project – standard bullets and casings" in Proc. XVII IMEKO World Congress, IMEKO, Dubrovnik, Croatia (2003), VIII-142.

[6] **Song, J.,** Vorburger, T., Clary, R., McGlauflin, M., Whitenton, E., Evans, C., "NIST random profile roughness specimens and standard bullets," in Proc. 2000 MSC, Measurement Science Conference, CA, 2000.

[7] **Song, J.,** Vorburger, T., "Development of NIST standard bullets and casings status report," NIJ Technical Report 603-00, National Institute of Justice, 2000.

[8] **Song, J.,** Vorburger, T., Renegar, T., Zheng, A., Thomson, R., Silver, R., Ols. M., "NIST SRM (standard reference material) 2460/2461 standard bullets and casings project" in the Proceedings of 4th International Conference on Forensic Weapons Study (ICFWS 2009), Saratov, Russia, October 13 - 14, 2009.

[9] **Song, J.,** Vorburger, T., Ols, M., "Progress in developing NIST standard casings," in Proc. 2002 MSC, Measurement Science Conference, CA, 2002.

[10] **Song, J.,** Vorburger, T., Clary, R., Whitenton, E., Ma, L., Ballou, S., "Standards for optical imaging systems in forensic laboratories," in Proc. 2002 ISIST, International Symposium on Instrumentation Science and Technology, Jinan, China (2002), 3001-3008 .

[11] **Song, J.,** Vorburger, T., "A novel parameter proposed for 2D and 3D topography measurements and comparisons," in Proc. SPIE 6672: 0M1-0M8, SPIE, Bellingham, WA, 2007.

[12] **Song, J.,** Vorburger, T., "Proposed bullet signature comparisons using autocorrelation functions," in Proc. 2000 NCSL, National Conference of Standards Laboratories International (NCSL), Toronto, Canada, 2000.

[13] **Song, J**., Vorburger, T., Ma, L., Libert, J., Ballou, S., "A metric for the comparison of surface topographies of standard reference material (SRM) bullets and casings," in Proc. 2005 ASPE Conference, America Society for Precision Engineering, VA, 2005.

[14] **Song, J.,** Ma, L., Whitenton, E., Vorburger, T., "2D and 3D surface texture comparisons using autocorrelation functions," *Key Engineering Materials*, **295**: Trans. Tech. Publications, Swaziland (2005), 437-440.

[15] **Song, J.,** Ma, L., Whitenton, E., Vorburger, T., "Bullet signature measurements at NIST," in Proc. 2003 MSC, Measurement Science Conference, CA, 2003.

[16] **Song, J.,** Vorburger, T., Thompson, R., Ballou, S., Zheng, A., Renegar, T.B., Silver, R., Ols, M., Wenz, E.W., Koch, S.A., Braune, M., Lohn, A., "Topography Measurements and Performance Comparisons between NIST SRM 2460 Standard Bullet Masters and BKA Bullet Replicas", *AFTE Journal*, **44**, 3 (2012), 201-217.

[17] **Song, J.,** Whitenton, E., Ma, L., Zheng, A., Vorburger, T., "Initial measurement results for 20 NIST SRM 2460 standard bullets," in Proc. 2004 MSC, Measurement Science Conference, CA, 2004.

[18] **Song, J.,** Ma, L., Vorburger, T., Ballou, S., "Optimizing Gaussian filter long wavelength cutoff for improving 3D ballistics signature correlations," in Proc. 2008 ASPE Conference, America Society for Precision Engineering, Portland, 2008.

[19] **Song, J.,** Ma, L., Vorburger, T., "The effect of Gaussian filter long wavelength cutoff λc in topography comparisons and measurements," in Proc. 2006 ASPE Conference, America Society for Precision Engineering, CA, 2006.

[20] **Song, J.,** Rubert, P., Zheng, A., Vorburger, T., "Topography measurements for determining the decay factors in surface replication," *Measurement Science and Technology*, **19** (8): 1-4, London, UK, 2008. DOI:10.1088/0957-0233/19/8/084005.

[21]* **Song, J.,** Vorburger, T., Ballou, S., Thompson, R., Yen, J., Renegar, T.B., Zheng, A, Silver, R., Ols, M., "The national ballistics imaging comparison (NBIC) project," *Forensic Science International*, **216** (2012), 168-182, online publication at: http://dx.doi.org/10.1016/j.forsciint.2011.09.016.

[22] **Song, J.,** Vorburger, T., Clary, R., Whitenton, E., Ols, M., "Establishment of ballistics measurement traceability using NIST SRM 2460 standard bullets," in Proc. 2002 NCSL, National Conference of Standards Laboratories International, San Diego, 2002.

[23] **Song, J.,** Vorburger, T., Ols, M., "Establishment of measurement traceability for NIST standard bullets and casings," in Proc. 2001 MSC, Measurement Science Conference, CA, 2001.

[24] **Song, J.,** Thompson, R., Vorburger, T., Ballou, S., Yen, J., Renegar, T.B., Zheng, A., Silver, R., "Establishing a Traceability and Quality System for U.S. Ballistics Identification Using NIST SRM Standard Bullets and Cartridge Cases," Proceedings of Saratov University, **12,** 3 (2012), 49-53.

[25] **Song, J.,** Vorburger, T., Ballou, S., Ma, L., Renegar, T., Zheng, A., Ola, M., "Three steps towards metrological traceability for ballistics signature measurements," *Measurement Science Review*, **10,** 2 (2010), 19-21, DOI: 10.2478/v10048-010-0004-8.

[26] **Song, J.,** Vorburger, T., Ballou, S., Ma, L., Renegar, T.B., Zheng, A., Ols. M., "Traceability for ballistics signature measurements in forensic science", *Journal of Measurement,* DOI: 10.1016/j.measurement.2009.07.006. 2009.

[27] **Song, J.,** Vorburger, T., Renegar, T.B., Rhee, H., Zheng, A., Ma, L., Libert, J., Ballou, S., Bachrach, B., Bogart, K., "Correlations of topography measurements of NIST SRM 2460 standard bullets by four techniques", *Meas. Sci. Technol.* **17** (2): 500-503, London, 2006. DOI:10.1088/0957-0233/17/3/S07.

[28] **Song, J.,** Chu, W., Vorburger, T., Thompson, R., Yen, J., Renegar, T.B., Zheng, A, Silver, R., "Development of ballistics identification – From image comparison to topography measurement in surface metrology," *Meas. Sci. Technol.* **23,** 4 (2012), 054010 (6pp), http://stacks.iop.org/0957-0233/23/054010.

[29]* **Song, J.,** Theodore T., Chu, W., Yen, J., Soons, J.A., Ott, D., Zhang, N.-F., "Estimating Error Rates for Firearm Evidence Identifications in Forensic Science," passed NIST review, to be submitted to *Forensic Science International* for publication, G2014-0557, 910556.

[30]* **Song, J.,** "Proposed Congruent Matching Cells (CMC) method for ballistics identification and error rate estimation," *AFTE Journal*, **47**, 3 (2015), 177-185.G2012-0898, 911193.

[31] **Song, J.,** "Proposed NIST Ballistics Identification System (NBIS) based on 3D Topography Measurements on Correlation Cells", *AFTE Journal*, **45**, 2 (2013), 184-194.

[32] **Song, J.,** Chu, W., Tong, M., Soons, J.A., "3D Topography Measurements on Correlation Cells – A New Approach to Forensic Ballistics Identifications," *Meas. Sci. Technol.*, **25**, 6 (2014) 064005 (6pp). G2013-0641, 913418.

[33] Vorburger, T., Yen, J., **Song, J.,** Thompson, R.M., Renegar, T.B., Zheng, A., Tong, M., Ols, M., "The Second National Ballistics Imaging Comparison (NBIC-2) Project," *Journal of Research of NIST*, **119**, 4 (2014), 644-673.

[34] Ma, L., **Song, J.,** Whitenton, E., Zheng, A., Vorburger, T., "NIST bullet signature measurement system for SRM (standard reference material) 2460 standard bullets," *Journal of Forensic Sciences*, **49,** 4 (2004), 649-659, ASTM International, PA, 2004.

[35] Tong, M., **Song, J.,** Chu, W., Thompson, R., "Cartridge Case Identifications Using Optical Images and Congruent Matching Cells (CMC) Method," *Journal of Research of NIST,* **119** (2014), 575-582.

[36] Chu, W., Thompson, R., **Song, J.,** Vorburger, T., "Automatic Identification of Bullet Signatures Based on Consecutive Matching Striae (CMS) Criteria," *Forensic Science International*, **231,** 1–3 (2013), 137–141.

[37] Chu, W., Tong, M., **Song, J.,** "Validation Tests for the Congruent Matching Cells (CMC) Method Using Cartridge Cases Fired with Consecutively Manufactured Pistol Slides," *AFTE Journal*, **45**, 4 (2013), 361-366.

[38] Chu, W., **Song, J.,** Vorburger, T., Thompson, R., Silver, R., "Selecting Valid Correlation Areas for Automated Bullet Identification System Based on Striation Detection", *J. of Research of NIST*, **116,** May – June (2011), 647-653.

[39] Chu, W., **Song, J.,** Vorburger, T., Yen, J., Ballou, S., Bachrach, B., "Pilot study of automated bullet signature identification based on topography measurements and

correlations," *Journal of Forensic Sciences*, **55** (2): 2010, 341-347. DOI: 10.1111/j.1556-4029.2009.01276.x

[40] Vorburger, T., **Song, J**., Chu, W., Renegar, T., Zheng, A., Yen, J., Thompson, R., Silver, R., Bachrach, B., Ols. M., "Topography measurements for correlations of standard cartridge cases," SPIE Scanning Microscopy Conference, *Proc. SPIE*, **7729**, 77291D, 2010. DOI: 10.1117/12.859858.

[41] Chu, W., **Song, J.,** Vorburger, T., Thompson, R., Renegar, T., Silver, R., "Optimal compression and binarization of signature profiles for automated bullet identification systems," *Proc. SPIE, **7729**,* 77291C, 2010, DOI: 10.1117/12.859858.

[42] Vorburger, T., **Song, J.,** Chu, W., Ma, L., Bui, S., Zheng A., Renegar, T., "Applications of cross-correlation functions," *Wear*, 2010.

[43] Chu, W., Ma, L., **Song, J.,** Vorburger, T., "An iterative image registration algorithm by optimizing similarity measurement," *Journal of Research of NIST*, **115** (2):1-6, 2010.

[44] Chu, W., **Song, J.,** Vorburger; T., Ballou, S., "Striation density for predicting the identifiability of fired bullets," *Journal of Forensic Sciences.* **55** (5): 2010, 1222–1226. DOI: 10.1111/j.1556-4029.2010.01438.x

[45] Chu, W., **Song, J.,** Vorburger, T., "Pilot Study of Automated Bullet Signature Identification Based on Topography Measurements and Correlations," *J. Forensic Sciences* **55**(2), 341-347 (2010); DOI: 10.1111/j.1556-4029.2009.01276.x.

[46] Vorburger, T., **Song, J.,** Chu, W., Ma, L., Bui, S., Zheng, A., Renegar, T., "Applications of cross-correlation functions," in Proc. of 12th International Conference on Metrology and Properties of Engineering Surfaces, Rzeszow, Poland, July, 2009.

[47] Vorburger, T., Yen, J., Bachrach, B., Renegar, T., Filliben, J., Ma, L., Rhee, H., Zheng, A., **Song, J.,** Riley, M., Foreman, C., Ballou, S., "Surface topography analysis for a feasibility assessment of a National Ballistics Imaging Database," *NISTIR 7362*, NIST, 2007.

[48] Whitenton, E., Johnson, C., Kelley, D., Clary, R., Dutterer, B., Ma, L., **Song, J**., Vorburger, T., "Manufacturing and quality control of the NIST standard reference material 2460 standard bullet," in Proc. 2003 ASPE Conference, America Society for Precision Engineering (ASPE), Saint Louis, 2003.

A. Microform Metrology Supports Rockwell Hardness Standardization

[49]* **Song, J**., "Random profile precision roughness calibration specimens," *Surface Topography*, **3** (2): 303-314, Kogan Page, UK, 1988.

[50] **Song, J**., Vorburger, T., "Standard reference specimens in quality control of engineering surfaces," *J. Res. NIST*, **96** (3) 271-289, NIST, 1991**.**

[51] **Song, J**., Vorburger, T., "Surface texture, "*ASM Handbook* (Volume 3)-- *Friction, Lubrication and Wear Technology*," p.334-345, ASM, PA, 1992.

[52] **Song, J**., Vorburger, T., Rubert, P., "Comparison between precision roughness master specimens and their electroformed replicas," *Precision Engineering* **14** (2): 84-90, ASPE, 1992.

[53] **Song, J**., Vorburger, T., "Stylus profiling at high resolution and low force," *Applied Optics* **30** (1): 42-50, OSA, 1991.

[54] **Song, J**., Vorburger, T., "Stylus flight in surface profiling," *J. Manufacturing Science and Engineering*, **118** (2): 188-198, ASME, 1996.

[55] **Song, J.,** Evans, C., McGlauflin, M., Whitenton, E., Vorburger, T., Yuan, Y., "NIST virtual/physical random profile roughness calibration standards," in Proc. SPIE'98, Scattering and Surface Roughness, SPIE 3426: 213-221, SPIE, Bellingham, WA, 1998.

[56] Dongmo, S., Villarrubia, J., Jones, S., Renegar, T., Postek, M., **Song, J.,** "Experimental test of blind tip reconstruction for scanning probe microscopy," *Ultramicroscopy*, **85**: 141-153, 2000.

[57] Dongmo, S., Villarrubia, J., Jones, S., Renegar, T., Postek, M., **Song, J**., "Tip characterization for scanning probe microscope width metrology," in Proc. International Conference on Characterization and Metrology for ULSI Technology, Gaithersburg, MD, 1998.

[58] Dongmo, S., Villarrubia, J., Jones, S., Renegar, T., Postek, M., **Song, J**., "Experimental test of scanned probe tip reconstruction," in *Proc. of the 44th National Symposium of the American Vacuum Society*, San Jose, CA, 1997.

[59] **Song, J**., Vorburger, T., "Measurement comparison of stylus radii," in *Proc. ICPE1997*, International Conference on Precision Engineering, p.823-828, Taipei, 1997.

[60]* **Song, J**., Vorburger, T., "Verifying measurement uncertainty using a control chart with dynamic control limits," *MEASURE* (Journal of NCSL-International), NCSL-International, **2** (3): 76-80, 2007.

[61] **Song, J**., Vorburger, T., "Working and check standards for NIST surface and microform calibrations," in Proc. 1995 NCSL, 291-302, National Conference of Standards Laboratories International, Dallas, 1995.

[62] **Song, J**., Vorburger, T., "Standard deviation or standard deviation of the mean – How to report statistical variations in surface calibrations," in Proc. 2004 ASPE Conference, America Society for Precision Engineering, FL, 2004.

[63] **Song, J**., Vorburger, T., "Topography measurement and applications" in Proc. SPIE -The 3rd International Symposium on Precision Mechanical Measurements (ISPMM), SPIE 6280: 1T1-1T8, SPIE, Bellingham, WA, 2006.

[64] **Song J,** Renegar T.B., Soons J, Muralikrishnan B, Villarrubia J, Zheng A, Vorburger T, "The Effect of Tip Size on the Measured Ra of Surface Roughness Specimens with Rectangular Profiles," *Precision Engineering*, **37,** 4 (2013), 217-220 (PubID: 911850, ERB Control #: G2012-1325), http://dx.doi.org/10.1016/j.precisioneng.2013.07.001.

[65] **Song, J.**, "The guidelines for expressing measurement uncertainties and the 4:1 test uncertainty ratio (TUR)," in *Proc. 1997 NCSL*, p.5-12, National Conference of Standards Laboratories International, Atlanta, 1997.

[66] **Song, J.,** Vorburger, T., "Uncertainty procedure for NIST surface finish and microform calibrations," in Proc. 1996 MSC, p.403-417, Measurement Science Conference, CA, 1996.

[67] **Song, J**., Vorburger, T., "NIST microform calibrations – How does it benefit U.S. industry?" in Proc. 1998 ASPE Conference, p.583-586, ASPE, Saint Louis, 1998.

[68] Vorburger, T., **Song, J**., Giauque, C., Renegar, T.B., Whitenton, E., Croarkin, M., "Stylus-laser surface calibration system," *Precision Engineering*, **19** (2): 157-163, ASPE, 1996.

[69] Yuan, Y., Vorburger, T., **Song, J.,** "A recursive algorithm for Gaussian filtering of three-dimensional engineering surface topography," in Proc. International Symposium on Metrology and Quality Control, 31-40, NIS, Cairo, Egypt, 2001.

[70] Yuan, Y., **Song, J**., Vorburger, T., "High accuracy high speed Gaussian filter in surface metrology," in Proc. 1st Int'l EUSPEN Conf., Vol. 1, Shaker Verlag, Aachen, 1999.

[71] Yuan, Y., Vorburger, T., **Song, J**., Renegar, T.B., "A simplified realization for the Gaussian filter in surface metrology," in Proc. X Int'l Colloq. On Surfaces, Chemnitz, Germany, M. Dietzsch, H. Trumpold, eds. Shaker Verlag GmbH, Aachen, 2000.

[72] Vorburger, T., **Song, J.,** Fu, J. , Tundermann, M., Renegar, T., Doiron, T., Barclay, G. and Orji, N. , "Dimensional metrology of millimeter- and sub-millimeter-scale components," in Proc. ICALEO 2000 *Conf. on Laser Microfabrication, p.B-38, Laser Inst. of America, Orlando, 2000.*

[73] Yuan, Y., Qiang, X., **Song, J**., Vorburger, T., "A fast algorithm for determining the Gaussian filtered mean line in surface metrology," Precision Engineering, 24 (1): 62-69, ASPE, 2000.

[74] Rudder, F., **Song, J**., "Calibration uncertainties for microform of Rockwell diamond indenters," in *Proc. 1995 MSC,* Measurement Science Conference, CA, 1995.

[75] Vorburger, T., **Song, J.,** Giauque, C., Renegar, T., "Stylus-laser surface calibration system," in *Proc. 8th Int. Precision Engineering Seminar*, Compiegne, France, 1995.

[76] Vorburger, T., Rhee, H., Renegar, T., **Song, J**., Zheng, A., "Comparison of optical and stylus methods for measurement of surface texture," *Int. J. Adv. Manuf. Technol.,* **33** (1): 110-118, 2007. DOI: 10.1007/s00170-007-0953-8.

[77] Vorburger, T., Zheng, A., Renegar, T.B., **Song, J.,** Ma, L., "An Iterative Algorithm for Calculating Stylus Radius Unambiguously," Proceedings of the 13th International Conference on Metrology and Properties of Engineering Surfaces, Met & Props 2011.

[78] McWaid, T., Vorburger, T., Fu, J., **Song, J.,** Whitenton, E., "Methods divergence between measurements of micrometer and sub-micrometer surface features," *Nanotechnology*, **5** (1): 33-43, 1994.

[79] Marx, E., Leridon, B., Lettieri, T., **Song, J**., Vorburger, T., "Autocorrelation function from optical scattering for one-dimensionally rough surfaces," *Applied Optics*, **32** (1): 67-76, OSA, 1993.

[80] Vorburger, T., **Song, J**., Marx, E., Scace, B., Lettieri, T., "Present and future standard specimens for surface finish metrology," in *Proc. SPIE **1720***, p.78-81, SPIE, Bellingham, WA, 1992.

[81] McWaid, T., Vorburger, T., **Song J.**, Chandler-Horowitz, D., "The effects of thin films on interferometric step height measurements," in *Proc. SPIE **1776***, p.2-13, SPIE, Bellingham, WA, 1992.

[82] McWaid, T., Fu, J., Vorburger, T., **Song, J.**, "A comparison of stylus interferometric and scanning probe measurements" in *Proc. ASPE Conference,* ASPE, Orlando, 1992.

[83] Cao, L., Vorburger, T., Lieberman, A., Lettieri, T., **Song, J**., "Light scattering measurement of the RMS slopes of rough surfaces," *Applied Optics,* **30** (4): 3221-3227, OSA, 1991.

[84] Lettieri, T., Marx, E., **Song, J.,** Vorburger, T., "Light scattering from glossy coatings on paper," *Applied Optics*, **30** (5): 4439-4447. OSA, 1991.

[85] Geist, J., Schaefer, A., **Song, J.,** Wang, Y., Zalewski, E., "An accurate value for the absorption coefficient of silicon at 633 nm," *Journal of Research of NIST*, **95** (5): 549-558, NIST, 1991.

[86] Marx, E., **Song, J.,** Vorburger, T., Lettieri, T., "Light scattered by coated paper," in *Proc. SPIE **1332***, San Diego, SPIE, Bellingham, WA, 1990.

[87] Lettieri, T., **Song, J.,** Vorburger, T., "Light scattering measurement of the surface roughness of glossy paper," in *Proc. 1989 Optical Society of America*, OSA, 1989.

[88] Vorburger T., **Song J.,** Petraco N., Topography measurements and applications in ballistics and tool mark identifications, *Surface Topography: Metrology and Properties*, Topical review, 2015. Open access at http://dx.doi.org/10.1088/2051-672X/4/1/013002.

C. Microform Metrology Supports Rockwell Hardness Standardization

[89]* **Song, J**., Low, S., Pitchure, D., Germak, A., DeSogus, S., Polzin, T., Yang, H., Ishida, H., Barbato, G., "Establishing a worldwide unified Rockwell hardness scale with metrological traceability," ***Metrologia,* 34** 4 (1997), 331-342, BIPM, Paris.

[90] **Song, J.,** Smith, J., Vorburger, T., "A metrology approach to unifying Rockwell C hardness scales," in Proc. 9th Int. Hardness Testing in Theory and Practice, VID Berichte 1194: 19-32, Dusseldorf, Germany, 1995.

[91] **Song, J.,** Rudder, F., Vorburger, T., Smith, J., "Development of Rockwell hardness standards: from performance comparisons to fundamental metrology," *Standard Engineering*, **47** (4): 6-11, Standard Engineering Society, 1995.

[92]* **Song, J.,** Rudder, F., Vorburger, T., Smith, J., "Microform calibration uncertainties of Rockwell diamond indenters," *Journal of Research of NIST*, **100,** 5 (1995), 543-561, NIST.

[93] **Song, J.,** Low, S., Pitchure, D., Germak, A., DeSogus, S., Polzin, T., Yang, H., Ishida, H., "Establishing a common Rockwell hardness scale using geometrically calibrated standard diamond indenters," in Proc. XIV IMEKO World Congress, 258-263, IMEKO, Tampere, Finland, 1997.

[94] **Song, J.,** Rudder, F., Vorburger, T., Hartman, A., Scace, B., Smith, J., "The geometric characterization of Rockwell diamond indenters," in Proc. XIII IMEKO World Congress, 79-784, IMEKO, Torino, Italy, 1994.

[95] **Song, J.,** Rudder, F., Vorburger, T., Smith, J., "Stylus technique for the direct verification of Rockwell diamond indenters," in Proc. 9th Int. Hardness Testing in Theory and Practice, VID Berichte 1194: 129-138, Dusseldorf, Germany, 1995.

[96] **Song, J.,** Rudder, F., Vorburger, T., Hartman, A., Scace, B. , Smith, J., "Microform calibrations in surface metrology," Int. *J. Mech. Tools Manufact.* **35** (2).301-310, 1995.

[97] **Song, J.,** Low, S., Zheng, A., Gu, P., "Geometrical measurements of 28 NIST SRM Rockwell hardness diamond indenters," in the Proc. of HARDMEKO-2010, Thailand, November 2010.

[98] **Song, J.,** Low, S., Zheng, A., "Geometric measurement comparisons for Rockwell diamond indenters" in Proc. of the IMEKO XIX World Congress, September, 2009, Lisbon, Portugal.

[99] **Song, J.,** Low, S., Zheng, A., "NIST microform calibration system for Rockwell hardness standardization," in Proc. SPIE - The 4th International Symposium on Precision Mechanical Measurements (ISPMM), SPIE 7130, p.I-7, Bellingham, WA, 2008.

[100] **Song, J.,** Low, S., Ma, L., "Tolerancing form deviations for NIST standard reference material (SRM) 2809 Rockwell diamond indenters," in Proc. International Symposium on Advances in Hardness Measurement (HARDMEKO 2007), 97-102, NMIJ, Tsukuba, Japan, 2007.

[101] **Song, J.,** Low, S., Ma, L., "Tolerancing form deviations for Rockwell diamond indenters," in Proc. IMEKO TC3/TC5/TC20 Joint International Conference, IMEKO, Celle, Germany, 2002.

[102] **Song, J.,** Low, S., Zheng, A., "Calibration reproducibility test for NIST No 3581 standard Rockwell diamond indenter," in Proc. XVIII IMEKO World Congress, p.TC5-2, IMEKO, Rio de Janeiro, Brazil, 2006.

[103] **Song, J.,** Vorburger T., "Standard grade Rockwell diamond indenters - A key to a worldwide unified Rockwell hardness scale," *Journal of Material Testing Research Association of Japan*, **41** (4): 365-373, Tokyo, 1996, (in Japanese)

[104] **Song, J.,** Vorburger, T., "Standard grade Rockwell diamond indenters - A key to a worldwide unified Rockwell hardness scale," in Proc. 1996 NCSL, National Conference of Standard Laboratories, CA, 1996.

[105] **Song, J.,** Low, S., Pitchure, D., Germak, A., DeSogus, S., Polzin, T., Yang, H., Ishida, H., "Establishing a world-wide unified Rockwell hardness scale using standard diamond indenters," *Measurement*, **4**: 199-205, London, 1998.

[106] **Song, J.,** Low, S., Pitchure, D., Vorburger, T., "Advances in NIST standard Rockwell diamond indenters," in Proc. International Symposium on Advances in Hardness Measurement (HARDMEKO'98), 71-76, NIM, Beijing, 1998.

[107] **Song, J.,** Liggett, W., Pitchure, D., Vorburger, T., "Measurement traceability for NIST standard Rockwell diamond indenters," in Proc. IMEKO-XV World Congress, V45-50, IMEKO, Osaka, Japan, 1999.

[108] **Song, J.,** Low, S., Ma, L., "Form error and hardness performance of Rockwell diamond indenters," in Proc. 16th IMEKO World Congress, I-95, IMEKO, Vienna, Austria, 2000.

[109] **Song, J.,** Low, S., "Worldwide comparisons of Rockwell hardness scales that use a diamond indenter," in Proc. 2002 NCSL, National Conference of Standards Laboratories International, San Diego, 2002.

[110] Ma,L., Low, S., **Song, J**., "An approach to determining the Brinell hardness indentation diameter based on contact position," *ACTA IMEKO*, **3**, 3 (2014), 9-14.

[111] Ma, L., Low, S., **Song, J.,** "A method to determine the spherical indentation contact boundary diameter in elastic-plastic materials," *Mechanics of Materials*, **69**, 1 (2014), 213-226. DOI information: 10.1016/j.mechmat.2013.11.001, http://authors.elsevier.com/sd/article/S0167663613002317.

[112] Ma, L., Low, S., **Song, J**., "Investigation of Brinell indentation diameter from confocal microscope measurement and FEA modeling," in Proc. International Symposium on Advances in Hardness Measurement (HARDMEKO 2007), 65-70, NMIJ, Tsukuba, Japan, 2007.

[113] Ma, L., Low, S., **Song, J**., Zhou, J., "Determining mechanical properties of O1 steel from reverse computation of indentation measurement" in *Proc. XVII IMEKO World Congress*, Dubrovnik, V-113, IMEKO, Croatia, 2003.

[114] Ma, L., Low, S., **Song, J**., "FEA modeling and experimental comparisons of deformable ball indenters' effect on Rockwell B hardness (HRB) tests," *Journal of Testing and Evaluation*, **31** (6): 514-523, ASTM International, PA, 2003.

[115] Ma, L., Low, S., **Song, J**., "Comparison of Rockwell hardness B (HRB) tests using steel and tungsten carbine ball indenters," in *Proc. IMEKO TC3/TC5/TC20 Joint International Conference*, IMEKO, Celle, Germany, 2002.

[116] Ma, L., Low, S., Zhou, J., **Song, J**., DeWit, R., "Simulation and prediction of hardness performance of Rockwell diamond indenters using finite element analysis," *Journal of Testing and Evaluation*, **30** (4): 265-273, ASTM International, PA, 2002.

[117] Ma, L., Low, S., **Song, J**., Zhou, J., "FEA modeling and hardness performance prediction of Rockwell diamond indenters," in *Proc. 2001 NCSL*, National Conference of Standards Laboratories International, Washington DC, 2001.

[118] Liggett, W., Low, S., Pitchure, D., **Song, J.,** "Capability in Rockwell C scale hardness," *J. Res. NIST*, **105** (4): 511-533, NIST, 2000.

[119] Liggett, W., Low, S., Pitchure, D., **Song, J**., "Assessment of error sources in Rockwell hardness measurements," *Proc. XV IMEKO World Congress*, p.V37-44, IMEKO, Osaka, Japan, 1999.

[120] Low, S., Gettings, R., Liggett, W., **Song, J**., "Rockwell hardness - A method-dependent standard reference material," *Proc. 1999 NCSL*, National Conference of Standards Laboratories International, Atlanta, 1999.

(Publications from 1965 to 1987 in China are not included.)